Dealkylation of HMPA and DMPU

Thesis

The Open University
Department of Chemistry

DEALKYLATION

OF HMPA AND DMPU

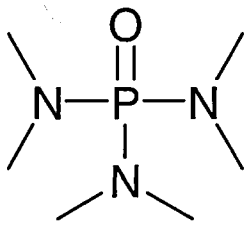

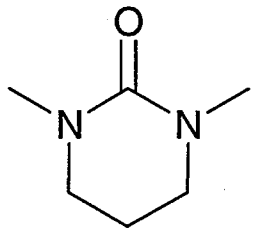

Thesis submitted by:

AUSTIN BARCLAY

In partial fulfilment of the requirements for the degree of Master of Philosophy of the Open University

June 2002

DATE OF SUBMISSION: 28 JUNE 2002
DATE OF AWARD : 13 AUGUST 2002

Table of Contents

Acknowledgements

I would like to thank my supervisors Dr. Jim Iley and Prof. Ray Jones for their guidance and advice throughout and in the writing this thesis.

My thanks go to the Open University for funding this degree.

I would also like to Graeme Jeffs for his technical support and finally Isabelle Carrus for her continual support throughout.

Abstract

Cytochrome P450 metabolises N,N-dialkylamides to their corresponding N-dealkylated products *via* the formation of an N-hydroxyalkyl-N-alkylamide intermediate. Studies by Iley et. al. have shown that the oxidative dealkylation of these amides occurs *via* hydrogen abstraction from the alkyl carbon atom α- to the amide nitrogen. This leads to the formation of a carbon-centred radical; it is believed that this radical is the cause of toxicity for these amides. The amide solvents, HMPA and DMPU have similar functional groups. Because of this similarity it is believed that HMPA and DMPU may undergo an analogous metabolic pathway to that of previously studied amide solvents.

Interestingly HMPA is toxic whereas DMPU is not. Investigation into why this is the case would be of use in designing other non-toxic solvents. This model study has shown that methyl group oxidation in HMPA is subject to a deuterium isotope effect of ~10. This would imply that H-atom abstraction occurs with the formation of a highly reactive C-centred radical. A deuterium isotope effect was not attempted for DMPU, but product analysis showed single oxidation of the ring to form 4-hydroxy-1,3-dimethyltetrahydropyrimidin-2-one and subsequent oxidation to afford 1,3 dimethyl-5,6-dihydropyrimidine-2,4-dione.

Abbreviations

HMPA	hexamethylphosphoramide
PMPA	pentamethylphosphoramide
FPMPA	N-formylpentamethylphosphoramide
TetraMPA	tetramethylphosphoramide
TriMPA	N,N′,N″-trimethylphosphoramide
FTetraMPA	N-formyl-N,N,N′,N″-tetramethylphosphoramide
DMF	N,N-dimethylformamide
NMF	N-methylformamide
DMBA	N,N-dimethylbenzamide
NMBA	N-methylbenzamide
DMPU	1,3-dimethyl-3,4,5,6,-tetrahydro-2(1H)-pyrimidin-2-one previously known as dimethylpropylurea
TMSCl	trimethylsilyl chloride
TFA	trifluoroacetic acid
TPPFeCl	5,10,15,20-tetraphenyl-21H,23H-porphine iron(III) chloride
TPPMnCl	5,10,15,20-tetraphenyl-21H,23H-porphine manganese(III) chloride
^{t}BuOOH	*tert*-butylhydroperoxide
^{t}BuOH	*tert*-butanol
ACN	acetonitrile
DCM	dichloromethane
THF	tetrahydrofuran
ΔH_f	heat of formation
$\Delta G^{\neq}$	Gibb's free energy

$\Delta\Delta G^{\neq}$	difference in Gibb's free energies
FAD	flavin adenine dinucleotide, oxidised form
$FADH_2$	flavin adenine dinucleotide, reduced form
FMN	flavin adenine nucleotide, oxidised form
$FMNH_2$	flavin adenine nucleotide, reduced form
NADP	nicotine adenine dinucleotide phosphate, oxidised form
NADPH	nicotine adenine dinucleotide phosphate, reduced form
GC	gas chromatography
GCMS	gas chromatography mass spectrometry
HPLC	high performance liquid chromatography
UV	ultra-violet spectroscopy
IR	infra-red spectroscopy
MS	mass spectroscopy
m.p.	melting point
M.O.	molecular orbital
MTBSTFA	N-methyl-N-*tert*-butyldimethylsilyltrifluroacetamide
$P450_{cam}$	bacterial cytochrome P450 responsible for the metabolism of camphor
DIBAL	diisobutylaluminium hydride
DIAD	diisopropyl azodicarboxylate

1 Introduction

1.1 Enzymology

In 1958 Klingenburg[1] and Garfinkel[2] independently reported a pigment in liver microsomes which, when carbon monoxide was added, exhibited a carbon monoxide difference spectrum with a very strong absorption band maximum at 450 nm. Six years later this pigment was identified as a protein containing heme (Figure 1) and was termed, cytochrome P450.

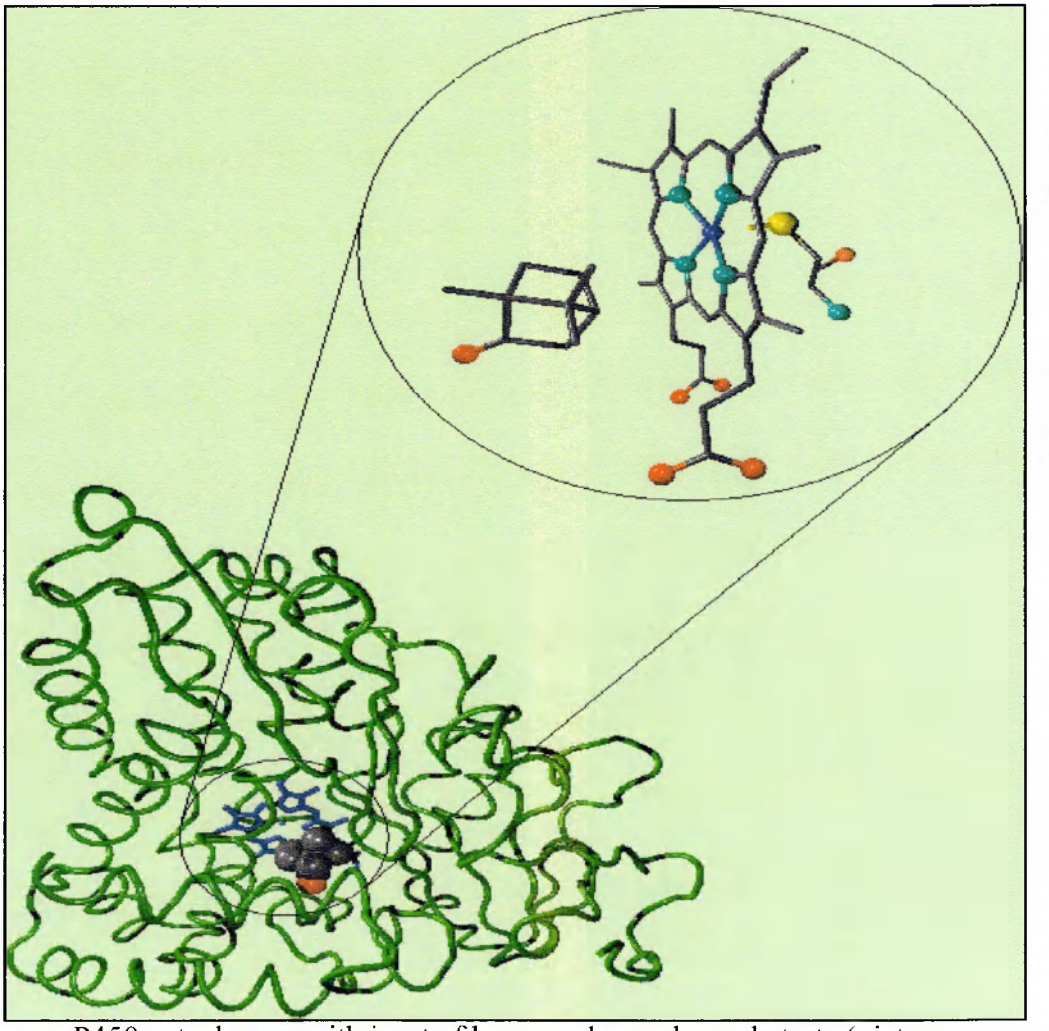

Figure 1 P450 cytochrome with inset of heme and camphor substrate (picture reproduced from http://www.tcm.phy.cam.ac.uk, site accessed June 2002)

Cytochromes P450 are heme-thiolate proteins widely distributed in prokaryotic and eukaryotic organisms. The thiolate is derived from a cysteine residue that is part of the heme protein. This acts as a tether anchoring the heme to the protein. Evidence for this has been obtained from X-ray crystallography.[3] The cysteine sulfur ligand (yellow) can be seen in Figure 2.

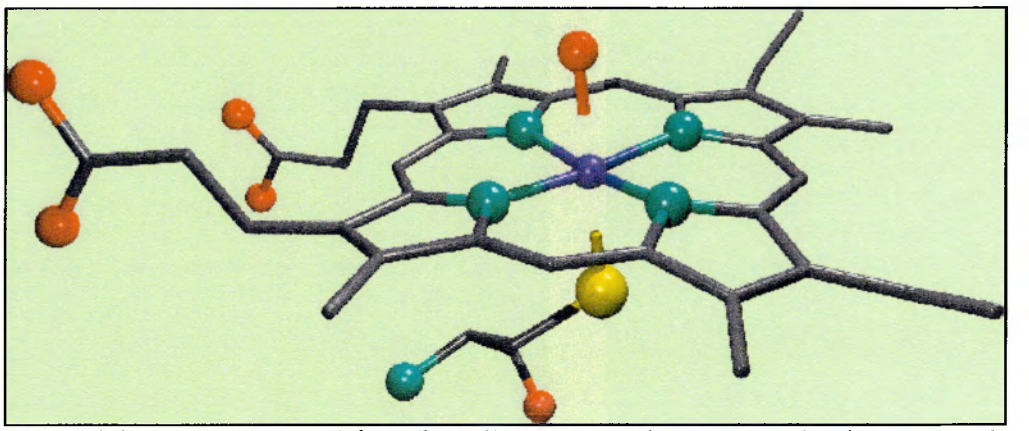

Figure 2 (picture reproduced from http://www.tcm.phy.cam.ac.uk, site accessed June 2002)

Cytochromes P450 have been isolated from numerous mammalian tissues (liver, kidney, lung, adrenal cortex, and intestine), insects, plants, yeasts and bacteria.[4] Cytochromes P450 exist in a number of forms known as **isozymes** or **isoforms**. About 500 different P450 isozymes have been reported. These are referred to collectively as the cytochrome P450 superfamily.

Cytochromes P450 are known to catalyse a range of reactions including hydroxylation of saturated alkanes and of arenes, N-, S-, and O- dealkylations, sulfur oxidation, N-oxygenation, dehalogenations and epoxidations.[5] All of these reactions require the oxidising agent O_2 as well as a reducing agent, which is either NADH or NADPH.

Because they require both a reducing agent and an oxidising agent, these enzymes are called **mixed-function oxidases.**

These reactions are essential for the body to monooxygenate many endogenous substrates, such as fatty acids, which are converted into essential prostaglandins, and also a wide range of xenobiotics. The importance of these enzymes in drug metabolism, toxicology, carcinogenesis, and fatty acid metabolism has made the cytochrome P450 family one of the most widely investigated classes of enzyme.

1.2 Location and physical characteristics of P450

Cytochromes P450 are obtained from two main sources, that is bacteria and the membrane of mammalian endoplasmic reticulum. Both sources give rise to P450s, but due to the different environments in which the P450 enzymes are produced it is easier to extract a pure P450 from bacterial, rather than mammalian sources. This is due to the ease with which a gene can be inserted into bacteria. Such a gene will express a single isoform of P450. The removal of these single isoforms is possible because the bacterial P450s are water soluble and crystallisable. In mammalian species P450s are found in most tissues, though the greater proportion is found in the liver where P450 enzymes are located in the smooth endoplasmic reticulum membrane of hepatocytes. In mammalian tissues there tends to be a large number of different P450s present, which makes purification rather difficult. X-ray crystallographic data have mainly

been obtained for bacterial P450s because they are crystallisable, whereas mammalian P450s are membrane bound and not crystallisable in their natural form.

The eventual purification and reconstitution of individual mammalian isoforms provided evidence for enzyme multiplicity and allowed for the characterisation of substrate and product selectivities. Examples of two different P450s are shown below (Figure 3).

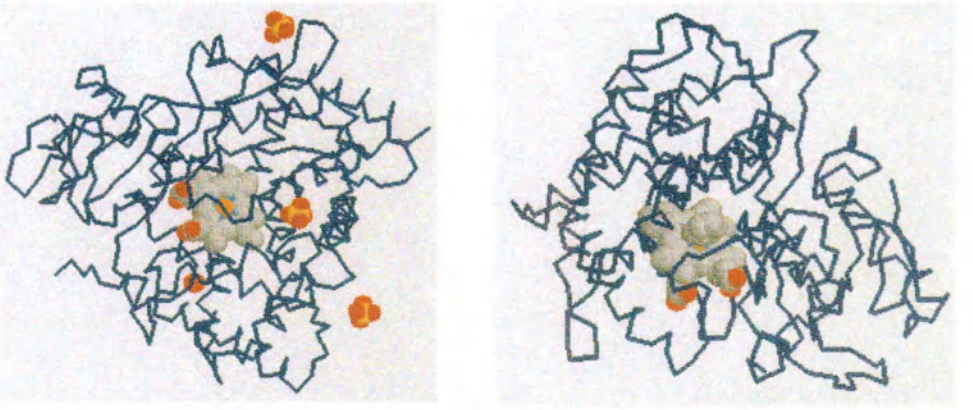

Figure 3 Examples of two different P450s; on the left mammalian cytochrome P450 2C5 and on the right cytochrome $P450_{CAM}$ (camphor monooxygenase (pictures from http://pdb.ccdc.cam.ac.uk).

In the pictures above, the two P450s have differing proteins surrounding the heme unit, which is identical in both. The 3D structure of P450 has been determined using three different bacterial P450s and, although the sequence homology for these proteins is less than 10 per cent, the overall folding of the proteins is quite similar (Figure 4).[5]

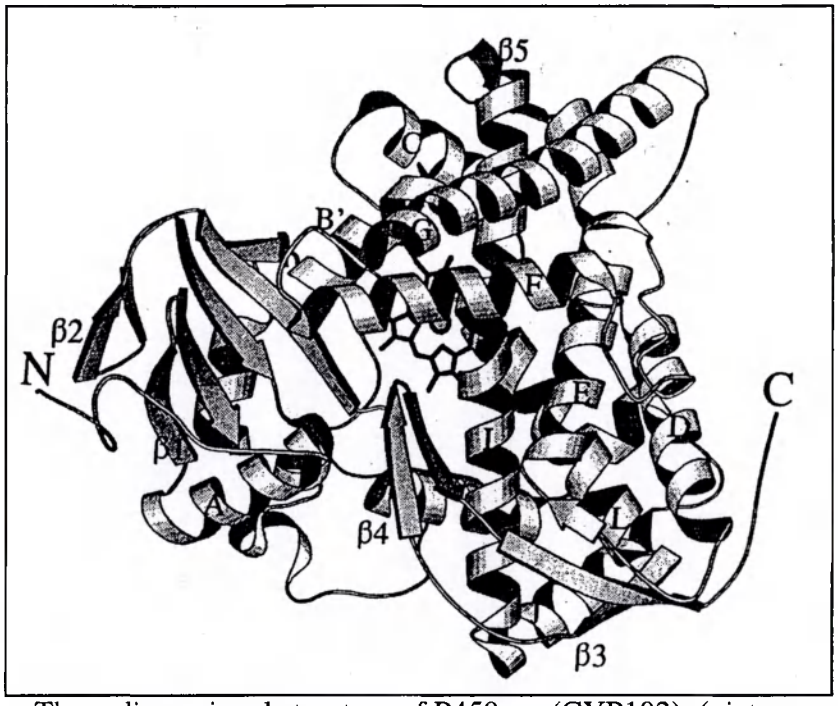

Figure 4 Three dimensional structure of $P450_{BM-3}$(CYP102). (picture reproduced from Cytochrome P450, Kluwer Academic / Plenum Publishers, 2nd edition, Paul R. Ortiz de Montellano (Editor), p154, 1995)

The proteins exhibit a two-domain structure comprising a β-sheet-containing domain (the ribbon arrows to the left in Figure 4) and an α-helix-rich domain (the spirals to the right in Figure 4). The dominant element is an α-helix (the I helix) that traverses the entire protein (top to bottom in the centre of Figure 4) and participates with three other helices (D, E and L) in defining the heme binding region and the substrate oxidation site. In addition, there is a depression in the protein that allows close approach (8-10Å) of a redox partner (a flavoprotein or an iron-sulfur protein) to the heme group. The path of the reductase to the heme is not certain.[5]

All members of the P450 family show absorption at 450 nm upon formation of the reduced P450-carbon monoxide complex. The overall absorption of these enzymes

varies from 447 – 452 nm with an absorption maximum at 450 nm, the so called Soret peak (Figure 5).

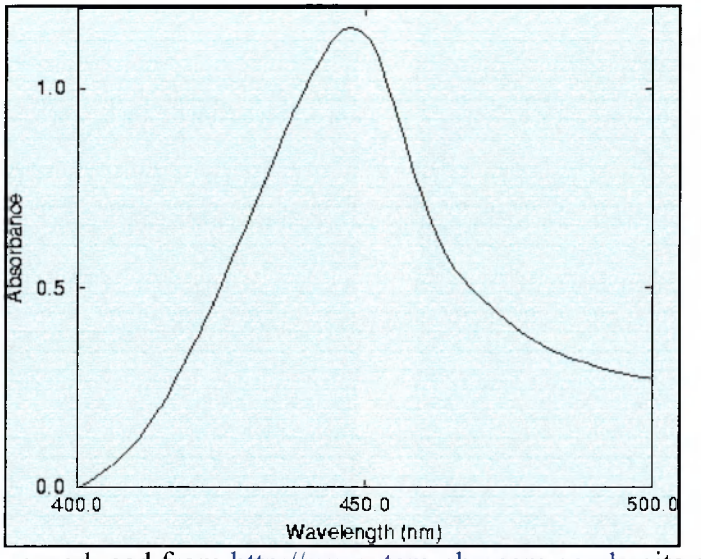

Figure 5 (picture reproduced from http://www.tcm.phy.cam.ac.uk, site accessed June 2002)

This peak is due to a $\pi \rightarrow \pi^*$ electronic transition (Figure 6).

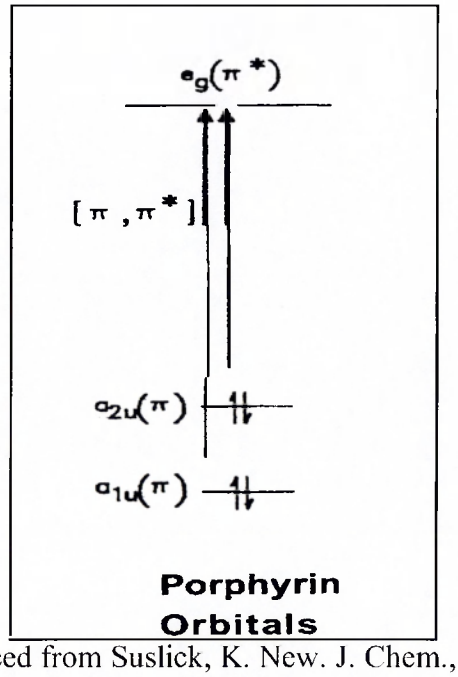

Figure 6 (Reproduced from Suslick, K. New. J. Chem., 1992, 16, 634)

This may be explained by Gouterman's four orbital model (Figure 7).[6]

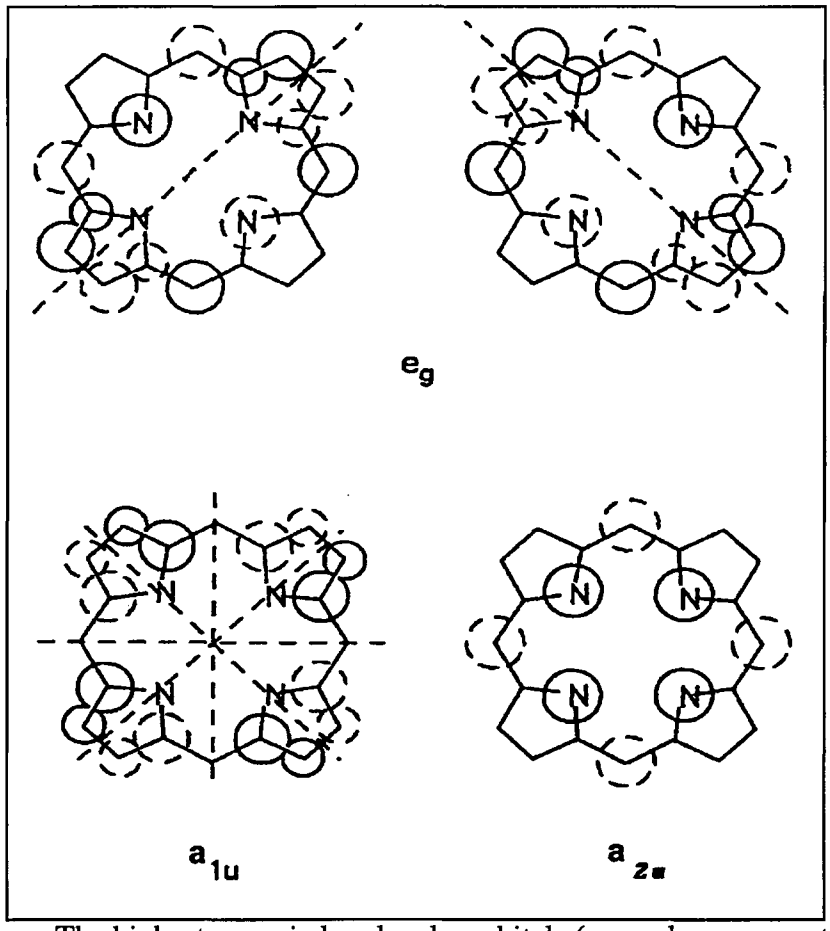

Figure 7 The highest occupied molecular orbitals (a_{1u} and a_{2u} symmetry) and the lowest unoccupied molecular orbital (e_g symmetry) of metalloporphyrins (Reproduced from Suslick, K. New. J. Chem., 1992, 16, 634).

In this model the four orbitals are porphyrin π and π^* orbitals; the two highest occupied molecular orbitals (HOMOs) of a_{1u} and a_{2u} symmetry, and the two lowest unoccupied molecular orbitals (LUMOs) are of e_g symmetry (Figure 7). Two major absorbances arise from coupling of the two transitions between the HOMOs and the LUMOs (Figure 7). A linear combination of the two transitions occurs with reinforcing transition dipoles, resulting in a very intense absorption.

Further characteristic peaks are found in heme at ~570 nm, though of a less intense nature than that of the Soret peak. This is a result of ligand to metal charge transfer (LMCT) and d→d* electronic transitions (Figure 8) in the hemoprotein caused by the ligation of the sulfur containing residue to the heme prosthetic group.[7,8]

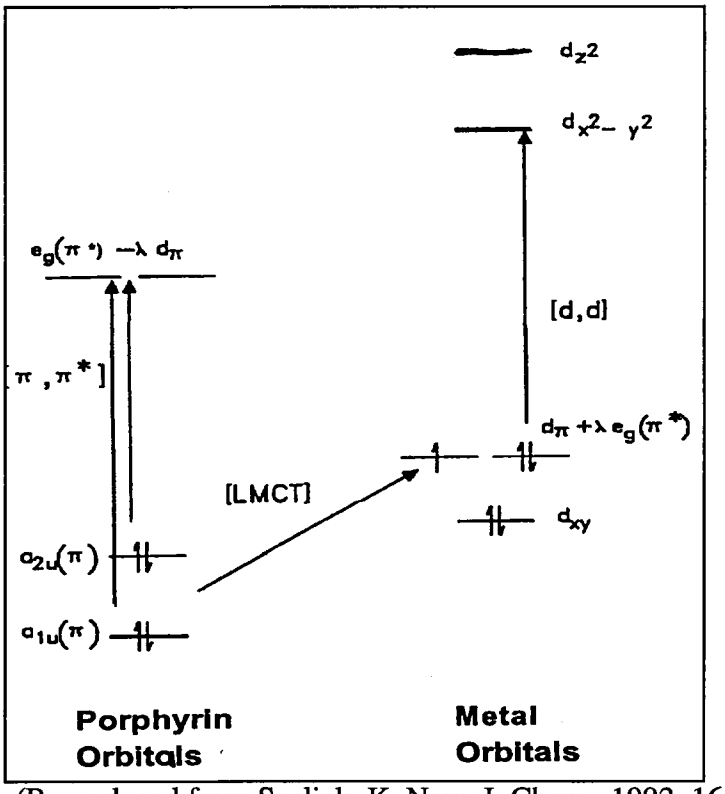

Figure 8 (Reproduced from Suslick, K. New. J. Chem., 1992, 16, 634)

This was first suggested by Mason,[8] and later the Fe-S stretch was proven by Champion[9] when a perturbation was observed in the Fe-S stretch frequency after direct sulfur and iron isotope substitution. Substrate (and carbon monoxide) free P450 exhibits a UV Soret absorption maximum at approximately 420 nm. This is associated with the low-spin state of Fe^{3+}. Spectral,[5] NMR[10] and crystallographic[11] data indicate that a water molecule forms a sixth axial ligand of the Fe^{3+} in the substrate-free form (Figure2, the red ligand *trans* to the thiolate), thus stabilising the low-spin state of the iron.

There are three types of ligand binding, which may be identified by changes in the UV spectrum. These are known as type I, type II and reverse type I.

Type I binding is associated with the binding of a molecule that is a substrate for P450 oxidation (Figure 9). It is identified by a reduction in the Soret absorption band at 420 nm, and a corresponding increase in a maximum at 390 nm, with an isobestic point at 407 nm. This is indicative of a change from a low-spin state to a high-spin state of the Fe^{3+}. X-ray crystallography of substrate-bound complexes of the enzyme[3] shows that the iron-ligated water molecule is displaced in these cases, changing the Fe^{3+} from a six-fold to a five-fold co-ordination state. The iron is also seen to move out of the plane of the heme.

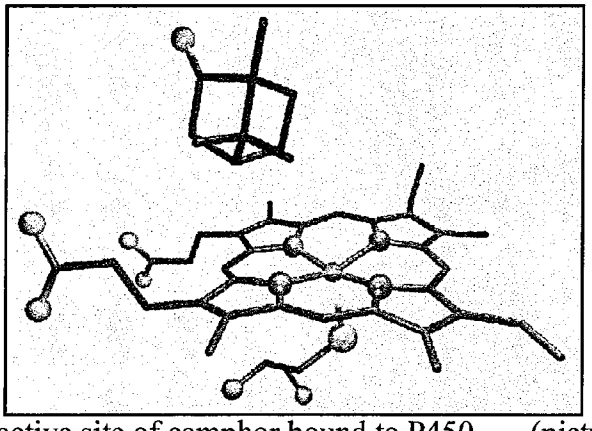

Figure 9 The active site of camphor bound to $P450_{CAM}$ (picture reproduced from http://www.tcm.phy.cam.ac.uk, site accessed June 2002).

A type II spectrum is characterised by an increase in the absorption between 425 nm and 435 nm and a decrease in the 390 nm maximum with an isobestic point at approximately 419 nm.[12] This is correlated with an increase in the low-spin character of the Fe^{3+}. This spectral change is associated with the interaction of inhibitors, which

bind directly to the Fe^{3+}, replacing the water molecule as the sixth axial ligand (Figure 10).[13,14]

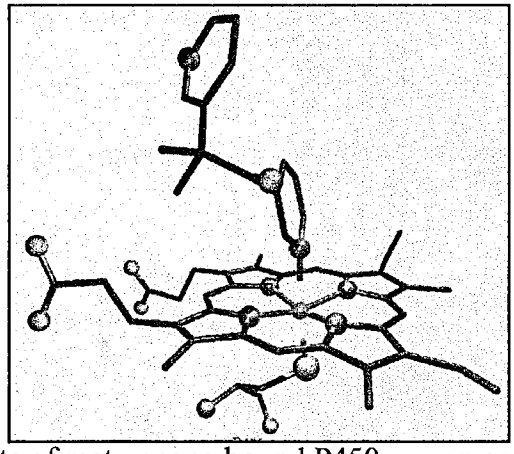

Figure 10 The active site of metyrapone-bound $P450_{CAM}$, an example of an inhibitor-bound system. Note that the inhibitor binds directly to the heme replacing the water molecule as the sixth axial ligand.

The reverse type I spectrum, not surprisingly, is a 'mirror image' of the type I spectral change, with an increase in the 420 nm band and a decrease in absorbance at 390 nm. This is similar to a type II change, except that there is no shift in the location of the maxima. The exact nature of this interaction is not known and it may be that the ligand binds to a different site on the enzyme.

Figure 11 displays typical type I and type II absorption traces. These are difference spectra; that is the difference in absorption between that of a reference sample and that of the sample to be recorded. This accounts for the occurrence of negative absorption in the spectrum due to lower absorption at specific wavelengths compared to that of the reference.

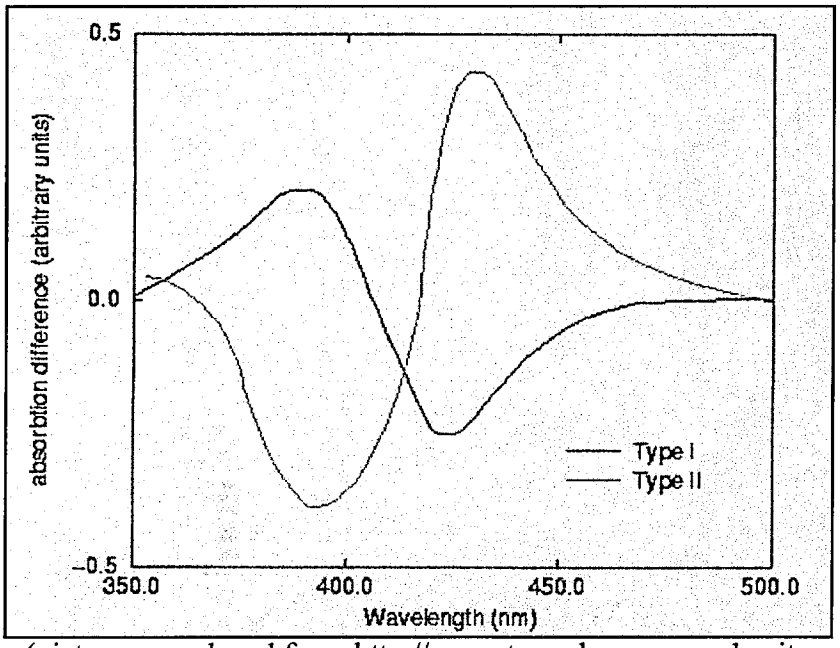

Figure 11 (picture reproduced from http://www.tcm.phy.cam.ac.uk, site accessed June 2002)

1.3 Nomenclature

There are several distinct types of redox proteins and enzymes, which have historically been termed cytochromes. It appears that the only feature in common between these is the possession of a heme group, with the primary, secondary and tertiary features being quite different. Cytochrome P450 may be regarded as a heme-thiolate protein. Other cytochromes tend to possess at least one histidine residue that ligates to the heme iron. Thus, the P450 family can be separated into a unique group of its own with corresponding nomenclature.

There is a systematic naming of P450s that has been in place since 1989. The symbol CYP is used as an abbreviation for cytochrome P450, which is italicised when referring to the gene. An alphanumeric designation is used in the naming of P450 families, subfamilies and individual proteins. For example, CYP2A1 implies

cytochrome P450 family 2, subfamily A, protein 1. The nomenclature of new P450 sequences is determined by their similarity to others previously assigned. There is a general rule that assignment of a P450 gene requires a ≤40% identity between a P450 in one family and that in another family, and that there is a >40% identity between subfamilies of a given P450 family. Table 1 shows a summary of P450 superfamily nomenclature.

Table 1 Cytochromes P450 and the species they metabolise

CYP	Functionality or species
1-3	Metabolism of foreign compounds
4	Metabolism of long chain fatty acids
5	Thromboxane biosynthesis
6	Insect forms
7	Steroid forms
8	Prostacyclin biosynthesis
9	Insect forms
10	Mollusc forms
11-21	Steroid biosynthesis
24	Vitamin D_3 metabolism
26	Retinoid metabolism
27	Bile acid biosynthesis
51-70	Fungal forms
71-100	Plant forms
101-140	Bacterial forms

1.4 Catalytic cycle of P450

The catalytic cycle of P450 (Scheme 1) has been well researched over the past 30 years. Even so, this cycle is still not completely understood, and the species in brackets have not been fully characterised. Nevertheless, the cycle affords the best model for the balancing of electrons and nuclei throughout the oxidation reaction.

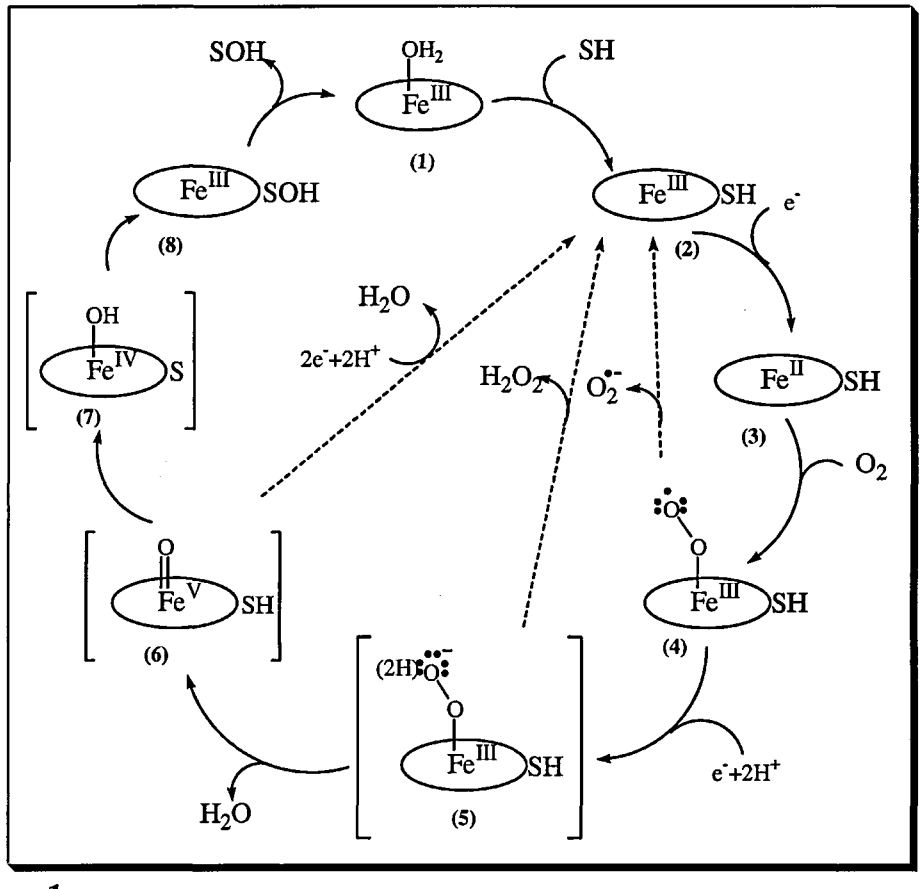

Scheme 1

The first steps of the catalytic cycle, involving substrate binding, electron transfer, and dioxygen association, have been fairly well characterised because these intermediates are fairly stable and have a UV/visible spectrum that makes them amenable to investigation.

Beginning the catalysis at **(1)**, with the substrate-free, oxidised (Fe^{3+}) state, this has a redox potential of about –300 mV with the heme iron in the low-spin six co-ordinated form. Solution X-ray of the substrate-free cytochrome has unambiguously documented water or OH^- as the sixth ligand. In **(2)** the binding of the substrate (SH) results in displacement of water from the active site and a change in the redox potential from –300 mV to about –170 mV. Hence substrate-bound P450 becomes more easily reduced. Substrate binding to P450 causes a spectral change related to spin state conversion of the heme iron. This is caused when **(1)**, a low-spin six co-ordinate heme iron, loses water upon addition of substrate to form a five co-ordinate high-spin state, with the iron out-of-plane of the porphyrin ring.[15,16]

An electron transfer then occurs to reduce ferric heme to ferrous heme. This electron is made available from NADH or NADPH. However, NAD(P)H prefers to donate two electrons. Therefore these electrons are transferred to an electron transport protein, then to a co-enzyme which can transfer single electrons. This reduction of **(2)** to **(3)** results in the heme having a higher affinity for dioxygen to bind as the sixth axial ligand,[17] to form **(4)**. Oxygen binding forms a low-spin heme peroxy radical or ferric superoxide species **(4)**. This has been characterised by Sligar[18]. If **(4)** is reduced further by electron transfer, then formation of **(5)** can occur, which, upon addition of two protons and loss of water, results in **(6)**, a high valent iron-oxo species. This species, drawn in Scheme 2 as **(10)** can also be described by the more stable resonance form **(9)**[19] or the other forms shown in Scheme 2.

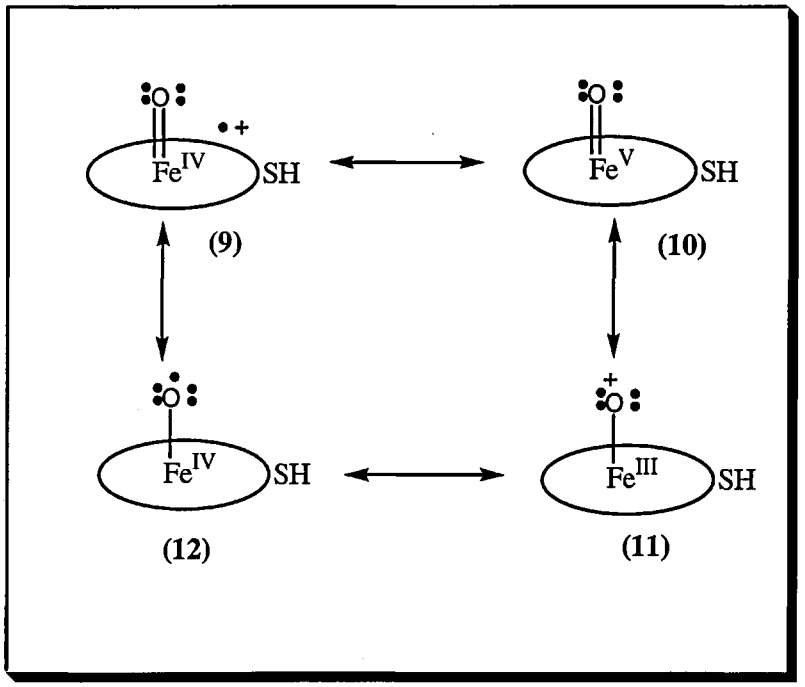

Scheme 2

The abstraction of an H atom from the substrate by this species gives the formation of **(7)** and a substrate radical species. This collapses *via* oxygen rebound to form **(8)**. It is not known if any of the bracketed species exist and it is possible that **(5)**, **(6)**, **(7)** may proceed through a concerted mechanism up to formation of the ferric alcohol complex **(8)**. This oxygenated substrate may then be released to regenerate the initial state of P450.

1.5 Enzymology of cytochrome P450 reductase

Mammalian NADPH-cytochrome P450 reductase (CPR) was first identified by Horecker in 1950.[20] These studies identified it as a flavoprotein (a group of enzymes containing flavin bound to protein and acting as dehydrogenation catalysts in biological reactions), although it was not recognised until the studies of Lyanagi and

Mason[21] in 1973 that the enzyme contains both FAD (a coenzyme of some flavoproteins) and FMN (a yellow crystalline phosphoric ester of riboflavin that is a coenzyme of several flavoprotein enzymes) in equal proportions. The role of the flavins in electron flow through the enzyme was elucidated in a series of studies from Coon,[22] that were based on the redox mid-point potentials determined by Lyanagi et al.[23] These studies established that FAD is the electron acceptor flavin from NADPH and that FMN is the electron donor to acceptor proteins such as the cytochromes (Scheme 3).

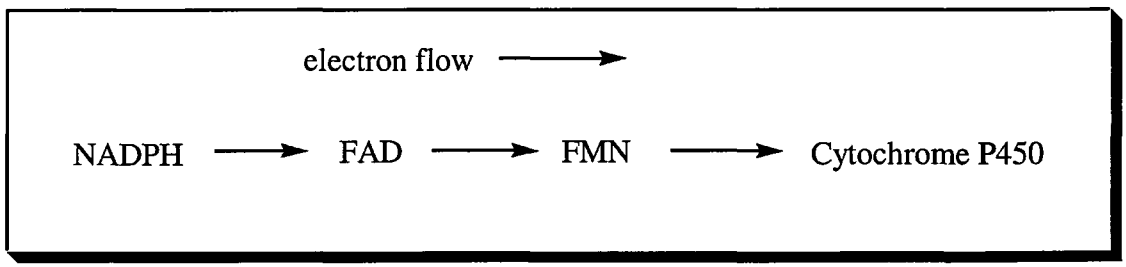

Scheme 3

Under physiological conditions the enzyme was proposed to cycle between 1- and 3-electron reduced states as shown below (Scheme 4):

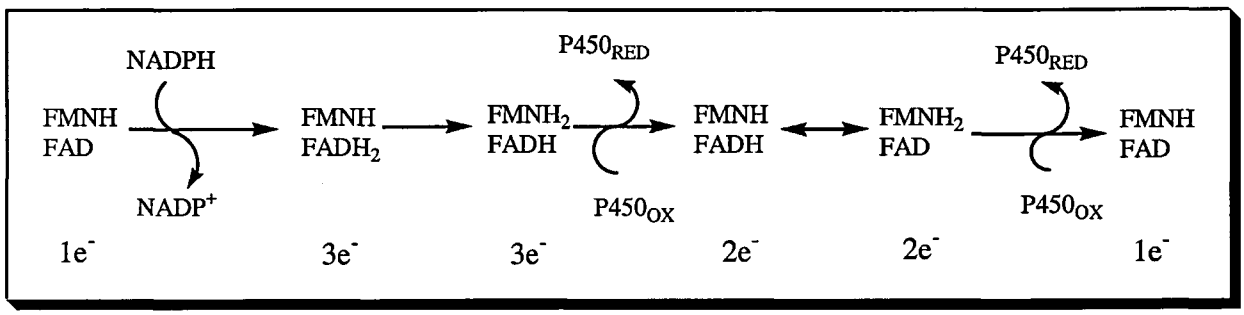

Scheme 4

1.6 Biomimetic oxidations catalysed by transition metal complexes

Metalloenzymes catalyse a host of biological oxidation reactions that are crucial to life processes. Cytochrome P450 is an oxidoreductase that activates molecular oxygen (O_2) and incorporates one of the oxygen atoms into a wide variety of biological substrates, with concurrent two-electron reduction of the other oxygen atom to water.[5] These oxygenation reactions metabolise steroids and prostaglandins, effect drug and xenobiotic detoxification and can bring about carcinogen activation. The active site of this enzyme has been determined from X-ray crystal structures[5] and has been shown to be extraordinarily simple, with an iron protoporphyrin IX (heme) (Figure 12) buried deep in a protein scaffold.

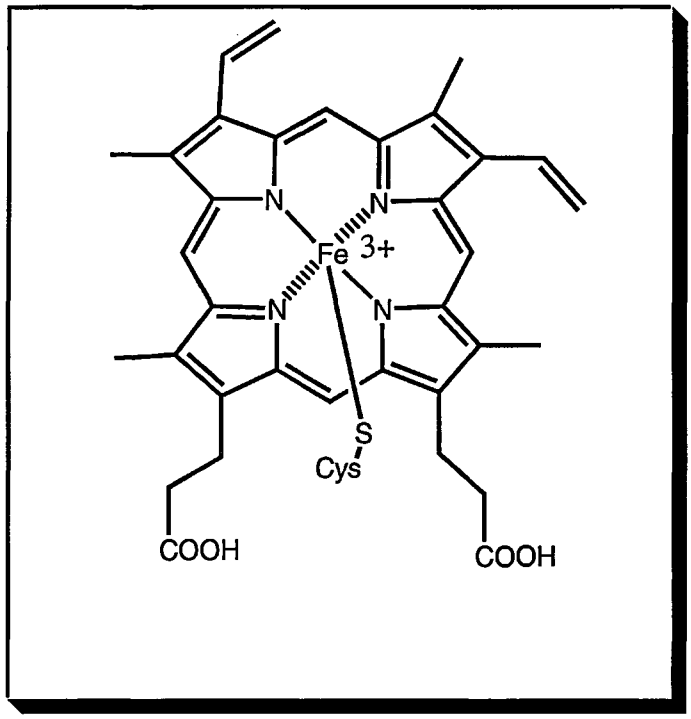

Figure 12

The heme has a cysteinate thiolate as the fifth ligand and an open co-ordination site to bind and activate molecular oxygen.

Small, synthetic active-site analogs are an invaluable tool in the study of metalloproteins. These so-called "enzyme models" can be used to obtain information about fundamental aspects of structure, reactivity and mechanism and are suitable for spectroscopic study of putative reactive intermediates.[24] Enzyme models can provide insights into aspects that are not so easily attainable from the study of the protein itself. The advantages of enzyme models are, first of all, that they are readily available in large quantities, whereas the natural systems are often difficult to isolate. Secondly, the study of mechanism and intermediates in model compounds can provide a basis for postulating biological reaction pathways and possible intermediates, or can be used to validate existing proposals. Finally, through systematic ligand variation information about structural and electronic aspects governing the reactivity can be obtained. Moreover, this may lead to new generations of biomimetic catalysts with improved selectivity, reactivity and stability.

Studies using metalloporphyrins as models for cytochrome P450 have afforded important insights into the nature of these enzymatic processes. The first synthetic system used to model the chemistry of cytochrome P450 was Fe(III)TPP(Cl) using iodosylbenzene as the oxidant. This was used to carry out epoxidation of olefins and the hydroxylation of hydrocarbons.[25] Many other metalloporphyrin-catalysed studies have been carried since that time. The first systems to be used employed metalloporphyrins containing metals such as iron, manganese, cobalt and chromium, and used oxygen atom donors such as peroxides, PhIO and NaOCl. Using these, it has been possible to generate species that give the same reactivity as in the O_2 system, a pathway known as the "peroxide shunt" (Scheme 5).[26]

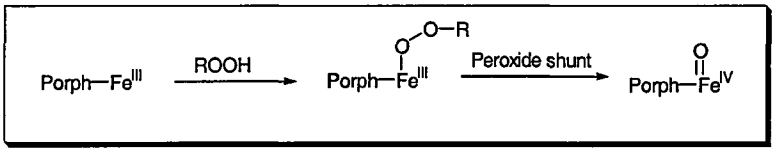

Scheme 5

The following (Table 2) show a selection of metalloporphyrins used in model studies.

Table 2 Different metalloporphyrins used in model studies

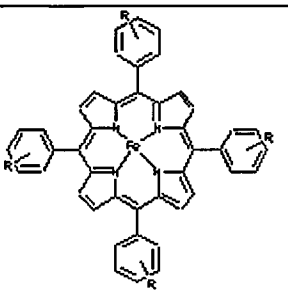

Metalloporphyrins	Substituent (R)		
	o	*m*	*p*
(TPP)Fe^{3+}(Cl)	H	H	H
(TPP)Cr^{3+}(Cl)	H	H	H
(TPP)Mn^{3+}(Cl)	H	H	H
(F_{20}TPP)Co^{3+}(Cl)	F	F	F
(Cl_8TPP)Fe^{3+}(Cl)	Cl	H	H
(Cl_8TPP)Mn^{3+}(Cl)	Cl	H	H

Much effort has been taken to improve the catalytic reactivity of iron porphyrin complexes[27,28]. An important finding for this was that the introduction of electron withdrawing substituents (eg F) into the phenyl groups of porphyrin ligands enhanced the reactivity of the iron porphyrins greatly and diminished the oxidative degradation of the porphyrin ligands dramatically[29-31]. Even more effective iron porphyrin catalysts were achieved when the porphyrin ring was fully halogenated[32]. These highly

electron-deficient iron porphyrins turned out to be remarkable oxidation catalysts with fast reaction rates and high product yields.

1.6.1 The metalloporphyrin-iodosylbenzene system

Organoiodine(III) species have unique properties and structures and are commonly described as hypervalent, owing to the increased valency of the iodine atom[33]. Iodosylbenzene (PhIO) is, perhaps, the most widely known and utilised organoiodine(III) reagent. Not only does this readily prepared reagent serve as a starting material for the synthesis of a wide variety of other organoiodine(III) species, but it also acts as an effective oxidant for many substrates[34-36]. Its oxidising ability is greatly extended when it is used in conjunction with appropriate transition metal catalysts, and it also has found extensive application as a primary oxo source for hydrocarbon oxidations and biomimetic studies[37,38]. Groves[25] has shown that oxidation reactions carried out by synthetic porphyrins in the presence of iodosylbenzene have similar mechanistic features to those of P450. There are two proposed mechanisms for the hydroxylation of hydrocarbons:

(1) oxygen rebound from the iodosylbenzene to the substrate *via* an iron-oxo intermediate **(13)**, and

(2) oxygen activation by the co-ordination of iodine to the porphyrin **(14)**.[39]

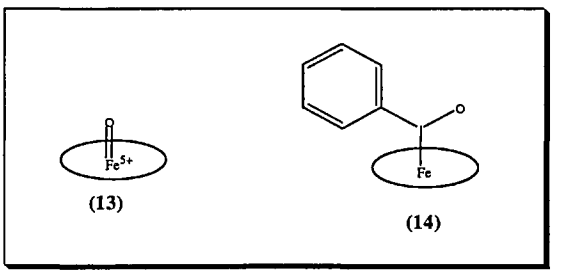

Scheme 6

The exact mechanism that is followed is still under investigation, but is most likely that of oxygen rebound.[25] For the hydroxylation of hydrocarbons this gives a mechanism as shown below (Scheme 7).[28]

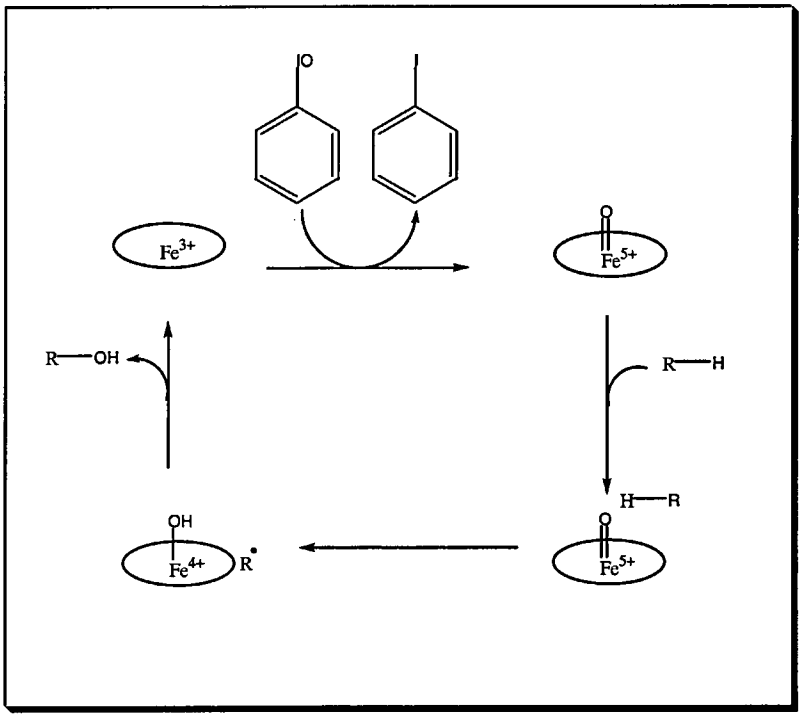

Scheme 7

1.6.2 The metalloporphyrin-alkylhydroperoxide system

Studies of reactions utilising metalloporphyrins with iodosylbenzene and peracids have provided important insight into the nature of oxidations occurring from hemoproteins such as P450, peroxidases and catalase. Although PhIO is a useful mechanistic tool, it is of limited biological relevance since it doesn't occur in plant or animal metabolism. In contrast, hydrogen peroxide and fatty acid hydroperoxides are widely distributed in the plant and animal kingdom, and support a variety of oxidations by heme proteins. This makes the study of alkylhydroperoxides with metalloporphyrin systems an interesting, and relevant, area of research.

Similar to the I=O bond in iodosylbenzene, the O-O bond in hydroperoxides is cleaved heterolytically by the iron porphyrin complex resulting in a high valent iron(IV)-oxo porphyrin cation radical intermediate ($O=Fe^{IV}$-$porph^{+\cdot}$). Alternatively, unlike iodosylbenzene, homolytic cleavage of the O-O bond can also form $O=Fe^{IV}$-$porph^{+}$. Thus, the two proposed routes for O-O bond cleavage with hydroperoxides and metalloporphyrins are,

(1) heterolytic cleavage to form an $O=Fe^{IV}$-$porph^{+\cdot}$ complex (Scheme 8, pathway A)

(2) homolytic cleavage to form an $O=Fe^{IV}$-porph complex (Scheme 8, pathway B)

It is important to consider which of these routes is followed, because if the $O=Fe^{IV}$-porph complex is formed hydrogen abstraction from the substrate is not possible, but in its formation an alkoxyl radical species is formed in the homolytic breakdown of the hydroperoxide. The alkoxyl radical *is* able to abstract a hydrogen atom from the substrate.[40,41] However, the $O=Fe^{IV}$-$porph^{+\cdot}$ complex is able to abstract a hydrogen atom from the substrate forming a Fe^{IV}-OH species that hydroxylates the carbon centred radical formed.[10,42]

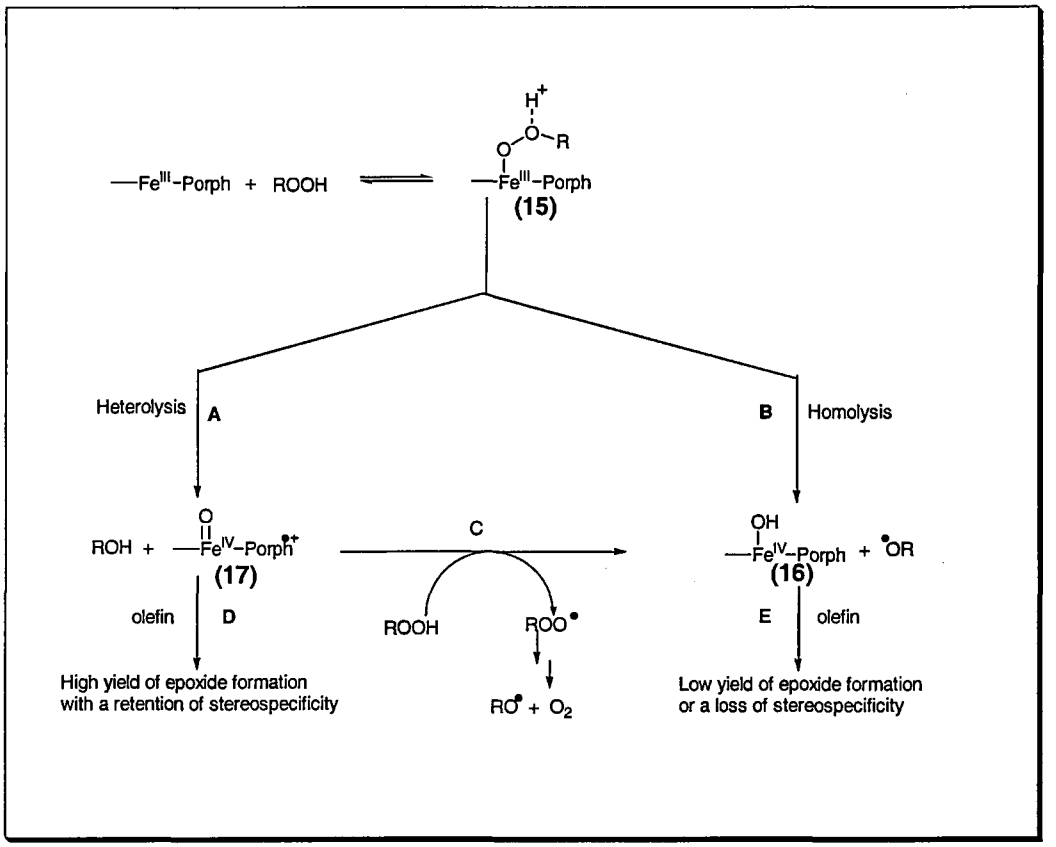

Scheme 8

Traylor has proposed that heterolytic cleavage of the O-O bond in **(15)** occurs to give the formation of **(17)** as the reactive species in olefin epoxidation.[28,42-45] This has been shown in protic alcohol solvents such as MeOH, with the protic solvents being proposed acid catalysts[46].

Bruice in contrast, has provided evidence that the initial step of the O-O bond cleavage of **(15)** in aqueous or aprotic solvents is homolytic, resulting in the formation of a ferryl-oxo complex **(16)**[47-49]. Several other groups also support the occurrence of O-O bond homolysis in aqueous and aprotic solvents. Traylor has proposed that product distributions may be accounted for by initial heterolytic cleavage of the O-O bond, with a subsequent side reaction between **(17)** and ROOH taking place at a high rate

(Scheme 8, Pathway A followed by pathway C). This would result in the expected product distribution from O-O bond cleavage.

Further studies by Nam have shown that the hydroperoxide bond is cleaved both homolytically and heterolytically in aqueous solution and in protic solvents. The ratio of each depends upon conditions, such as:

(1) the electronic nature of the iron porphyrin complexes, where iron porphyrins containing electron deficient porphyrin ligands result in an increase in heterolytic cleavage, and electron rich porphyrin ligands give an increase in homolytic cleavage, and

(2) the alkyl substituent of the hydroperoxide, with electron-donating *tert*-alkyl groups tending to give O-O bond homolysis and electron withdrawing groups, such as acyl, facilitating O-O bond heterolysis.[50-52]

2 Reactions catalysed by P450

2.1 Aliphatic hydroxylation

Hydroxylation of unactivated alkanes was initially thought to undergo a concerted insertion process (Scheme 9).

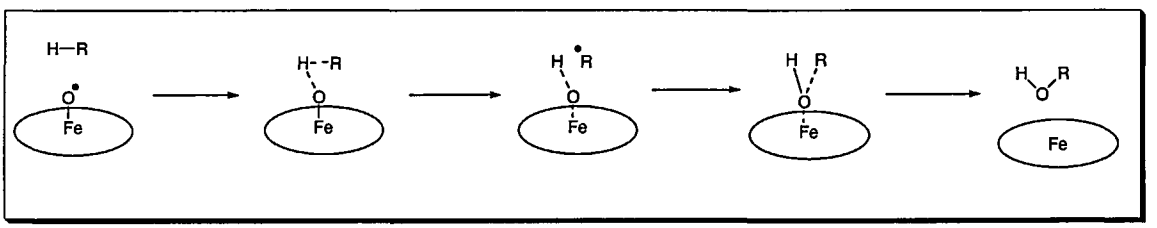

Scheme 9

This mechanism was proposed because of low deuterium isotope effects (k_H/k_D <2)[53] (Scheme 10).

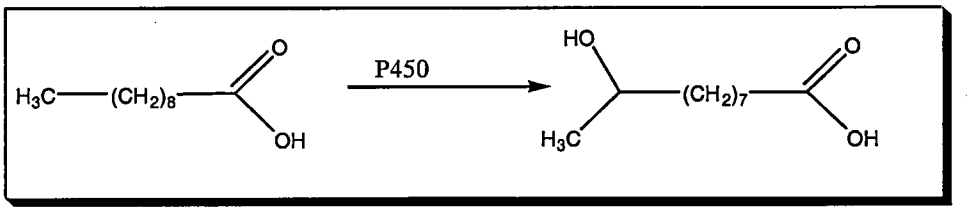

Scheme 10

However these results were shown to be erroneous by Hjelmeland and Groves,[54,55] who showed that the isotope effect on, for example, norbornane hydroxylation was much larger (k_H/k_D >11). These differences arise from the fact that the earlier studies utilised **intermolecular** isotope effects. These are obtained by comparing rate differences using unlabelled *versus* deuterium labelled substrates. However, if the C-H bond is not involved in the primary rate-determining step then the difference in rates between the isotopically labelled substrates will be small. The studies of Hjelmeland and Groves were carried out using a technique that measured the intramolecular isotope effect. This involves hydroxylation of a substrate containing two identical and symmetrical sites, one of which incorporates deuterium (Scheme 11).

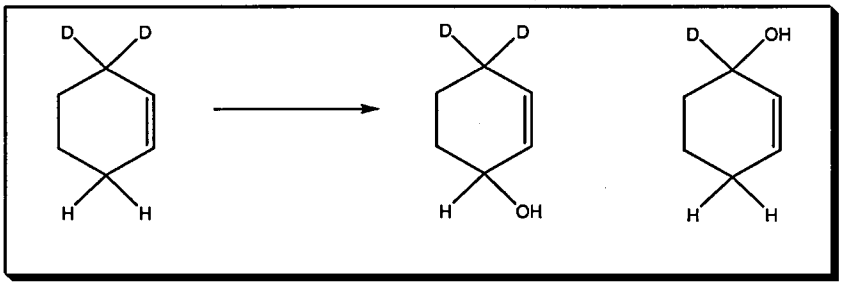

Scheme 11

Now the extent of C-H *vs.* C-D bond cleavage may be determined more accurately. The large deuterium isotope effect observed suggests that C-H bond cleavage is a chemically important step that is masked by other processes. The size of the isotope

effect suggests a two-step mechanism, either involving a radical pathway or *via* the formation of a carbocation.

Evidence for a two-step mechanism can be observed from the stereochemical scrambling of deuterated substrates incubated with P450. An appropriate example of this is with *exo*-2,3,5,6-tetradeuteronorbornane incubated with CYP2B4 (Scheme 11).[55] In this reaction four norbornanols are produced. This shows that the reaction does not proceed with retention of configuration and so supports a two step mechanism

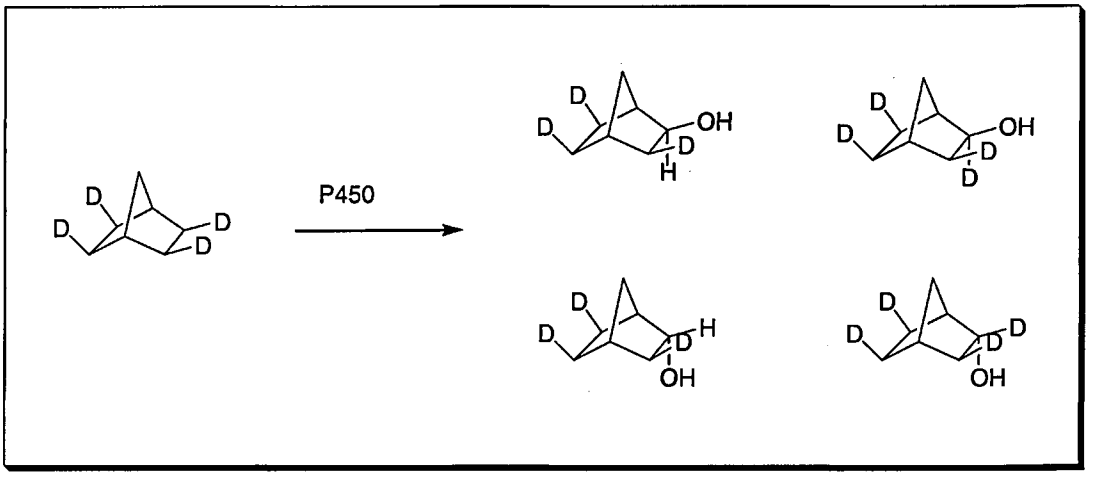

Scheme 12

If the reaction takes place *via* a radical mechanism, then abstraction of a hydrogen atom from the substrate will give a heme-bound hydroxyl radical and a carbon-centred radical (see Scheme 13). These two may then combine to form the hydroxylated product **(18)** a process termed **oxygen rebound.**[56]

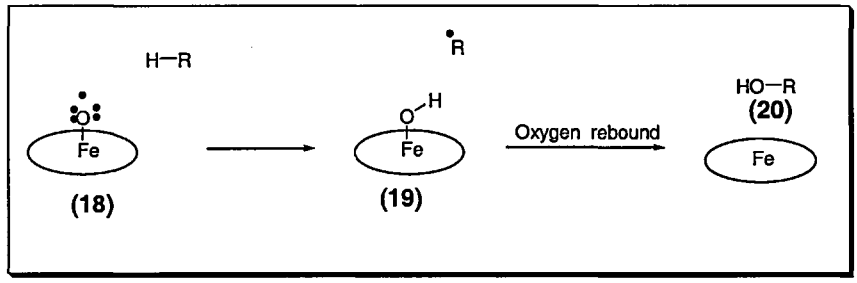

Scheme 13

Evidence to support a pathway involving formation of the carbon-centred radical comes from the use of ultrafast radical clock probes (Scheme 14)[57]. In this case a strained cyclopropyl compound, *trans*-1-methyl-2-phenycyclopropane **(21)**, whose radical rearranges at the remarkable rate of 3×10^{11} s^{-1}, was oxidised using P450 and three oxidation products **(23)**, **(24)** and **(26)** were observed (Scheme 14). Compound **(23)**, the product of simple hydroxylation is formed *via* pathway A, through the formation of the cyclopropylcarbinyl radical intermediate **(22)**. The latter can either undergo oxygen rebound to form **(23)** or rearrangement followed by oxygen rebound to form **(26)**. Pathway B accounts for the third product. Use of the perdeuteriomethyl analogue leads to an increase in the oxidation at the phenyl ring. This process is called **metabolic switching**, that is deuteration at one site changes the partition between two metabolic pathways due to the isotope effect on C-H bond cleavage at the first site.

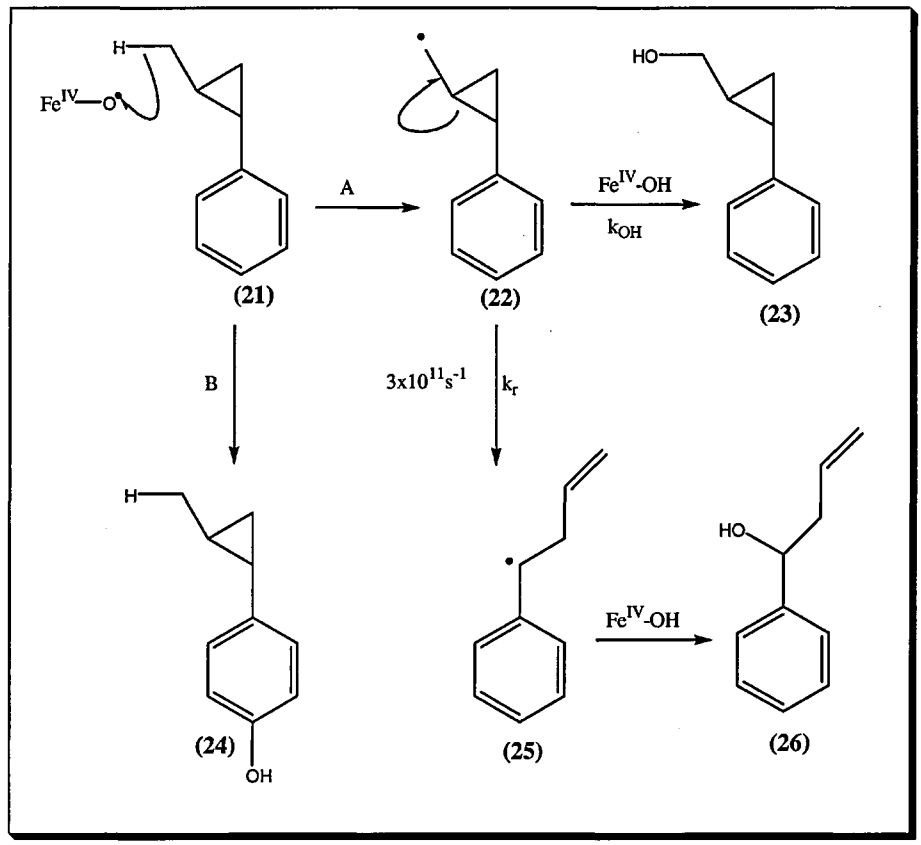

Scheme 14

Scheme 15 shows the most likely mechanism with oxygen rebound for the alkane oxygenation by heme-dependent monooxygenases.

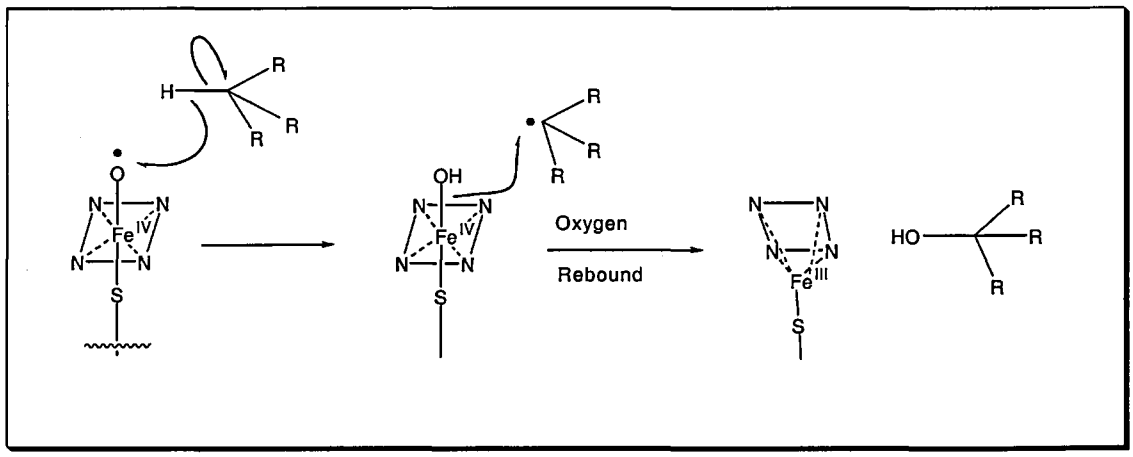

Scheme 15

2.2 Alkene epoxidation

Alkenes are oxidised by cytochrome P450 to epoxides. This can be explained by a radical mechanism (Scheme 16) similar to that for alkane hydroxylation. This mechanism shows radical addition to the π-bond of the alkene to give **(27)**. This collapses to the epoxide **(28)** leaving a high-spin ferric heme.

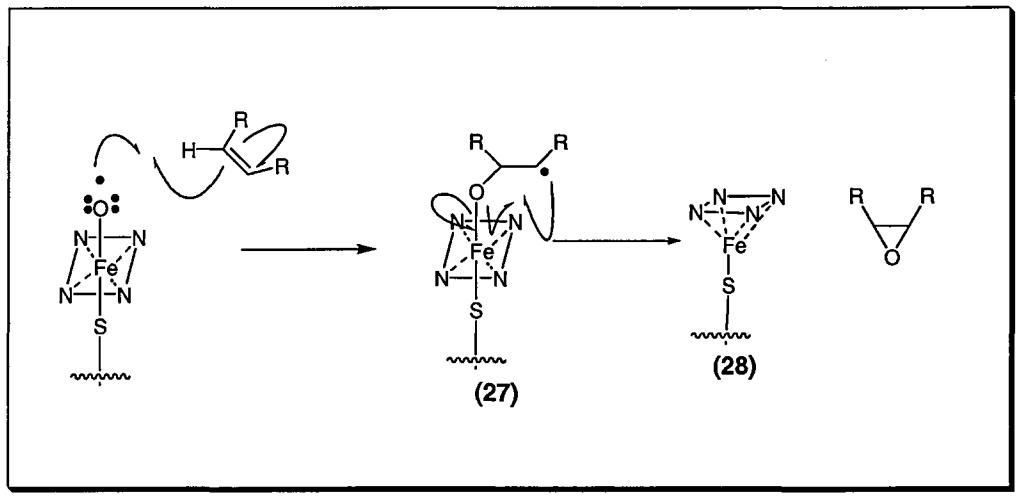

Scheme 16

This simple picture of alkene epoxidation may not tell the true story. Spectroscopic data from model studies have indicated that an intermediate is formed on the way to epoxide formation (Scheme 17). Groves has suggested either a π-complex **(29)** or a oxametallocycle **(30)** for this intermediate.[58]

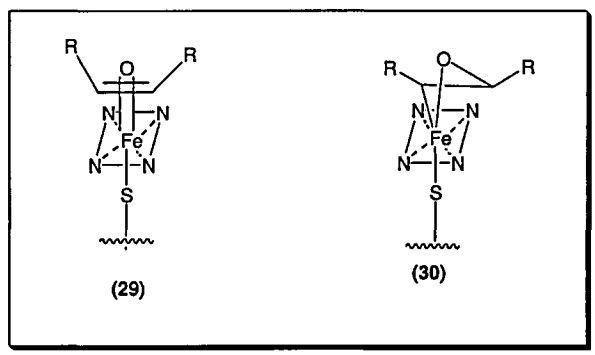

Scheme 17

Bruice, alternatively, has suggested epoxidation may involve a charge transfer complex between the iron-oxo species and the alkene followed by concerted epoxidation.[35,59]

With the epoxidation of terminal olefins it has been found that N-alkylation of the prosthetic heme group can occur[60]. It has also been observed, using *E*-1-deutero-1-octene, that:

(1) olefin stereochemistry is preserved, *i.e.* the oxygen and pyrrole-N add to the same face of the olefin, and

(2) the oxygen atom is delivered to the *re* face of the double bond[61]. This suggests a degree of stereochemical control in the reactions.

From the above results the following mechanism has been postulated (Scheme 18).

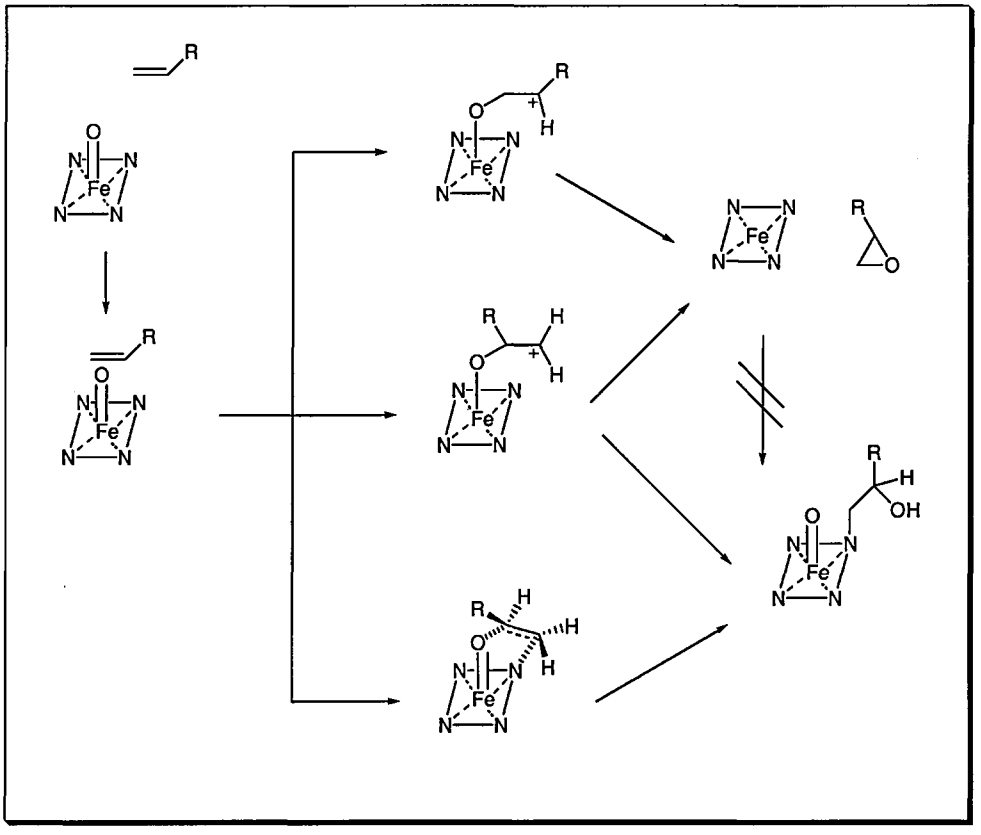

Scheme 18

2.3 Arene hydroxylation

Aromatic oxidation usually involves the introduction of a hydroxyl group (Scheme 19).

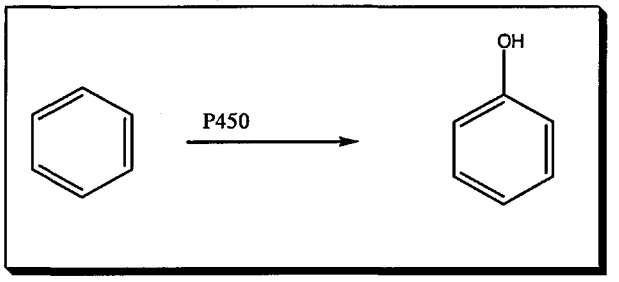

Scheme 19

This commonly involves epoxidation of the aromatic ring followed by epoxide ring opening, migration of a hydride to the carbocation generated, and tautomerisation of the ketone product formed, an overall process called the **NIH** shift. The NIH shift is evidenced by appropriate deuterium labelling (Scheme 20).

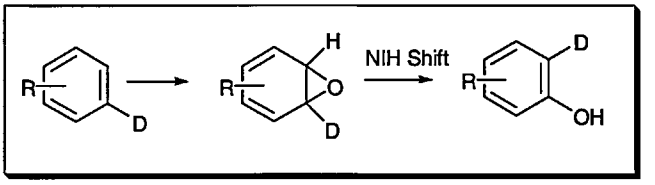

Scheme 20

The isolation of naphthalene 1,2-oxide **(32)** (Scheme 21) after P450 oxidation of naphthalene **(31)** is evidence in support of this pathway.

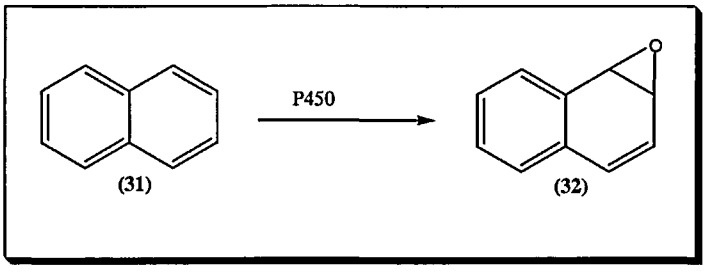

Scheme 21

Deuterium substitution does not markedly affect the hydroxylation rate because the hydrogen shift occurs after the rate-limiting enzymatic epoxidation step.

Decomposition of either [1-^{2}H] or [2-^{2}H] naphthalene 1,2-oxide yields 2-naphthol **(34)** having identical isotopic composition (Scheme 22), indicating a common intermediate **(33)** that originates from the two arene oxides.

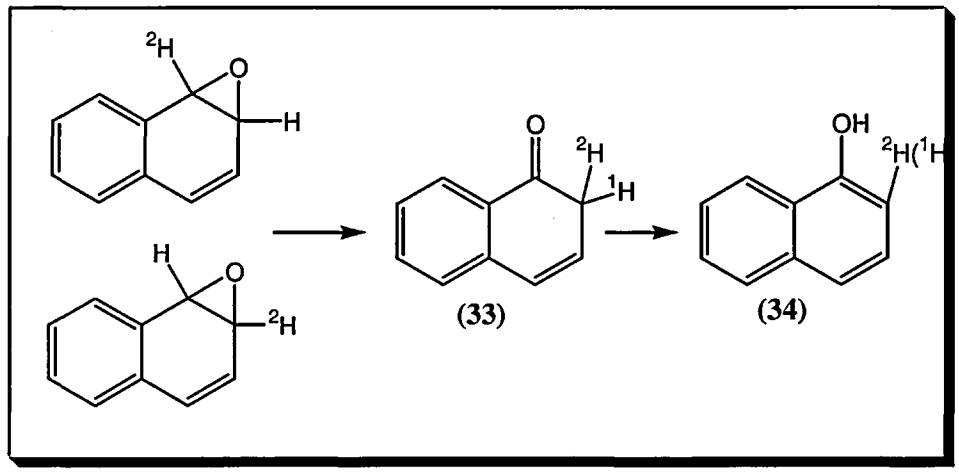

Scheme 22

Formation of **(33)** could come from two pathways (Scheme 23), one concerted (pathway A) the other stepwise (pathway B).

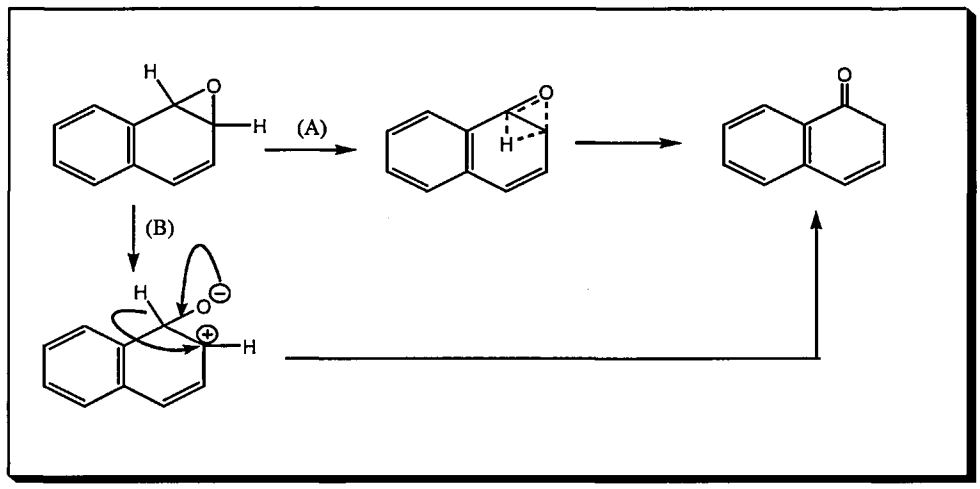

Scheme 23

Two pieces of evidence rule out the concerted pathway:

(1) there is no deuterium isotope effect observed,[62] and

(2) with various substituted arene oxides a Hammett plot shows a large negative ρ value, indicating that positive charge develops in the transition state.[63]

Other evidence, however, suggests that the arene oxide is not produced (but may be formed by an alternative pathway). The most likely route (Scheme 24) for the formation of phenols not involving the formation of arene oxides, involves oxidation of the π-system of the substrate to give a radical cation (**36**). The involvement of a singe electron transfer step is supported by a Hammett relationship between the rates of para-hydroxylation of monohalogenated benzene by CPY3B1 and the σ^+ values (which correlate to the $E_{1/2}$ values for benzene) of the substituents.[64] It should be noted however that oxidation of cyclopropylbenzene by cytochrome P450 gives 1-phenylcyclopropanol and phenol metabolites without detection of ring-opened products (Scheme 24).[65] This suggests no electron abstraction from the aromatic ring.

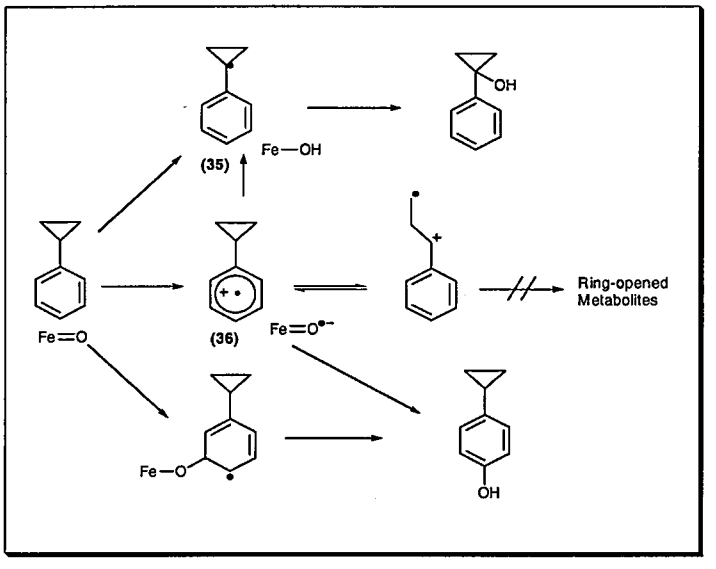

Scheme 24

For the moment, evidence for any mechanism is weak, the following (Scheme 25) gives an outline of the most likely routes.

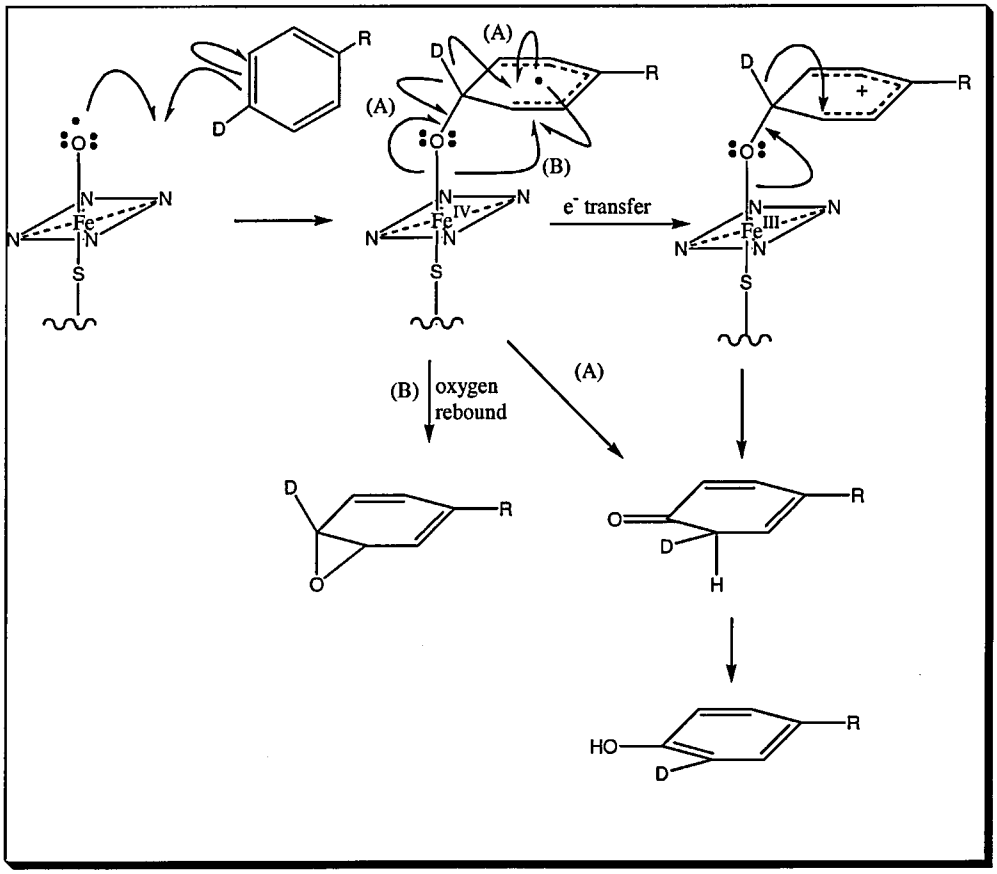

Scheme 25

2.4 Heteroatom oxidation

Sulfur-, phosphorus- and nitrogen- containing compounds may undergo oxidation to the corresponding S, P, or N-oxides. This happens particularly when there are no α-hydrogens adjacent to the heteroatom. The mechanism is believed to involve electron transfer followed by oxygen rebound (Scheme 26).

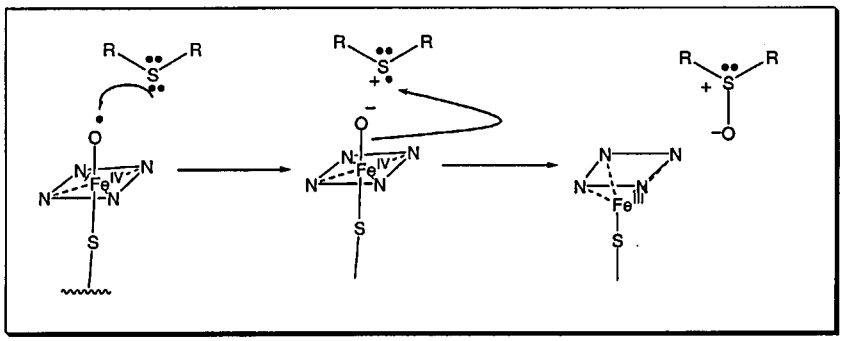

Scheme 26

Ethers on the other hand do not undergo oxygenation, since the oxygen atom has a much higher oxidation potential than the corresponding sulfur or phosphorus analogues[66-68]. The cytochrome P450 catalysed oxidation of alkylamines can result in N-oxygenation or N-dealkylation. The formation of N-oxides is not common but has been observed; N-dealkylation is the more common process. N-Oxide formation becomes the major pathway when the nitrogen has no α-hydrogen atoms available or the α-hydrogen atoms are inaccessible for abstraction (for example in strained cyclic systems).[69,70]

2.5 O-Dealkylation: ethers and esters

P450s are known to cleave the C-O bond of ethers through a mechanism that involves C-hydroxylation[71] to form a hemiacetal (Scheme 27).

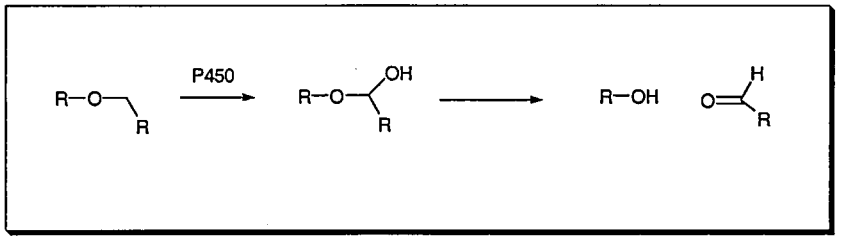

Scheme 27

A large deuterium isotope effect of ca. 8 is observed,[72] indicative of a hydrogen atom abstraction process.

Esters undergo a similar cleavage (Scheme 28). As esters are even more electron deficient than ethers they also will favour a hydrogen atom abstraction pathway, a deuterium isotope effect of ca. 8 confirming this.[73]

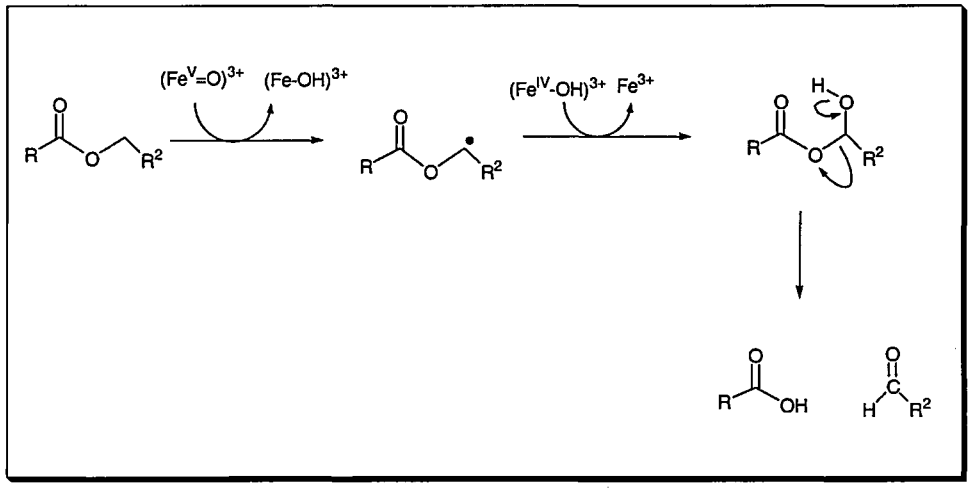

Scheme 28

2.6 N-Dealkylation: amines, amides and their differences

Like ethers and esters, amines and amides undergo P450 catalysed dealkylation (Scheme 29).

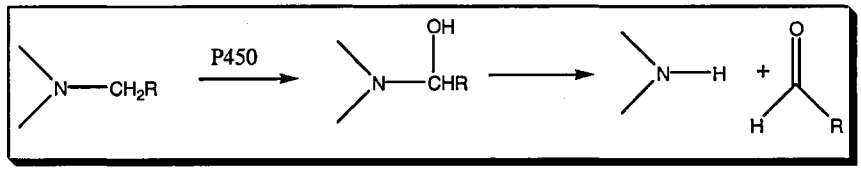

Scheme 29

In contrast to amides, amine P450-dependent metabolism has received extensive mechanistic attention. Both compounds generate N-dealkylation products through the formation of either a carbinolamine or carbinolamide, respectively. Because of these similarities it would be tempting to suggest that both follow the same metabolic pathway, but there are important physical and chemical properties to consider (Scheme 30).

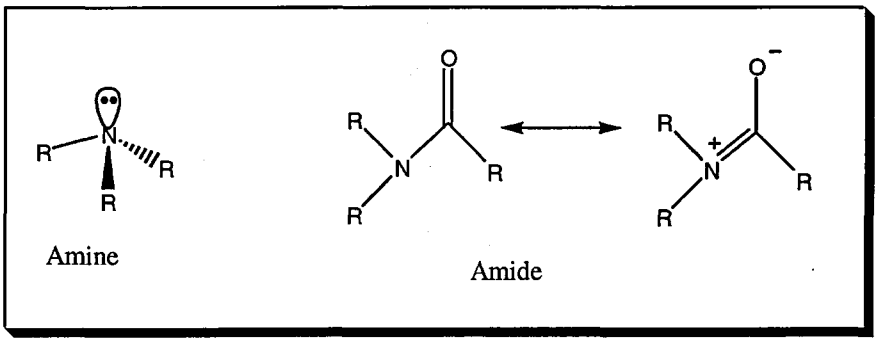

Scheme 30

Aliphatic amines have a non-bonding electron pair of electrons in an sp^3 orbital; these electrons are readily available for bonding and generally have low ionisation potentials (~7.8eV). This is not the case for amides, where the corresponding electron pair occupies a delocalised π-orbital that involves the carbonyl group; consequently these electrons are much less available and the ionisation potentials of amides (~9.1eV) are consequentially higher than those of amines.

Substituted amines bearing α-hydrogen atoms readily undergo cytochrome P450-catalysed N-dealkylation by a mechanism that is initiated by single electron transfer (Scheme 31).

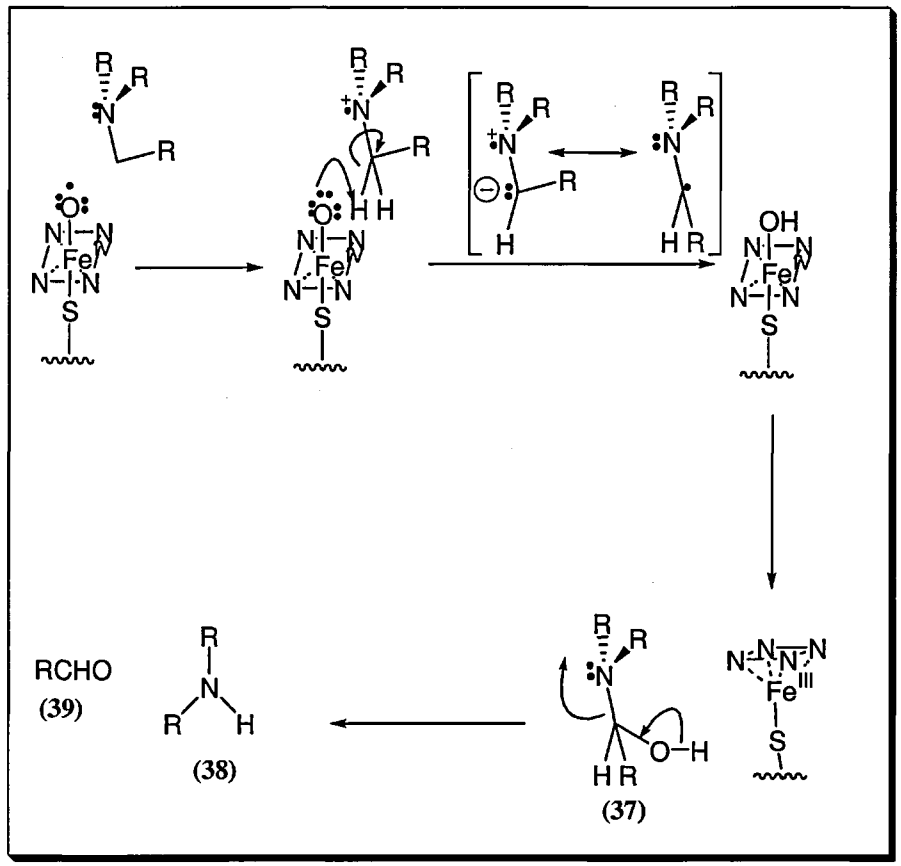

Scheme 31

From the so-formed amine radical cation proton abstraction can take place to afford a carbon-centred radical. Oxygen rebound at this stage gives a carbinolamine **(37)** that can readily decompose to the N-dealkylated amine **(38)** and corresponding aldehyde **(39)**.

Several lines of evidence support this mechanism:

- kinetic deuterium isotope effects for alkylamine dealkylation are small (1.3-3.0)[74], in contrast to O-dealkylation and carbon hydroxylation[73,75]
- cyclopropylamines are suicide substrates for P450 [76-79] (Scheme 32).

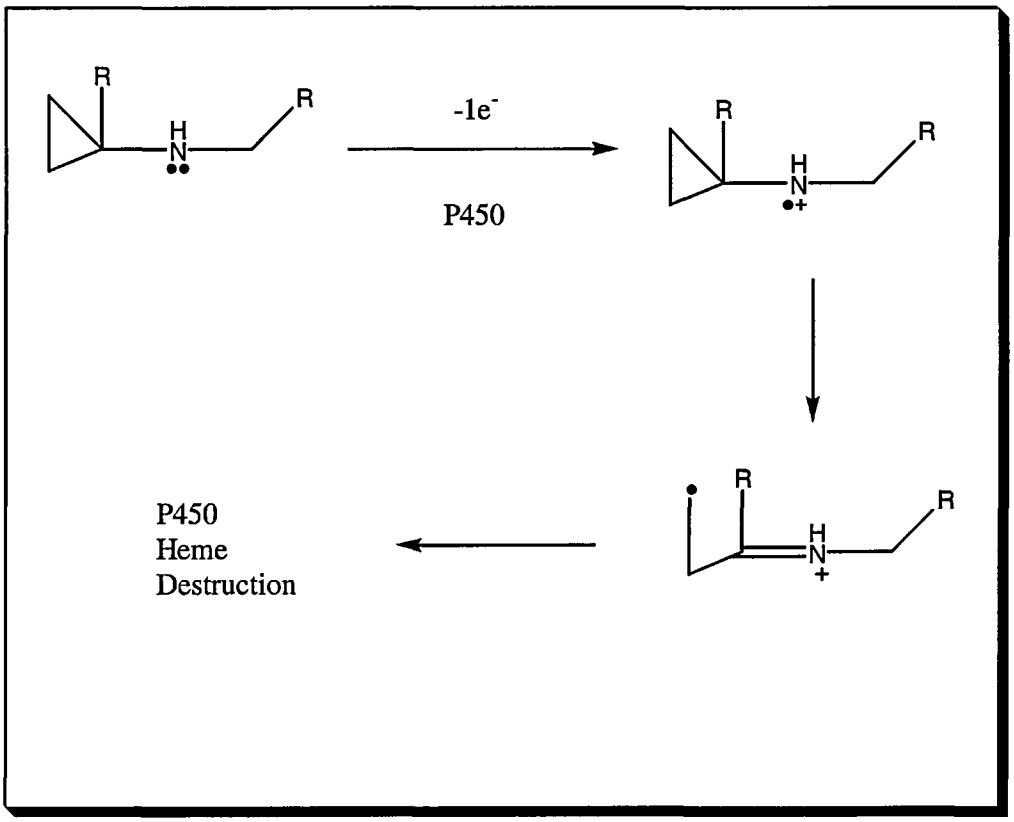

Scheme 32

Amides do not readily undergo one-electron oxidation but do exhibit N-dealkylation reactions. Scheme 33 outlines the possible routes of amide oxidation, They give relatively large kinetic deuterium isotope effects (k_H/k_D = 4-7).[78 80] Moreover, P450-mediated metabolism of N-cyclopropylamides does not lead to suicide activation of the enzyme, even though N-dealkylation occurs.[81] Taken together, these results suggest that N-dealkylation of amides involves direct hydrogen atom abstraction (path a) rather than nitrogen radical cation formation (path b, Scheme 33). This difference in mechanism must be related to the higher ionisation potential of amides as compared with amines.

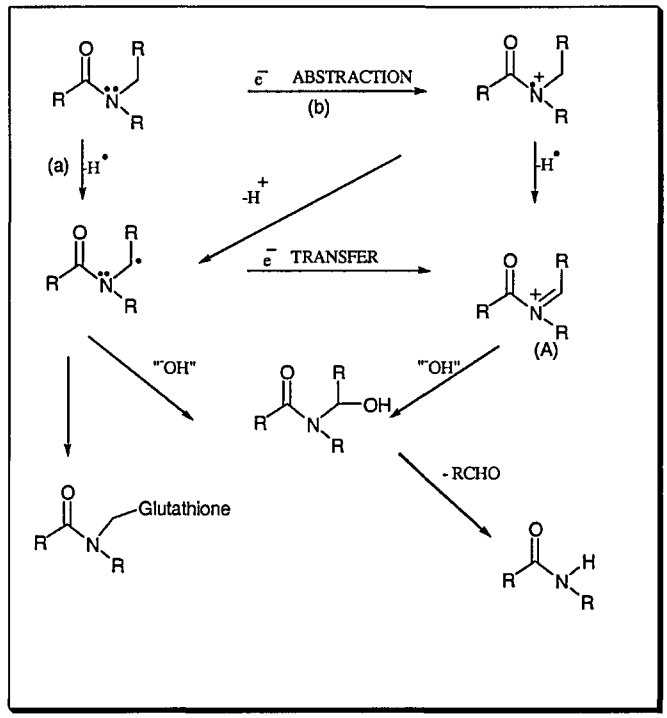

Scheme 33

2.7 Amide and amide-like solvents DMF, HMPA and DMPU

DMF, HMPA and DMPU (Scheme 34) are dipolar aprotic solvents that are used in large quantities both in industry and, to a lesser extent, research laboratories. Unfortunately, both DMF and HMPA have toxic properties, which has lead to the increasing use of the non-mutagenic DMPU as a 'safe' alternative. DMF and HMPA are pro-carcinogens, that is they require activation *via* oxidative metabolism to induce carcinogenic activity. During this metabolism, cytochrome P450 enzymes catalyse the removal of a methyl group by oxidative dealkylation. Toxicity is presumed to arise from the reactive intermediates formed during metabolism. One candidate for such an intermediate is the amide derived carbon-centred radical mentioned previously

(Section 2.6) and which has recently been intercepted using an intramolecular radical probe. However, all three dipolar aprotic solvents can potentially afford such an intermediate so the difference between DMPU on the one hand and DMF/HMPA on the other remains to be established.

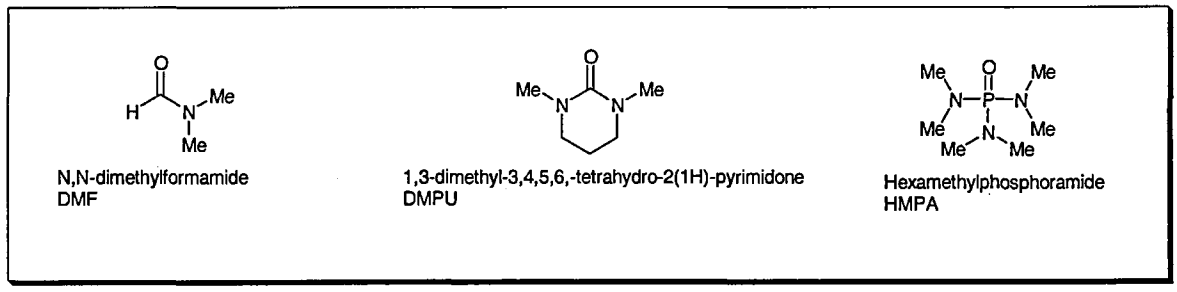

Scheme 34

Dimethylformamide

Dimethylformamide is a known toxic agent that can lead to gastric irritation, pancreatic disorders,[82] carcinogenesis,[82] and hepatotoxicity[82] and it is also known to affect skeletal muscle.[83] Microsomal oxidation of DMF has been shown to produce N-methylformamide NMF, probably *via* the route shown (Scheme 35).

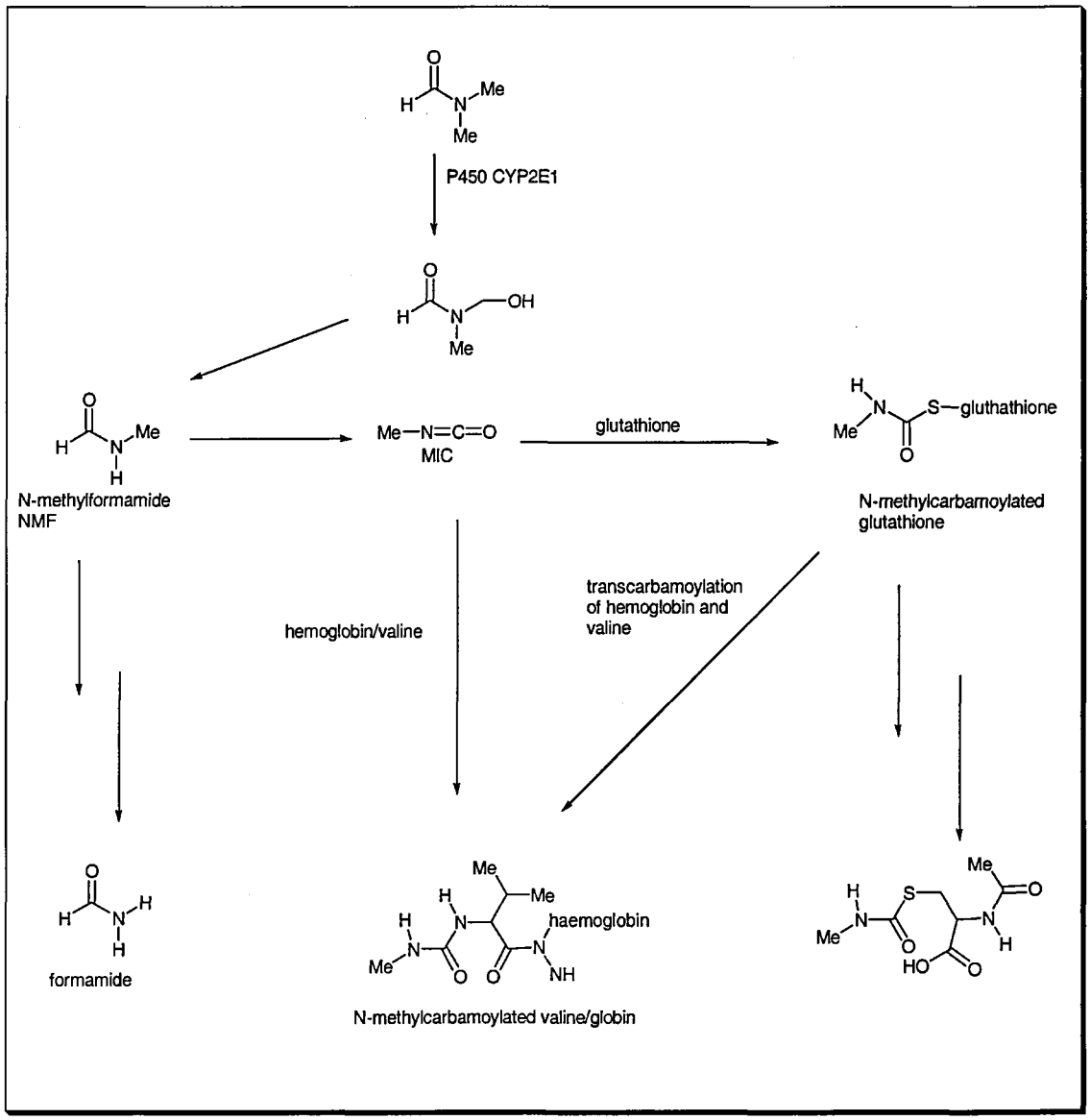

Scheme 35

Recent studies have shown that NMF and DMF themselves are probably not the cause of this toxicity and that metabolites involving glutathione have adverse effects.[84] Indeed, methylation of hemoglobin (a common process) increases 100 fold in the presence of DMF.[85] Although formaldehyde, a known carcinogen, is released during metabolism of DMF, this alone does not account for the degree of toxicity in DMF. The metabolic route shown (Scheme 35) has been postulated in the light of the metabolites isolated.[84,85] Several approaches have been taken to trap the possible

carbon-centred radical and iminium ion intermediates (Scheme 36) that form during amide metabolism.

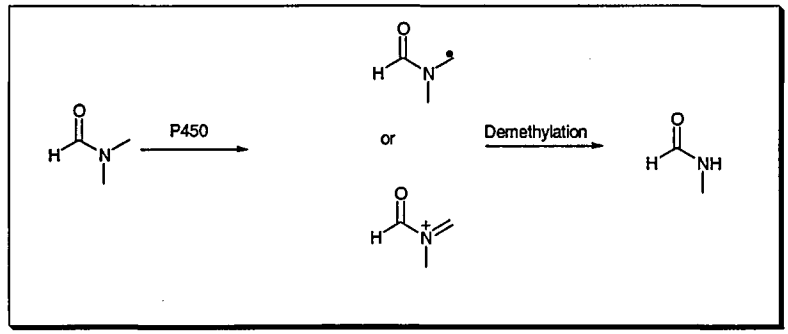

Scheme 36

One involves the use of an N-(3-butynyl) substituent as a radical trap (Scheme 37). Metabolism of N-(3-butynyl)-N-methylformamide **(40)** can potentially afford six products. In fact only A, B, and C were isolated.[86] The formation of B demonstrates that radical formation occurs at the α-carbon (Scheme 37).

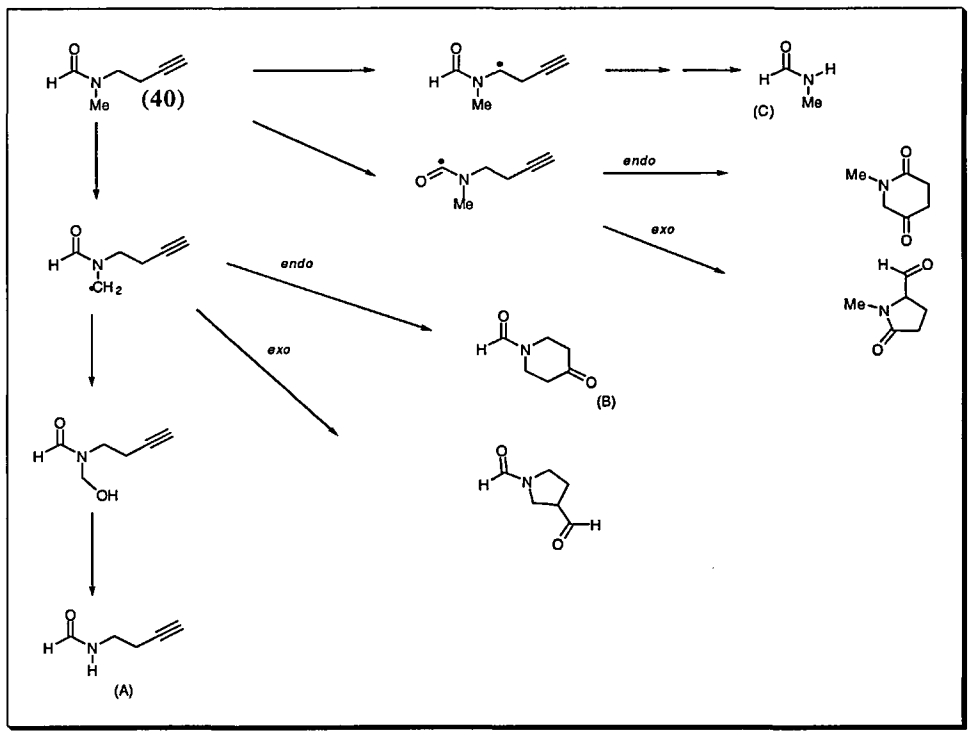

Scheme 37

Direct observation of radical formation by ESR is difficult because of the aqueous medium and because the lifetime of radicals tends to be too small to measure. However, radical trapping by N-*tert*-butyl-α-phenylnitrone yielded a stable nitroxyl radical **(41)** that has been observed[87] (Scheme 38).

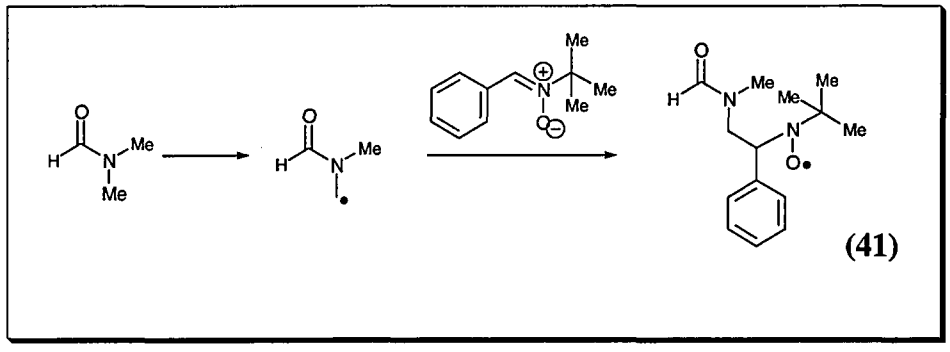

Scheme 38

The above results indicate that DMF undergoes demethylation *via* a carbon-centred radical. Formation of this carbon-centred radical may partly explain the toxicity associated with DMF. For example, there is evidence for the formation of a heme adduct with DMF that is metabolism dependent.[85] One explanation is that heme traps the carbon centred radical formed during metabolism. Certainly, there is a metabolism-dependent destruction of heme.[85]

HMPA

Hexamethylphosphoramide (HMPA) is a dipolar aprotic solvent possessing unique properties. It has been widely used in small-scale organic and organometallic syntheses in laboratories and for industrial processes such as UV inhibition in PVC and as a de-icing additive for jet fuels.[88] Unfortunately, it has been extensively reported that HMPA has severe toxicological effects on living organisms, giving side-

effects such as such as kidney disease, severe bronchiectasis, and bronchopneumonia, with squamous metaplasia and fibrosis in the lungs in rats.[88] Its mutagenic effects have been studied in both rats and house flies. The worst of these are located primarily in the nasal mucosa, and it is most harmful by inhalation.[89,90] Indeed HMPA is metabolised by P450 faster in nasal mucosa than in liver or lung. This implies tissue specific metabolism.

HMPA is known to undergo oxidative demethylation.[91] Given that the product of demethylation, pentamethylphosphoramide, is non-toxic, toxicity may be presumed to arise from an intermediate in the metabolic pathway. Several studies have attempted to establish the route of metabolism of HMPA, in order to better understand its toxicity. Metabolites so-far isolated[92-95] are: pentamethylphosphoramide (PMPA) **(42)**, N,N,N′,N″-tetramethylphosphoramide (TetraMPA) **(43)**, N,N′,N″-trimethylphosphoramide (TriMPA) **(44)**, N-formylpentamethylphosphoramide (FPMPA) **(45)**, N-formyl-N,N,N′,N″-tetramethylphosphoramide (FTetraMPA) **(46)** and formaldehyde (Scheme 39).

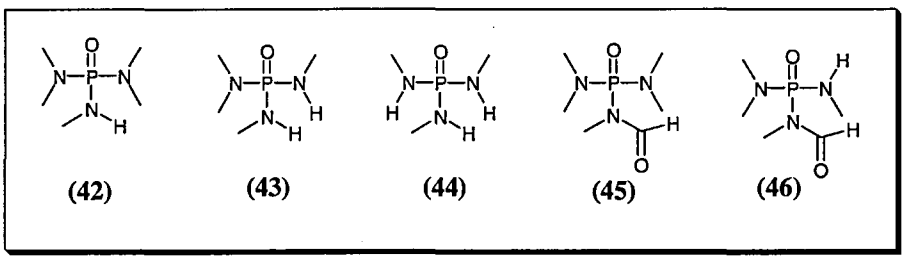

Scheme 39

Metabolism occurs by an oxidative mechanism;[96] in the absence of O_2, complete inhibition of PMPA formation is observed.[97]

Like DMF, metabolism of HMPA can occur primarily *via* two routes: oxidation at the N atom, or H-atom abstraction from the α-carbon. Ionisation potentials are inconclusive since the ionisation potential for HMPA (8.1 eV)[98] is between that of amide (9.11 eV for DMF)[99] and amine (7.82 eV for methylamine).[100] However, oxidation at the N atom is unlikely for following reasons:

a) no demethylation is apparent upon addition of hydrogen peroxide[94] or upon treatment with peracid[91]

b) inhibition by N,N-dimethylbenzylamine of FAD-containing dimethylaniline oxidase (an enzyme capable of N-oxidation) leads to an increase (rather than an expected decrease) in HMPA mutagenicity[101]

c) the putative N-oxide rearranges to N-((bis(dimethylamino)-phosphinyl)oxy)dimethylamine[91] **(47)**, which is non-toxic (Scheme 40).

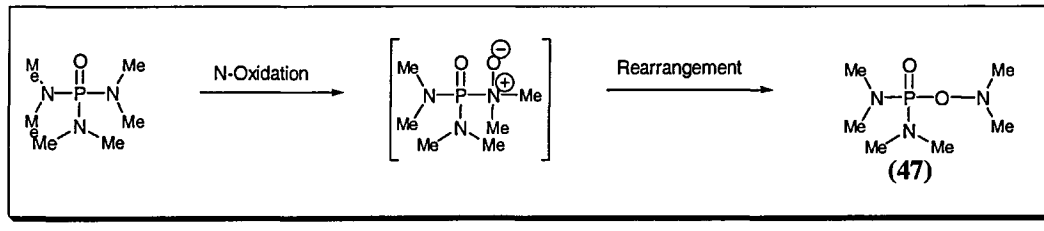

Scheme 40

The above imply that metabolism probably proceeds *via* H-atom abstraction, leading to hydroxylation of the methyl group and subsequent dealkylation. This is supported by:

(a) a ^{14}C study which gives lower than expected amounts of ^{14}C recovered (impling deformylation or absorption into body tissue)[95]

(b) isolation of formamide derivatives[94]

(c) isolation of formaldehyde[102]

(d) stepwise formation (supported by isolation) of main metabolites PMPA/ TetraMPA/ TriMPA. If PMPA is used instead of HMPA formation of FTetraMPA and FPMPA (Scheme 41) has also been observed. This would imply that appropriate formylation is involved at each stage, along with analogous methylol intermediate.

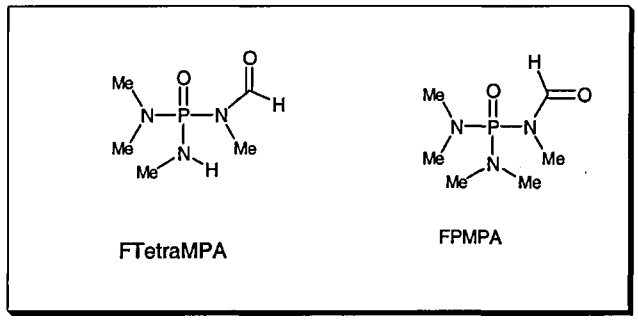

Scheme 41

Hence the following mechanistic route is postulated (Scheme 42).[101]

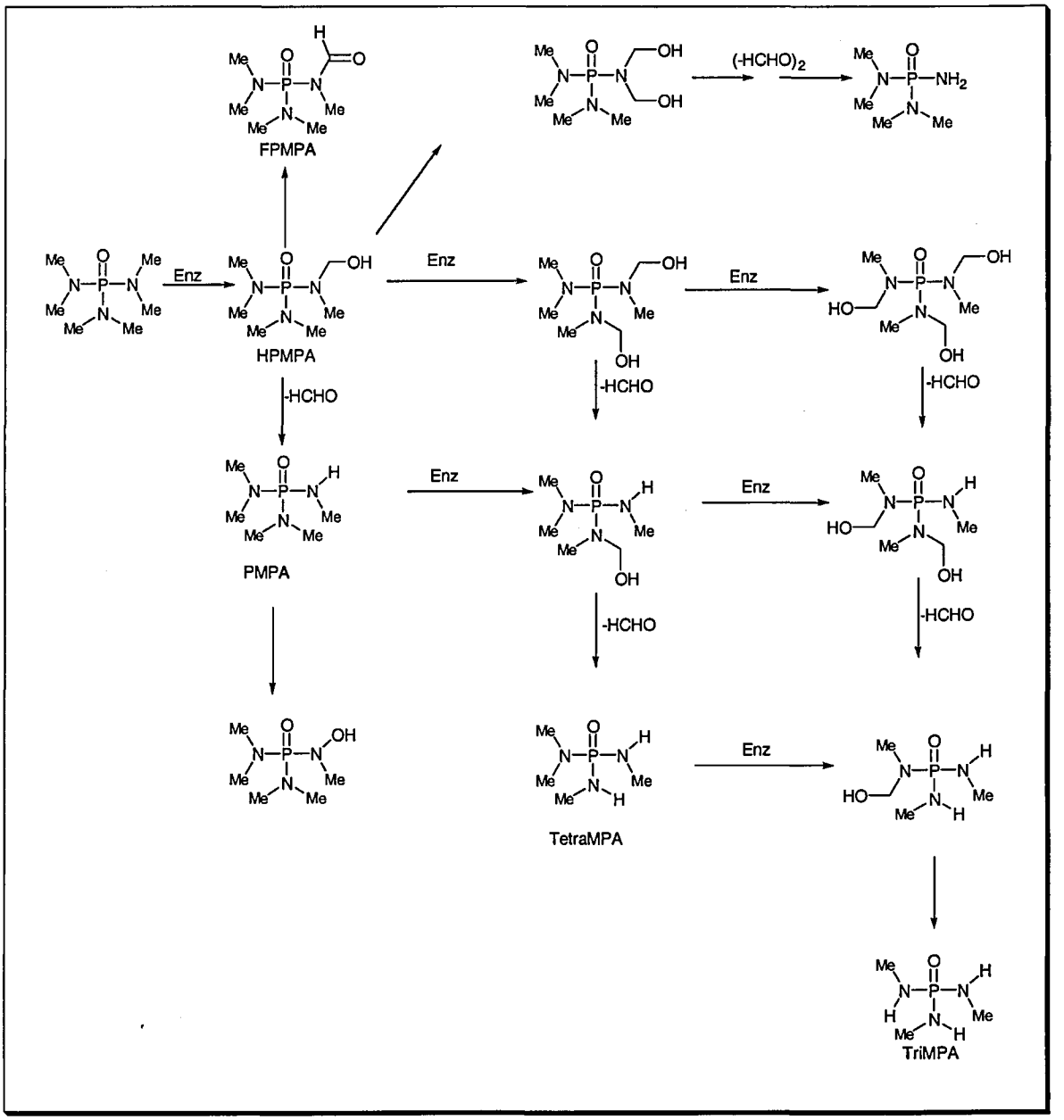

Scheme 42

DMPU

Surprisingly, given its recommended use in place of DMF and HMPA,[103] very little data exist regarding the metabolism and toxicity of DMPU. The data available reveal it to have an acute toxicity a little higher than that of HMPA, but there is no evidence for

mutagenic or chromosome damaging activity.[103] DMPU is a cyclic urea **(48)**, but may be thought of as being very much like an amide **(49)**. (Scheme 43)

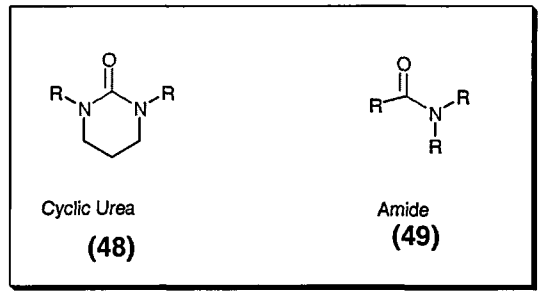

Scheme 43

It can be seen that both urea and amide have a nitrogen atom next to a carbonyl group but in the urea there is an extra nitrogen atom involved in bonding to the carbonyl. As might be expected, therefore, ureas and amides have similar ionisation potentials, but of the two the urea is the lower (urea ~ 8.4-8.7eV and amide ~ 8.7-9.1eV). Consequently, ureas may follow similar oxidative mechanisms to those of the amides. An important point to be considered is the site of attack; this is an issue since the DMPU is cyclic and so may be attacked at an α-carbon atom in the ring or at the N-methyl position. With N-methylpyrrolidinone it has been shown that chemical oxidation occurs only on the ring[104] but that P450 oxidation involves N-demethylation as well. Remarkably, there are as yet no published studies of the metabolism or chemical oxidation of DMPU. Scheme 44 gives the possible routes of metabolism.

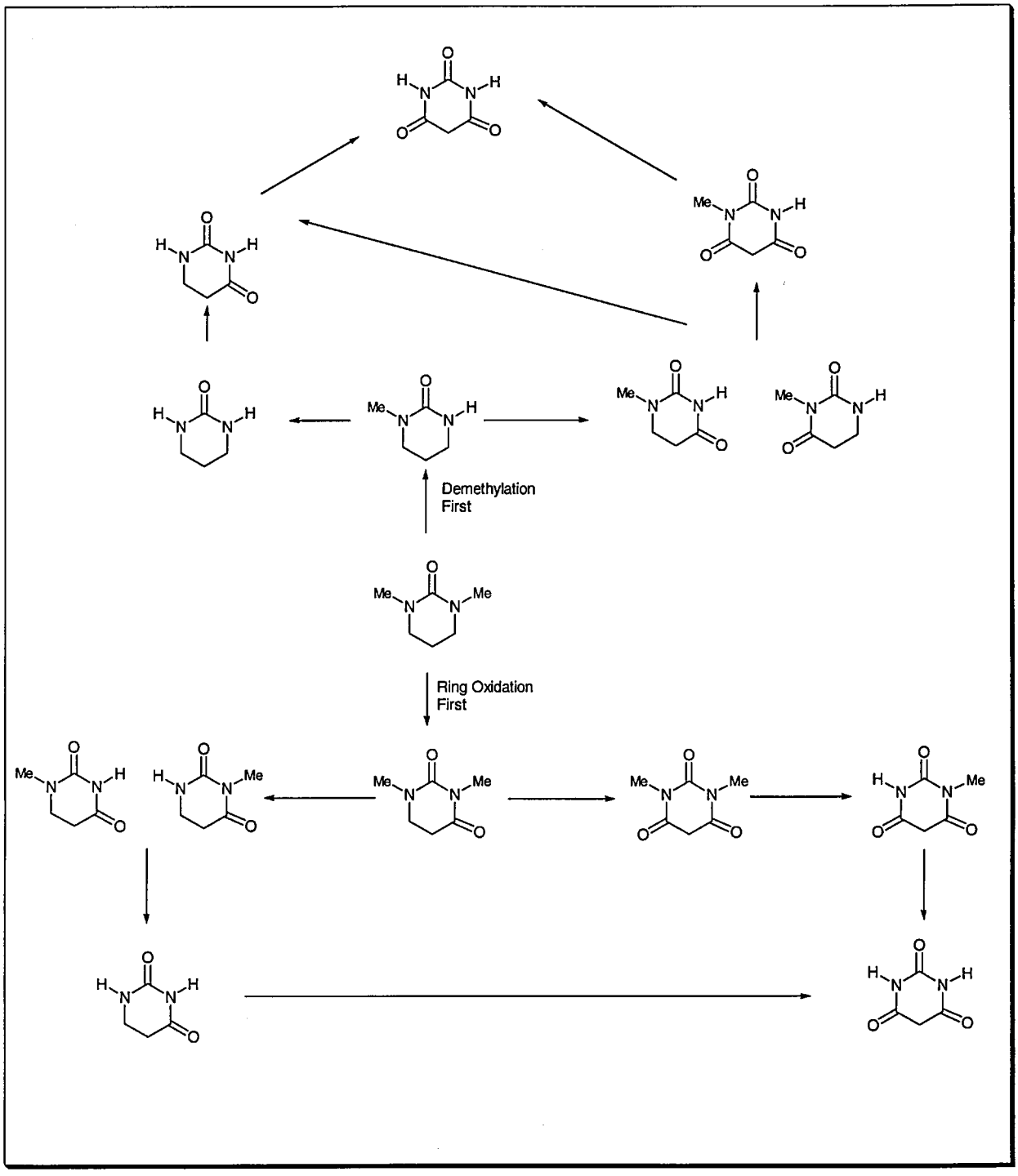

Scheme 44

Scope of thesis

It seems remarkable that although DMPU is recommended as a safe alternative for HMPA little data is available. In fact there have been no

- biomimetic studies

- metabolic pathways published
- toxicology studies

There have been no studies attempting to establish the metabolic intermediates. It was thought that by using the same strategies as that applied for DMF, it would be possible to determine whether a C-centred radical intermediate is formed from DMPU and HMPA in their oxidation.

It is possible to determine the kinetic deuterium isotope effect for the oxidation, with the use of deuterated HMPA. This will give an indication of whether the mechanism of P450 mediated N-dealkylation proceeds via an initial one electron abstraction like that of amines (small deuterium isotope effect)[72,76,77] or *via* hydrogen abstraction (large deuterium isotope effect) leading to either a carbon centred radical or an iminium ion.[78] If demethylation of HMPA occurs *via* hydrogen abstraction as expected then a carbon centred radical or an iminium ion could be formed. This thesis aims to determine this effect for HMPA using model studies, which will give further evidence as to whether N-demethylation is undergone *via* a C-centred radical.

3 Discussion

3.1 Analytical Techniques

In the introduction, oxidation of amide solvents is discussed. A suitable analytical technique must be developed to determine the products and allow quantitative analysis. Literature reports on the product study of microsomal dealkylation of HMPA

suggested gas chromatography (GC) might be a suitable technique, these reports also show that PMPA and FPMPA are formed under microsomal oxidation. Hence it was thought these would be the most probable oxidative products produced under model studies (using TPPFeCl/ ^{t}BuOOH) of HMPA. Following a procedure already used in the analysis of N,N-dimethylbenzamide[105] it was hoped that a similar system could be employed for HMPA (Scheme 45).

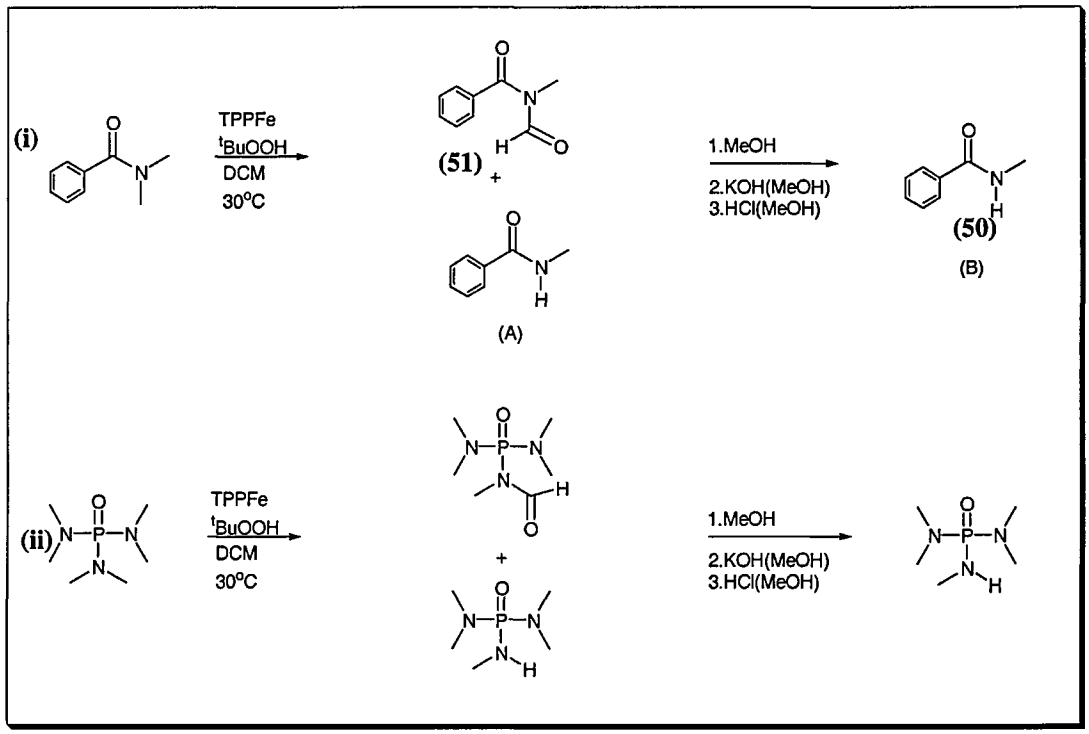

Scheme 45

In the benzamide system it has been shown that the formyl derivative produced is unstable. To determine accurately the quantity of oxidised products formed, the formyl product was treated with sodium hydroxide to form N-methylbenzamide **(50)**. It was decided that this methodology should also be applied to the HMPA system (Scheme 45, pathway ii). To develop a suitable analytical system, standard solutions of HMPA and PMPA were analysed by GC. These test experiments showed that HMPA and PMPA have similar GC retention times (Figure 13).

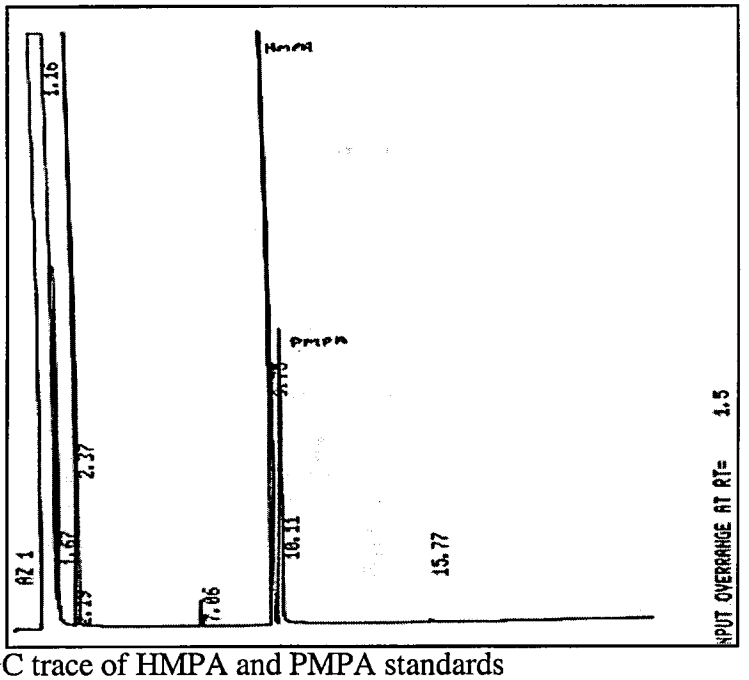

Figure 13 GC trace of HMPA and PMPA standards

Although this appears to have good separation, this posed a problem for the analysis of reaction mixtures where only 1-5 per cent of HMPA is oxidised to PMPA. Hence the large relative concentration of HMPA present swamped any PMPA produced. By using a derivatising agent it was hoped that the retention time of PMPA could be increased, thus allowing separation. N-Methyl-N-(*tert*-butyldimethylsilyl)trifluoroacetamide (MTBSTFA) was chosen since it could be demonstrated independently, that 98 per cent conversion to the silylated derivative was achieved after 10 min.

Using standards of HMPA and derivatised PMPA separation was indeed achieved, so several pilot experiments were carried out in which HMPA under went oxidation (0.001 M TPPFeCl in DCM as catalyst, 0.2 M *tert*-butylhydroperoxide as oxidant with 0.2 M of HMPA as substrate) with derivatisation of the PMPA. Unfortunately, after several kinetic runs repeat injections appeared to show varying amounts of derivatised PMPA present. To test if this was experimental or human error two identical

experiments were run in tandem. These yielded results that varied by 26 per cent, whereas independently we were able to verify that reproducibility was within 5 per cent. The possible variables contributing to these differences were examined, *viz.* the deterioration of PMPA in alkaline solution and the loss of phosphoramide during methanol removal.

To determine if HMPA decomposed in KOH, a test of the stability of HMPA in KOH solution was determined. HMPA was left in a 2M KOH solution overnight after which time the solution was analysed by ^{31}P and ^{1}H NMR and also by TLC. The results proved negative; that is, HMPA was found to be stable to alkaline solutions at room temperature.

To examine whether or not the product was being lost upon removal of the methanol that had been used to quench the reaction, HMPA in methanol was concentrated under reduced pressure. A cold trap (-78 °C) was put in place to collect the evaporated materials. Analysis of removed methanol showed HMPA present. Given the similar physical properties of HMPA and PMPA, this observation could account for varying amounts of PMPA present in the reaction mixtures.

To overcome this need for filtration (due to the salt formed after neutralisation of KOH by HCl) and evaporation, the following alternative procedure was employed. An aliquot of the reaction mixture was quenched in 100 µl of methanol. This aliquot was then treated with a solution of concentrated NH_3 in chloroform. This solution was then reduced in volume under a flow of nitrogen gas to remove any NH_3, the resultant solution was made up to 800 µl with diethyl ether and then derivatised using 200µl

MTBSTFA. Using this methodology the solution could be injected directly onto the GC column. However, subsequent independent tests with synthetic FPMPA indicated that NH_3 does not cause FPMPA to undergo deformylation to PMPA. It would appear that FPMPA has much greater stability to base than N-formyl-N-methylbenzamide. Because of this, it seemed possible that we could analyse for both the N-formyl and N-demethylated products. Even so, despite these improved methods being implemented, the problem of variable PMPA concentrations and increased amounts of unknown compounds persisted.

An increase/decrease in PMPA may have been due to poor injection technique, though this may be discounted since multiple injections of a PMPA standard gave identical results within experimental error (±5 per cent). However, it was decided that in order to eliminate inaccuracies by injection technique and for an improvement in overall accuracy, an internal standard should be employed. For an internal standard to work effectively it must have a similar retention time to the compound being studied, and a concentration giving similar peak height to that of the compound being studied.

n-Octadecane was chosen because it conformed to these factors (Figure 14).

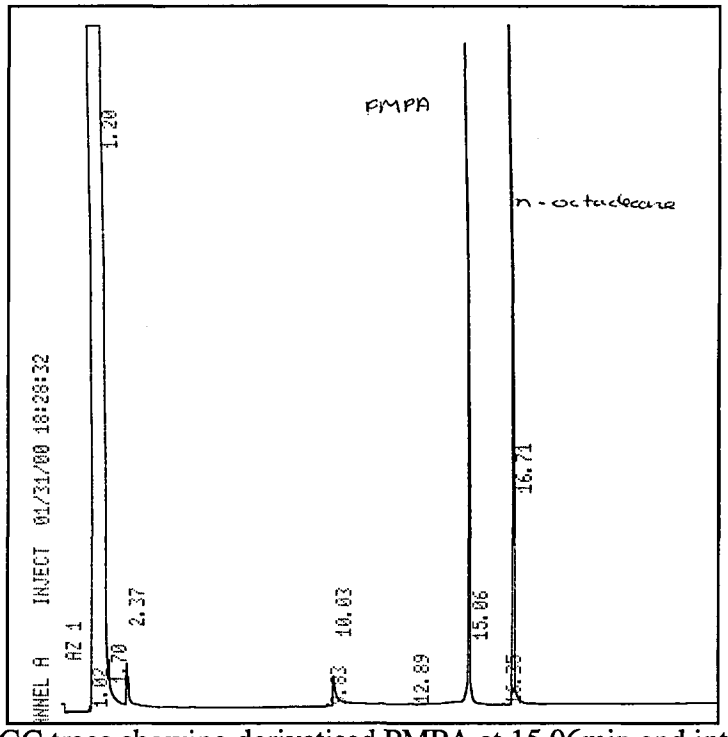

Figure 14 GC trace showing derivatised PMPA at 15.06min and internal standard n-octadecane at 16.71 min.

However, even with the use of an internal standard, erratic results still occurred.

The same oxidation experiments were carried out on a smaller scale, it was observed that the products were being catalytically decomposed on the column, possibly due to TPPFeCl build up. To test for this, a sample containing pure HMPA and PMPA was analysed by GC using a column which had previously been used to analyse model reaction mixtures. A large number of compounds was noted on the chromatogram. When the first 5 cm of the column was removed (where any catalyst might be absorbed), GC of this pure sample afforded only two peaks. Significantly, after several reaction mixtures were subsequently analysed the problem re-emerged. This indicates that a build-up of contaminant (probably TPPFeCl) occurs at the head of the column, which leads to catalytic decomposition of compounds injected into the system.

Attempts to remove the TPPFeCl by filtration and column chromatography were unsuccessful. Consequently, the use of GC was discontinued.

Following the failure of GC as an analytical technique, high performance liquid chromatography (HPLC) was investigated. Initially, to verify the method and to confirm experimental techniques, the known dealkylation of N, N-dimethylbenzamide was studied.[86] Analysis was carried out using a Waters C18 Symmetry column, separation was achieved using a water/acetonitrile (50%/50% v/v) eluent (Figure 15; N-methylbenzamide **(50)** at 5.4 min and dimethylbenzamide at 7.9 min).

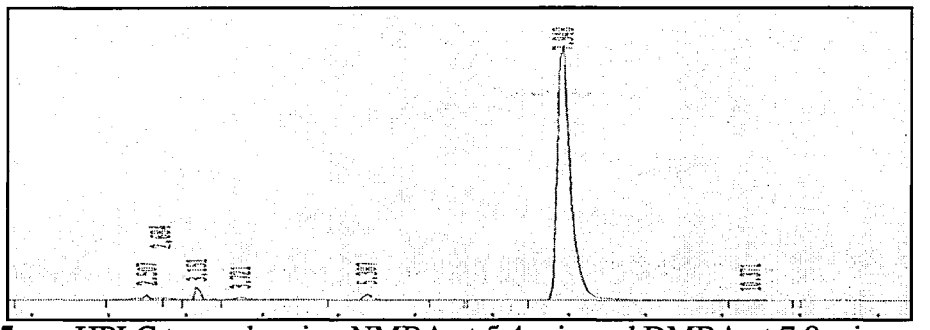

Figure 15 HPLC trace showing NMBA at 5.4 min and DMBA at 7.9 min

This compound undergoes reaction according to the pathway shown in Scheme 45. Two separate aliquots of reaction mixture A (Scheme 45) were taken at regular intervals and quenched in methanol. The latter terminates the reaction thus preventing any further oxidation of the benzamide. To one of these aliquots, potassium hydroxide was added to convert any unreacted N-formyl-N-methylbenzamide (FNMBA) **(51)** to N-methylbenzamide (NMBA) **(50)**. Both aliquots were then separately analysed by HPLC. Results for this can be seen in Figure 16, where increasing amounts of N-methylbenzamide (NMBA), are formed as the reaction proceeds. It is also apparent that a greater concentration of NMBA is present in the sample treated with hydroxide (B) due to conversion of FNMBA to NMBA (Figure 16).

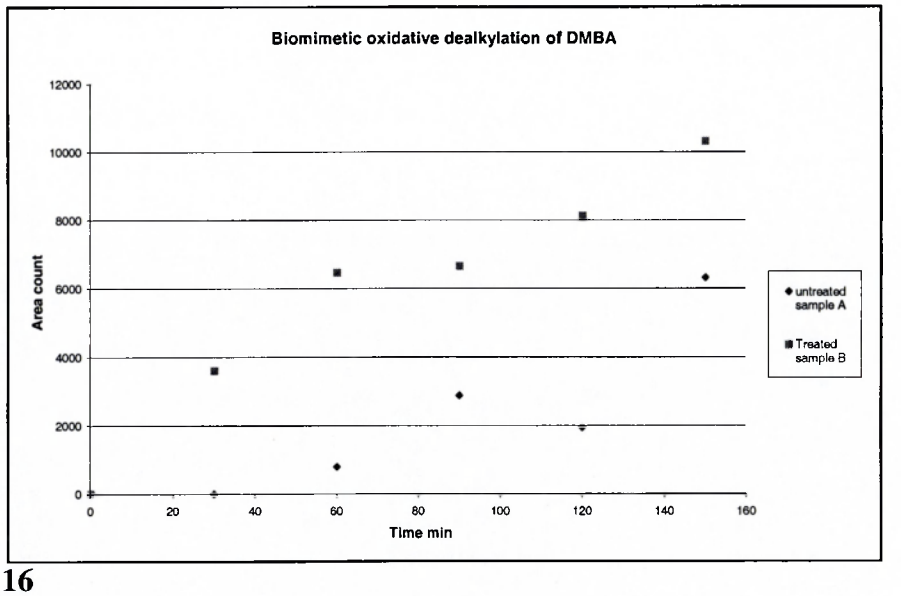

Figure 16

At this stage a study was performed to compare the relative efficiencies of tetraphenylphorphyrin iron (III) chloride and tetraphenylphorphyrin manganese (III) chloride for the oxidative dealkylation of DMBA. Using identical substrate concentrations and concentrations of oxidants this showed that the manganese catalyst was less efficient (Figure 17). For this reason, tetraphenylphorphyrin iron (III) chloride, it was chosen for all subsequent experiments.

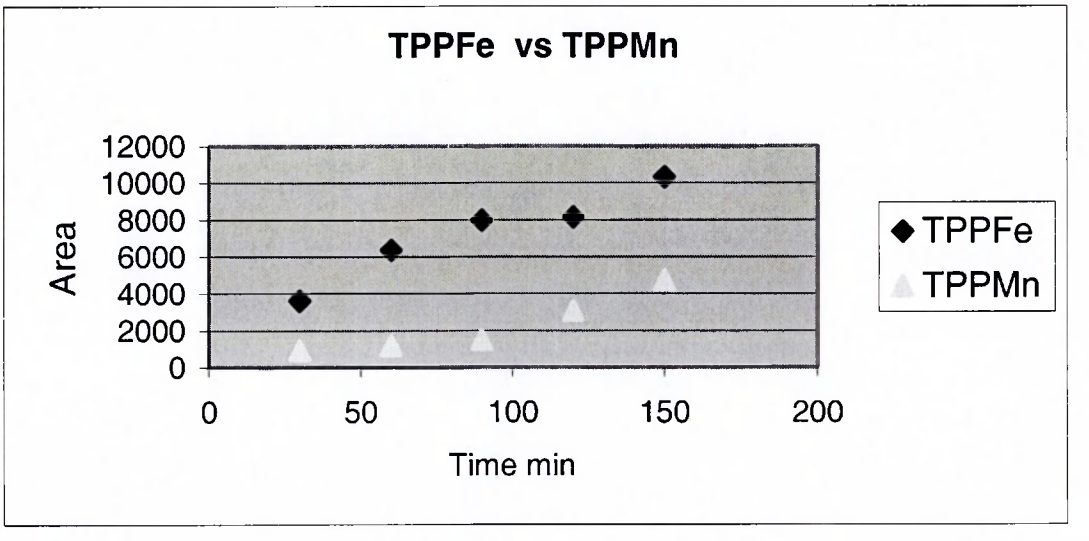

Figure 17

Unfortunately, when the HPLC system employed for the benzamides was used to investigate analogous HMPA reaction mixtures, insufficiently adequate separations were obtained (Figure 18, HMPA at 2.3min, PMPA at 2.2min). This proved a problem in reaction mixtures where HMPA was in excess and swamped the PMPA signal.

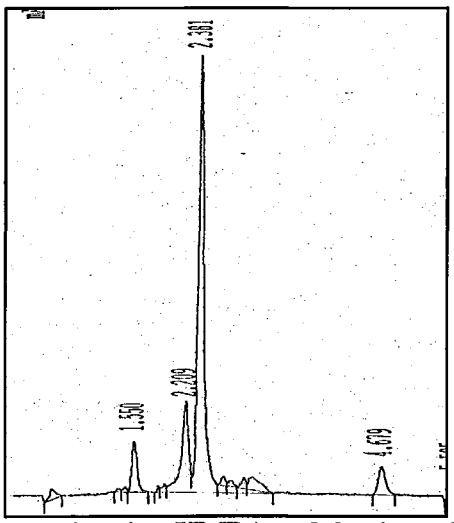

Figure 18 HPLC trace showing HMPA at 2.3 min and PMPA at 2.2 min.

HPLC was re-examined, this time employing a PLRPS (polymeric reverse phase) column. This column was found to give the necessary separation between HMPA, PMPA and FPMPA. This column is stable to chlorinated solvents, thus a system was developed where the reaction mixture was added directly to methanol (to quench the reaction) and then injected on to HPLC, removing the need for evaporation of chlorinated solvent. Figure 19 shows a reaction mixture of oxidised HMPA, with PMPA at 17.57min, FPMPA at 21.69min and HMPA being removed in the end wash.

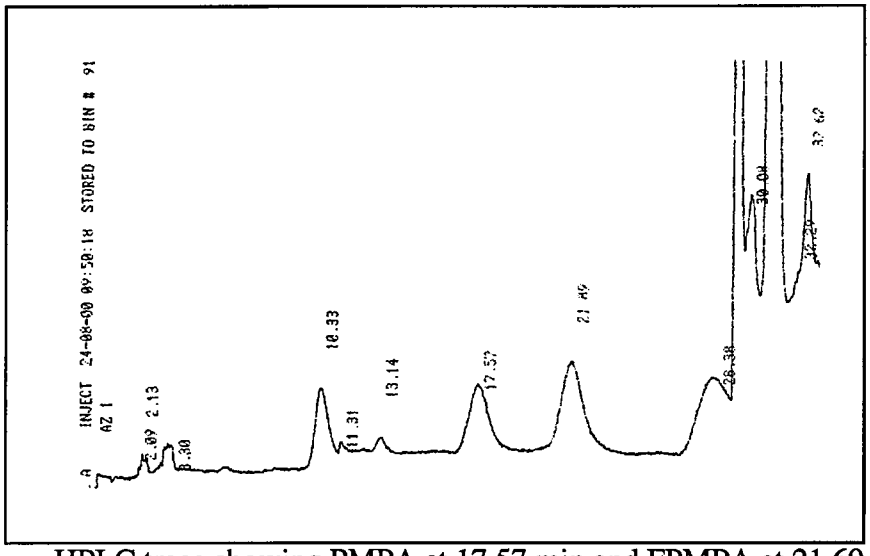

Figure 19 HPLC trace showing PMPA at 17.57 min and FPMPA at 21.69 min

3.2 HMPA reactions

By using the above-described analytical techniques, it proved possible to create a calibration graph of FPMPA and PMPA (Figure 20). This was used to analyse results of the reactions of HMPA without the need to convert FMPMA to PMPA.

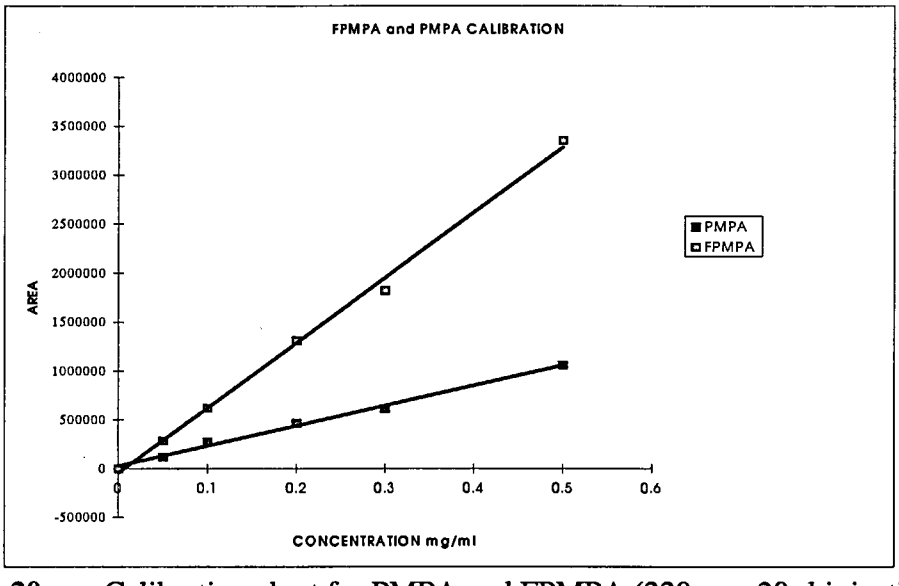

Figure 20 Calibration chart for PMPA and FPMPA (220 nm, 20µl injection, 1ml/min)

Using the calibration chart in Figure 20 it is possible to analyse the reaction of HMPA with TPPFeCl/^{t}BuOOH. Such a profile is shown in Figure 21

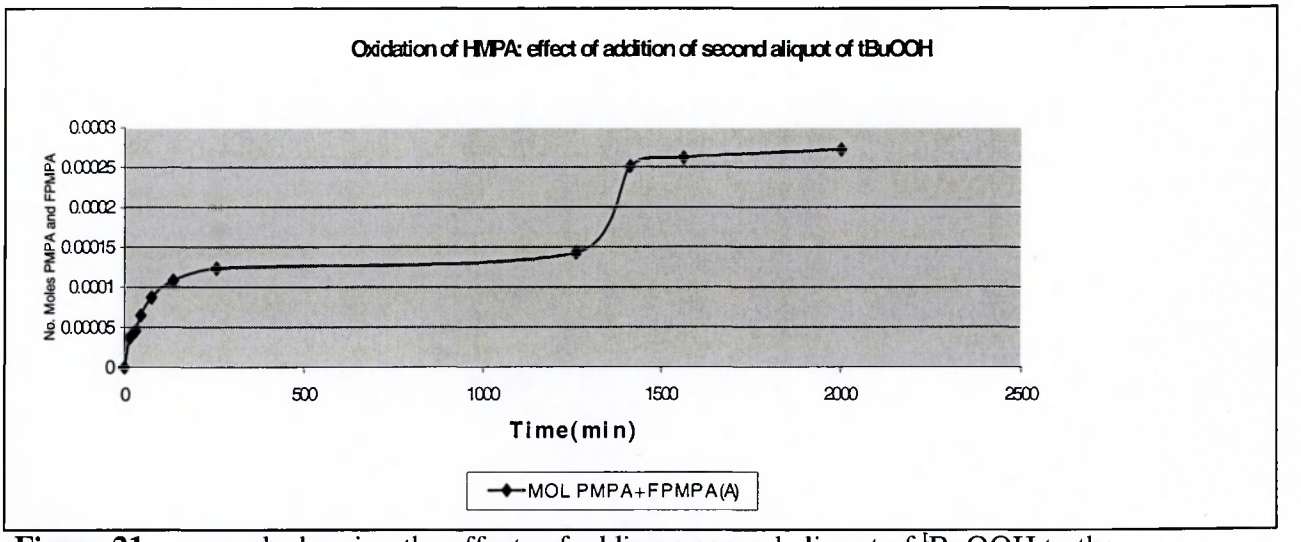

Figure 21 graph showing the effects of adding a second aliquot of ^{t}BuOOH to the oxidation system as per section 4.5.3 ([TPPFeCl] = 0.001 M, [^{t}BuOOH] = 0.2 M, [HMPA] =0.2 M, DCM 20cm^{3})

It is clear from this that the reaction tails off markedly after about 150 min. This corresponds to 5 per cent of reaction. Since this low conversion was thought to be due to the consumption of *tert*-butylhydroperoxide *via* a side reaction to form ^{t}BuOOH and H_2O, at 1260 min, a further aliquot of *tert*-butylhydroperoxide (of equal concentration to the first) was added. A further burst of reaction can be observed, the extent of which corresponds to that of the initial reaction.

Plots such as that shown in Figure 21 but taking a greater number of aliquots in the initial 20 min phase of the reaction, were used to examine the initial rate of oxidation. The initial rates at varying concentrations of HMPA for the demethylation of HMPA to PMPA and oxidation to FPMPA are shown in Figure 22.

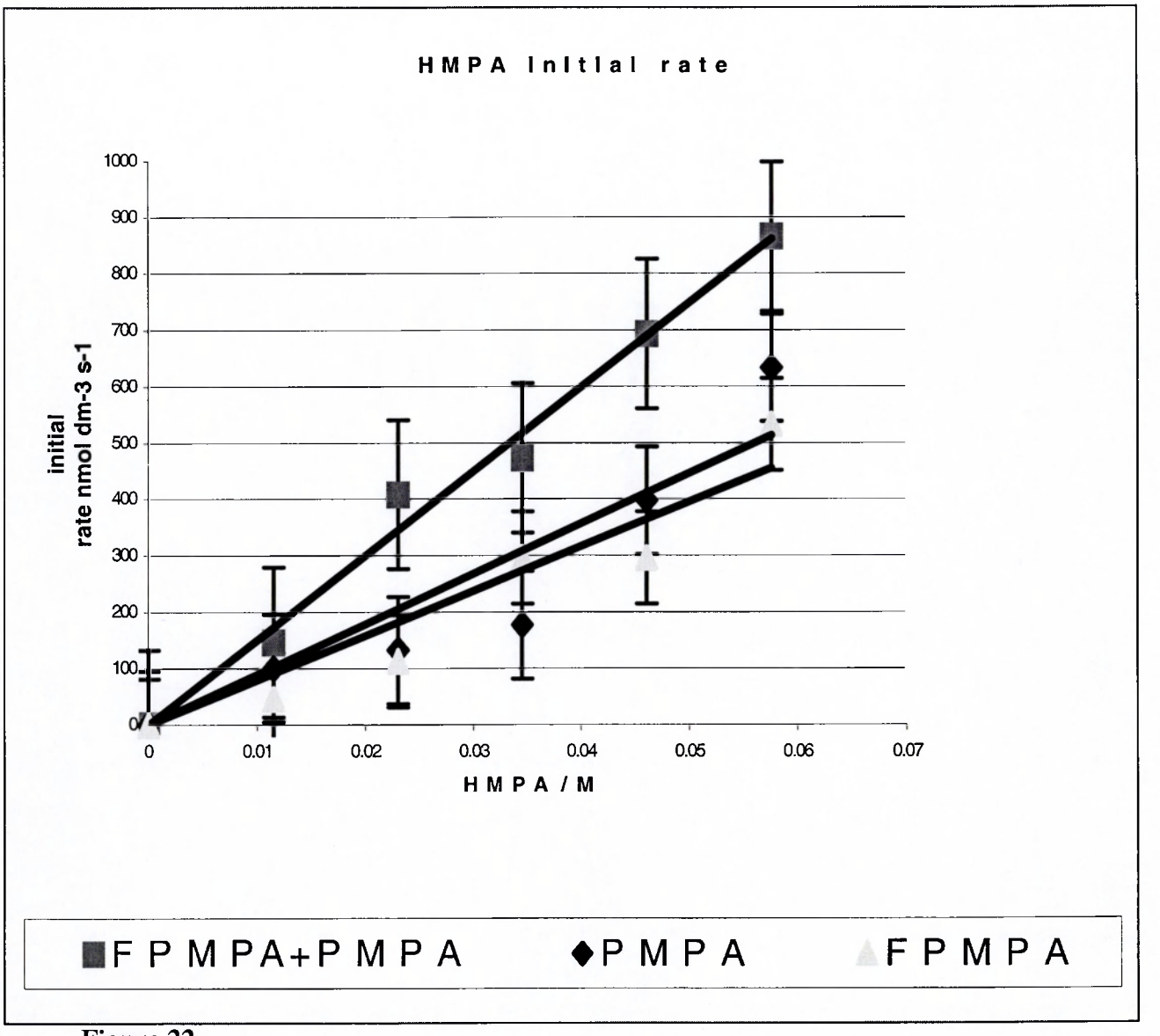

Figure 22

This gives a pseudo-first-order rate constant of 1.7 x 10^{-5} s^{-1} for the combined PMPA and FPMPA, 8.6 x $10^{-6}s^{-1}$ for PMPA and 8.5 x $10^{-6}s^{-1}$ for FPMPA. An analogous experiment was carried out using the perdeuterated HMPA analogue $^{2}H_{18}$-HMPA (Figure 23).

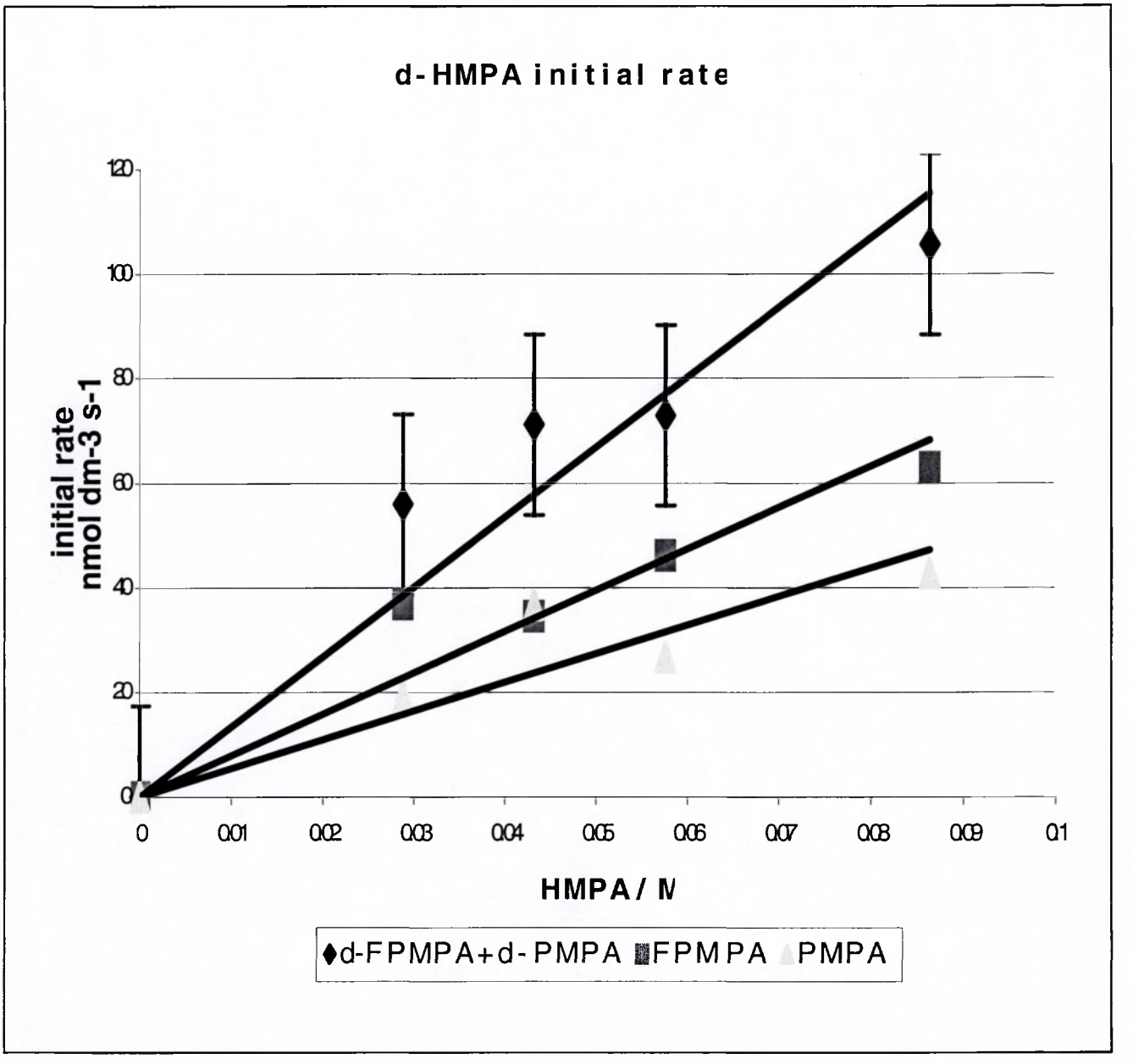

Figure 23

This gives a pseudo-first-order rate constant of 1.65 x 10^{-6} s^{-1} for combined PMPA and FPMPA, 8.5 x 10^{-6} s^{-1} for PMPA and 8.0 x 10^{-6} s^{-1} for FPMPA. Comparing this value with that for HMPA, affords a kinetic deuterium isotope effect, k_H/k_D, of *ca.* 10. This is a large kinetic deuterium isotope effect, which indicates that the reaction involves hydrogen atom transfer in the rate-limiting step.

The oxidation of N,N-dimethylbenzamide has been similarly examined.[106] This has been shown to give a pseudo-first order rate constant of 2.2 x 10^{-5} s^{-1}. Comparing this to that obtained for HMPA this gives a difference in rate of 1.3 fold, the amide being the more reactive. This does not take into account statistical factors where the benzamide has two methyl groups available for attack whereas HMPA has six. Taking these factors into account, the benzamide is more reactive than HMPA by a factor of 4. This reactivity difference is presumably due to electronic effects of the P=O group as compared with the C=O group.

To investigate the mechanism of formation of the demethylated and formyl products further, the following possible metabolites **(45)**, **(54)** were synthesised (Scheme 46).

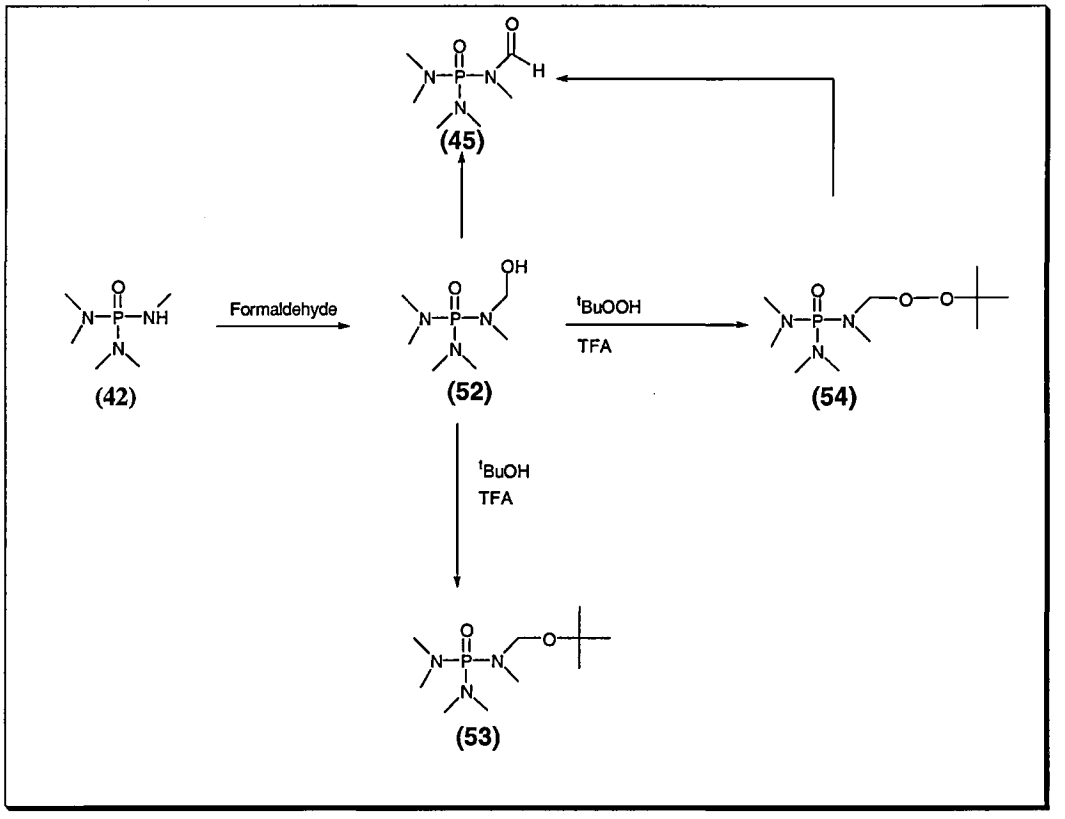

Scheme 46

When HMPA undergoes alkyl group oxidation, it is possible that *en route* it could form several intermediate compounds. One of the most likely is the alcohol **(52)**. Subsequent oxidation of this can yield the formyl compound **(45)**. The formyl compound may then undergo deformylation to give the demethylated HMPA derivative PMPA (alternatively, PMPA may arise directly from **(52)** by loss of formaldehyde). To account fully for all oxygenated products it was decided to try and synthesis the alcohol **(52)** since it may also have been detectable by HPLC. This was attempted using PMPA **(42)** and a 33 per cent formaldehyde solution. This method has been employed to form the corresponding amide derivatives.[107] Unfortunately, it prove impossible to isolate the alcohol from the reaction mixture; concentrating the product always resulted in an intractable tar. This polymer is not detectable by HPLC. Alternatively, the alcohol **(52)** may react with ^{t}BuOOH in solution or with ^{t}BuOH (from ^{t}BuOOH), and so could form either **(53)** or **(54)**, respectively. It can easily be seen how the peroxide **(54)** may be cleaved to form the corresponding formyl compound **(45)**, making this a prospective reaction route. The synthesis of both of these substances was attempted according to the two reactions in Scheme 47.

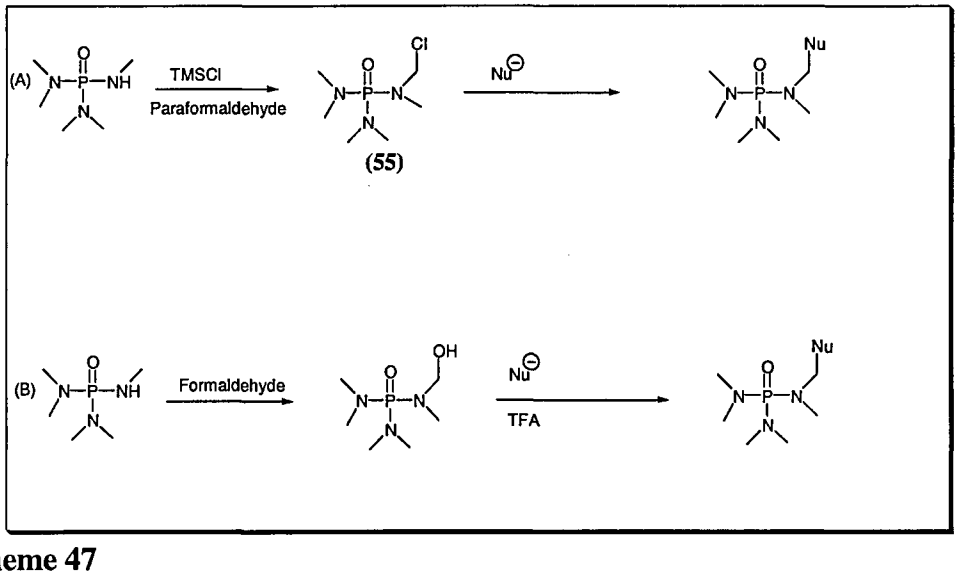

Scheme 47

In route (A), PMPA was treated with chlorotrimethylsilane (TMSCl) and paraformaldehyde[86] to form the N-chloromethyl derivative (**55**). This is a highly reactive species with the chloride easily substituted by the nucleophilic ^{t}BuOOH or ^{t}BuOH. However, with either of these nucleophiles a complex mixture of products was obtained and so route (B) was utilised. PMPA was reacted with aqueous formaldehyde to form a solution that was hoped to contain the alcohol (**52**). Reaction was then attempted of the solution of crude alcohol with the appropriate nucleophile (either ^{t}BuOOH or ^{t}BuOH), which is also the solvent for this latter reaction. For ^{t}BuOOH, this resulted in a very clean reaction affording (**54**) in quantitative yield. However, when ^{t}BuOH was used, addition of trifluoroacetic acid (TFA) was required to catalyse the reaction, probably because ^{t}BuOH is a weaker nucleophile than ^{t}BuOOH. However, this results in a mixture of products. From the ^{1}H NMR spectrum, the products appear to be reversion to PMPA (**42**), dimerisation (**56**) and formation of the *tert*-butyl ether (**53**) (Scheme 48).

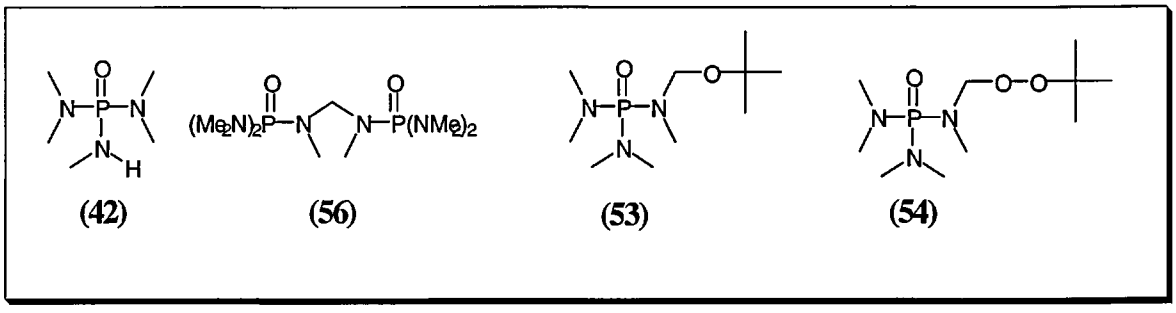

Scheme 48

Purification of this latter compound was attempted by column chromatography, which resulted in the labile ^{t}BuO group being removed. The acidity of the silica may catalyse the removal of the ^{t}BuO group. Consequently, chromatography on either a silica column pre-washed with NEt_3 to remove acidic sites, or on a basic alumina column

were attempted, but even so the compound still decomposed on-column. Thus an examination of the chemistry of a crude sample of **(53)** was required. To do this **(53)** was dissolved in water. Analysis of the reaction mixture after 60 min by ^{1}H NMR spectroscopy showed that dimerisation (to **56**)and demethylation (to **42**)occurs. Loss of ^{t}BuOH indicates that the ^{t}BuOH group is too labile to handle and in any case would be removed on column by HPLC. For **(54)** analysis by ^{1}H NMR at 60 min intervals showed that dimerisation and demethylation also occurs, although it does so at a slower rate. Because of the problems in handling these products they were not observed on HPLC, with only the decomposition product being observed. This is not a problem since it means all oxidised products may be accounted for, but does not allow determination of possible ^{t}BuOOH or ^{t}BuOH trapping.

That **(54)** could be an intermediate in the formation of FPMPA during oxidation of HMPA by TPPFeCl/ ^{t}BuOOH comes from subjecting it to the same reaction conditions as used for HMPA. This results in the instantaneous and exclusive formation of FPMPA. FPMPA itself is stable to the same reaction conditions. This observation implies that the formation of PMPA and FPMPA come in HMPA oxidation arise separate routes. It is possible that formation of **(54)** occurs from addition of a ^{t}BuOO radical to a carbon-centred radical. It is easily seen how the decomposition of **(54)** would result in the formation of FPMPA **(42)** (Scheme 49).

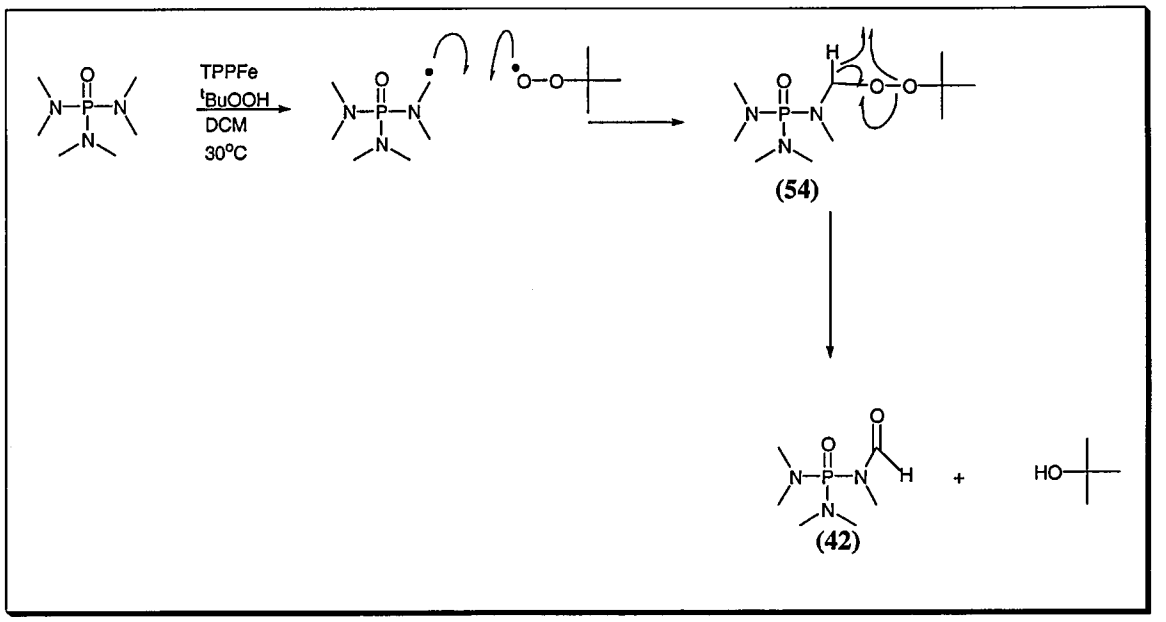

Scheme 49

PMPA is likely to arise form the oxidation of HMPA to **(52)** which may then undergo deformylation to **(42)** (Scheme 50).

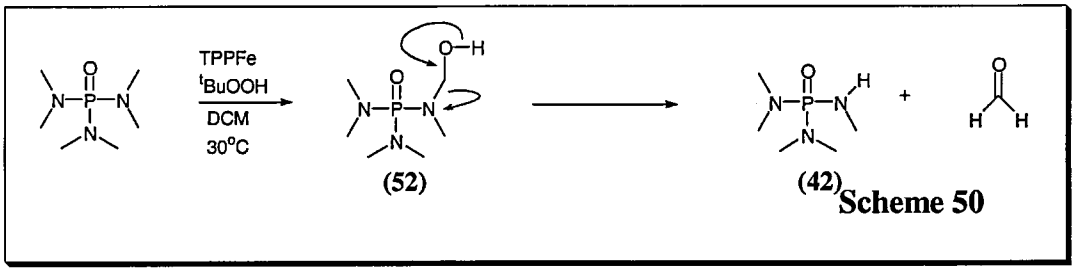

Scheme 50

3.3 DMPU reactions

Prior to investigating model reactions of DMPU **(57)**, several of the possible products were anticipated and obtained. Scheme 51 shows the most probable products that could be formed. These were either synthesised or purchased.

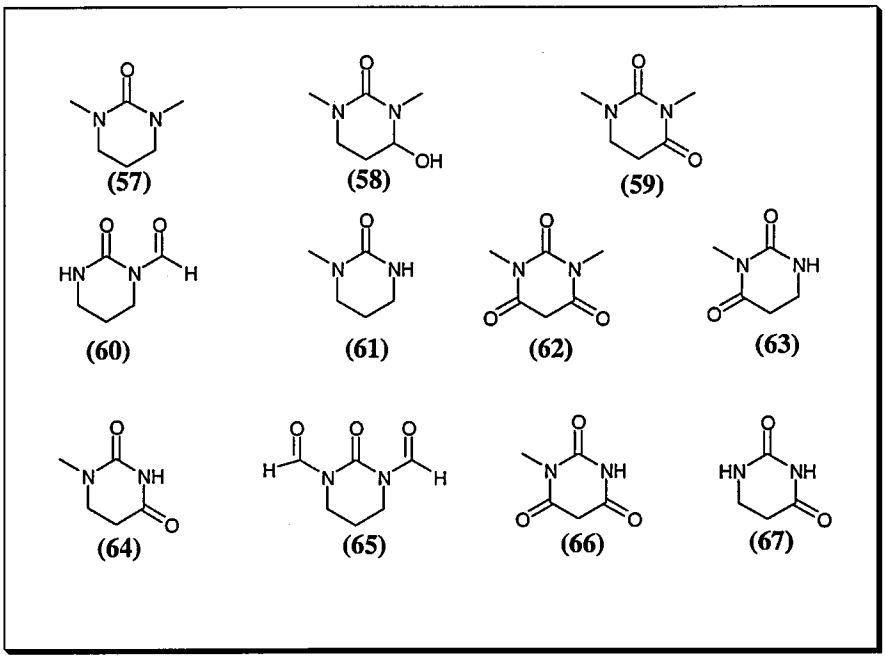

Scheme 51

The following procedures outline the synthesis of the above compounds. 1,3-Dimethyldihydropyrimidine-2,4-dione **(59)** and 1-methyldihydropyrimidine-2,4-dione **(64)** were synthesised by the route shown in Scheme 52, which involves initial Michael addition of the appropriate urea to acrylic acid.

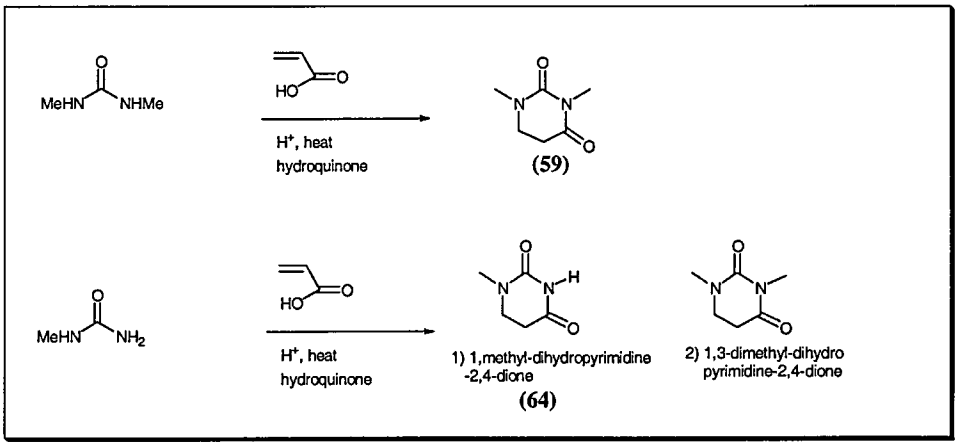

Scheme 52

However, in the latter, instead of giving the anticipated mixture of 1 or 3-methyldihydropyrimidine-2, 4-diones, a mixture of **(59)** and **(64)** was obtained. This

can be explained if the urea undergoes a disproportionation reaction (Scheme 53) prior to the reaction with acrylic acid.

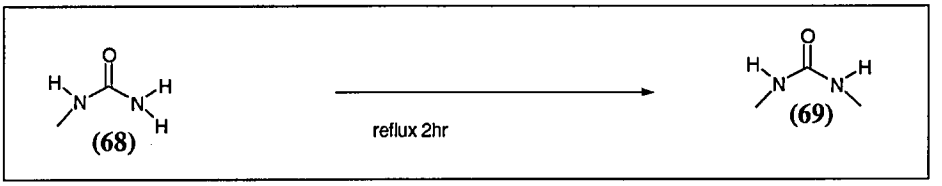

Scheme 53

To determine if this was the case N-methylurea **(68)** was subjected to the reaction conditions but in the absence of acrylic acid. Disproportionation would be expected to yield both 1,3-dimethylurea **(69)** and urea. Analysis of the products by ^{1}H NMR spectroscopy and TLC indicated that **(68)** does indeed undergo a disproportionation reaction to form **(69)** (Scheme 53) though urea was not observed although the disproportionation explains the presence of **(59)** in the synthesis of **(64)**. The formation of only ((**64**) rather than (**63**))can be attributed to the higher nucleophilicity of the urea NMe nitrogen atom over NH_2 nitrogen atom in the initial addition step of the reaction; this results in the formation of only one isomer.

To synthesise 3-methyldihydropyrimidine-2,4-dione **(63)** the following method was used (Scheme 54)

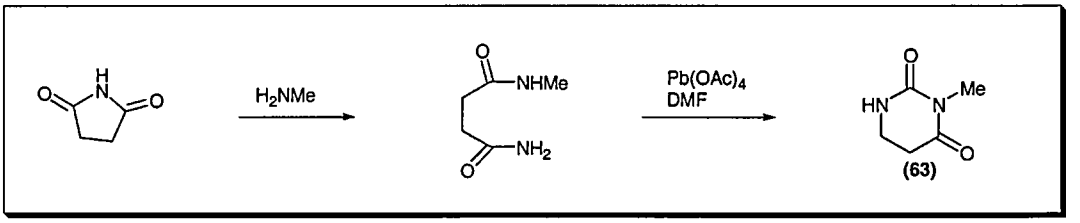

Scheme 54

In this synthesis, nucleophilic attack at the imide yields N-methylsuccinic diamide, which is subjected to oxidative cyclisation using DMF/lead tetra-acetate.
This compound could potentially arise from oxidation of DMPU by both ring and N-methyl oxidation, though the probability of formation of this compound is low since it requires four oxidations. Given that the substrate will be in large excess, the chances of an oxidised product being further oxidised are relatively low. In a biological system, the likelihood of multiple oxidations to occur on the same molecule is even lower, because the hydrophilicity of the metabolite is greater than the substrate thereby making it less likely to occupy the hydrophobic active site in the P450 enzyme.

The synthesis of 1-methyltetrahydropyrimidine-2-one **(61)** was achieved by reaction of dicarbonylimidazole with N-methylpropane-1,3-diamine (Scheme 55).

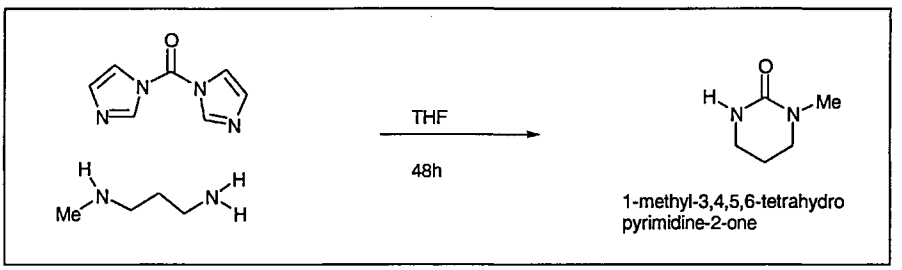

Scheme 55

In order for **(59)** to be formed DMPU must undergo double oxidation. It follows that DMPU is initially oxidised to **(58)**, which would subsequently undergo further oxidation to **(59)**. Synthesis of the alcohol **(58)** was carried out using the procedures shown in Scheme 56.

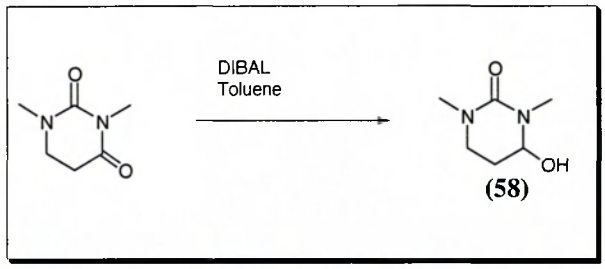

Scheme 56

Unfortunately, the purification of this material proved extremely difficult, with the compound decomposing on the chromatography column. To ascertain that the compound had been made, ^{1}HNMR (Figure 24) and HPLC mass spec (Figure 25) were obtained.

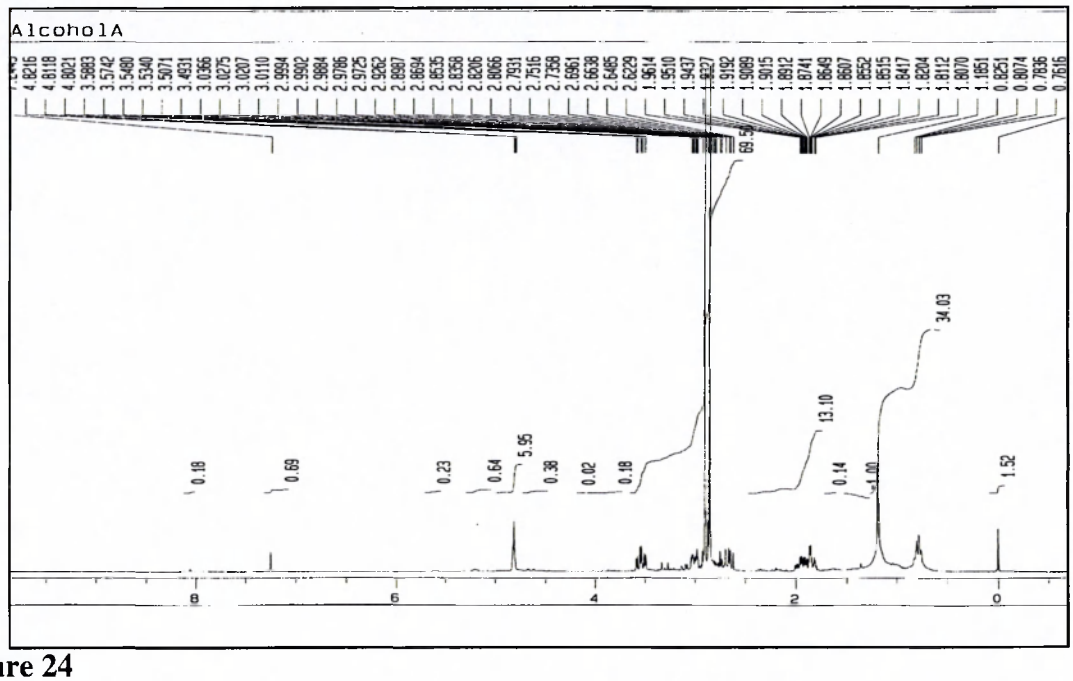

Figure 24

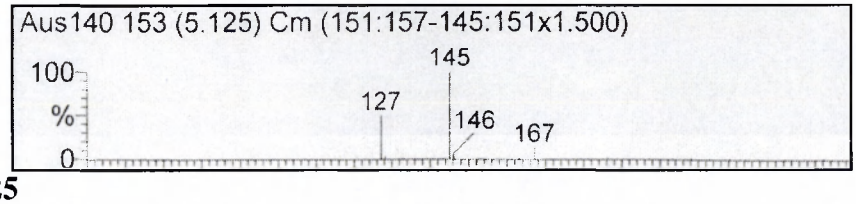

Figure 25

The mass spectrum showed that the compound had the expected mass of 145 for MH^+. Fragmentation at 127 is due to loss of OH and the peak at m/z=167 can be ascribed to ($M+Na^+$). Although the compound is not pure, ^1H NMR indicates the formation of **(64)**. In this spectrum two singlets of 6H δ_H =2.85, 2.90 show the two methyl groups (H^F, H^G) (Scheme 61). A triplet of 1H at δ_H =4.81 shows H^A, and a multiplet at δ_H =1.87, 2H shows H^B and H^C. Due to the puckered nature of the ring (Scheme 57) it can be seen that the OH group has a greater influence over H^D than H^E. This causes a down field shift for H^D resulting in a 1H doublet of triplets at δ_H =3.54, H^E arrives upfield from this at with a 1H multiplet at δ_H =3.14.

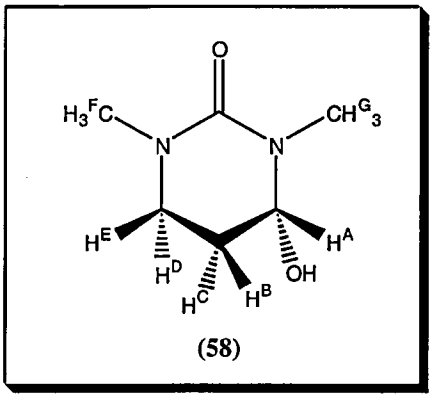

(58)

Scheme 57

Unfortunately, quantitative analysis for **(58)** could not be obtained due to the difficulty in obtaining a pure sample. Nevertheless, comparison of the synthesis reaction mixture and that from the model oxidation reaction mixture reveals the presence of a product that has an identical retention time for a major unknown in the model system thus indicating that the ring oxidised alcohol **(58)** is probably formed in the model oxidations.

Synthesis of the formylhydropyrimidinones was accomplished using a Vilsmeier salt (Scheme 62)

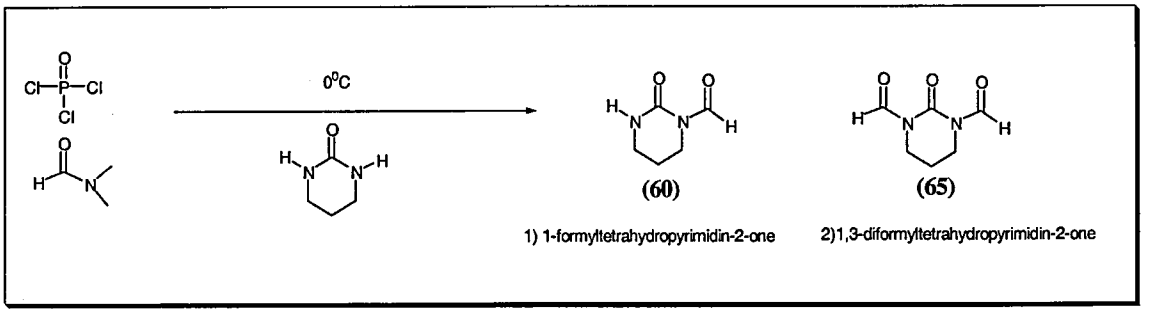

Scheme 58

Both the mono- and diformylated products were isolated. The monoformylated **(60)** is relatively stable compared to **(65)** which readily deformylates in water to afford **(60)**. The latter does not undergo deformylation to tetrahydropyrimininone and is stable in water over a two-day period. This increased stability can probably be ascribed to the formyl groups in **(65)** both being imide-like whereas the formyl group in **(60)** is more amide like, the latter allowing increased delocalisation of the nitrogen non-bonding electron pairs over the amide bond system.

3.4 DMPU model studies

DMPU model studies were carried out using a method similar to that used for HMPA. HPLC analysis was carried out using a Varian photodiode array. The solvent system was as detailed in experimental. Analysis of the reaction mixture reveals that oxidation of DMPU takes place in the ring rather than at the methyl groups. This conforms to previous studies involving N-methyl-2-pipieridinone although with this latter compound methyl group oxidation was observed[86].

Single oxidation of the ring to the corresponding alcohol **(58)** occurs. Unfortunately quantitative analysis could not be carried out since a pure sample of this compound was not obtained. Further oxidation of the alcohol then occurs, resulting in the formation of **(59)**, quantitative analysis of **(59)** allowed a initial rate graph to be constructed (Figure 26). By comparison of these results to that of a graph prepared from a standard solution at varying concentrations an extent of reaction of approximately 3.5 per cent was determined (experiment carried out as per section 4.5.3 [TPPFeCl] = 0.001 M, [tBuOOH] = 0.2 M, [DMPU] = 0.2 M)

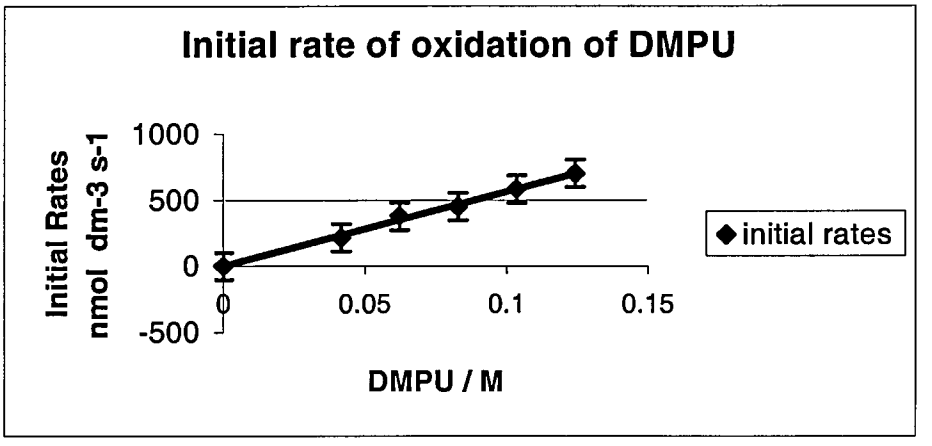

Figure 26

A similar ring system, N-methylpiperidin-2-one has been studied.[86] The observed rate of demethylation for N-methyl-2-piperidinone is 1.7 x 10^{-8} s^{-1} and ring oxidation is 9.4x10^{-5} s^{-1}, in DMPU the rate of ring oxidation is 6 x 10^{-6} s^{-1}. This gives a comparative rate of ring oxidation at 15 fold slower for DMPU. These rates may explain the lack of oxidative demethylation from DMPU since in N-methyl-2-piperidinone this occurs ~ 5000 fold slower than ring oxidation. Since this compound has chemistry similar to DMPU (ring oxidation only 15 fold slower) it can be argued that comparable rates may be observed for DMPU. If this is the case any demethylated product will not have been observed in the analytical system used.

3.4.1 AM1 semi-empirical molecular orbital calculations

Using the self-consistent field semi-empirical AM1 model the heats of formation of the postulated carbon-centred radical intermediates and the oxidised products of the reactions indicated in Scheme 43 were calculated (Table 3).

Table 3 Heats of formation of (ΔH_f) calculated by the AM1 model for DMPU and its postulated radical and oxidised intermediates

Compound	ΔH_f (kcal/mol)
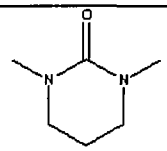	**-29.04**
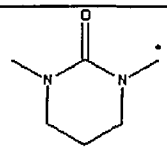	**-4.61**
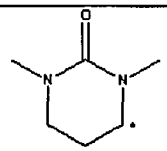	**-10.33**
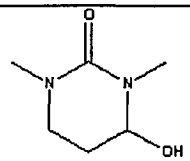	**-73.75**
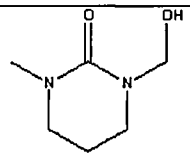	**-78.87**

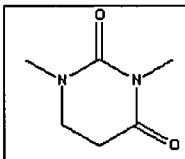	**-62.59**
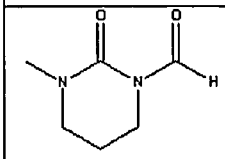	**-64.25**
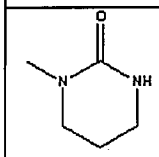	**-34.69**
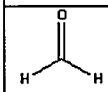	**-31.5**

Using the calculations below it can be seen that formation of a carbon-centred radical on the ring is favoured over that of the N-methyl position. Although the difference in heats of formation of the two radicals is only 5.72 kcal/mol, if this diffeence were reflected in the activation energies then the rate of formation of the ring oxidised intermediate would be 13000 times faster than oxidation of the N-methyl position. Thus, these data predict almost exclusive reaction at the ring carbon. Such calculations have also correctly predicted the reactivity of cyclic amides.[86]

Since $k = (\mathrm{k}T/h)e^{-\Delta G^{\neq}/RT}$

and $\ln k = \ln(\mathrm{k}T/h) - \Delta G^{\neq}/RT$

then $\ln k_1 = \ln(\mathrm{k}T/h) - \Delta G^{\neq}_1/RT$ for ring oxidation

and $\ln k_2 = \ln(\mathrm{k}T/h) - \Delta G^{\neq}_2/RT$ for methyl oxidation

Consequentely, $\ln k_1/k_2 = (\Delta G^{\neq}_2/RT) - (\Delta G^{\neq}_1/RT) = \Delta\Delta G^{\neq}_{2,1}/RT$

Assuming that the difference between ΔH_f of the radicals reflects the difference in $\Delta G^{\neq}$,

$$\Delta\Delta G^{\neq}_{2,1} \approx \Delta H_2 - \Delta H_1 \approx -4.61 + 10.33 = 5.76$$

So, $\ln k_1/k_2 = 5.76 \times (4.18 \times 10^3)/(8.31 \times 303.2) = 9.49$

and $k_1/k_2 = 13227$

Interestingly, the data for the putative radical intermediates contrast with those of the hydroxylated products where formation of N-hydroxymethylDMPU is thermodynamically favoured over the ring hydroxylated product. The model experiments described here have shown the formation of ring hydroxylated products in the form of singly and doubly oxidised DMPU. Thus, these are the kinetic, rather than the thermodynamic products of oxidation by TPPFeCl/^{t}BuOOH

3.5 Further work

3.5.1 Alkynes in C-centred radical trapping

For amides, it has been shown that microsomal oxidation results in N-dealkylation. The possible routes of demethylation are shown in (Scheme 32). This involves either electron abstraction from the heteroatom (nitrogen) or H-atom abstraction to form a C-centred radical. For the amide DMF, it has been demonstrated that H-atom abstraction results in C-centred radical formation. Due to the similarities between the amide, urea and phosphoramide functional groups, it was decided that H-atom abstraction would also be the most likely route of dealkylation for both HMPA and DMPU. To identify whether C-centred radicals are involved in the model reactions an attempt to synthesise substrates incorporating an alkyne probe would allow this to be determined.

Scheme 59, underlines the method development for making amide-derivatised alkyne probes. Several routes for the synthesis of alkyne probe derivatives have been attempted, it is hoped that this will form the basis for future work in this area.

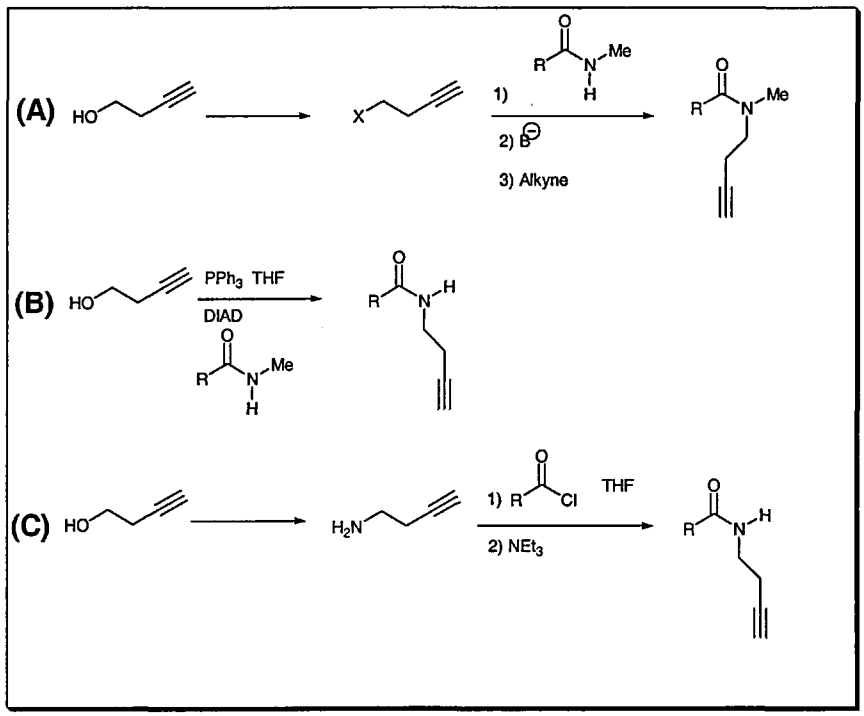

Scheme 59

Route A utilises a strong base to remove a hydrogen atom from the amide nitrogen to form an anion; which can undergo substitution reaction using an appropriately derivatised butyne. For the phosphoramide derivatives, PMPA was used as the equivalent amide. Scheme 60 shows the different butynes and bases used in the attempted formation of the phosphoramide derivative **(70)**.

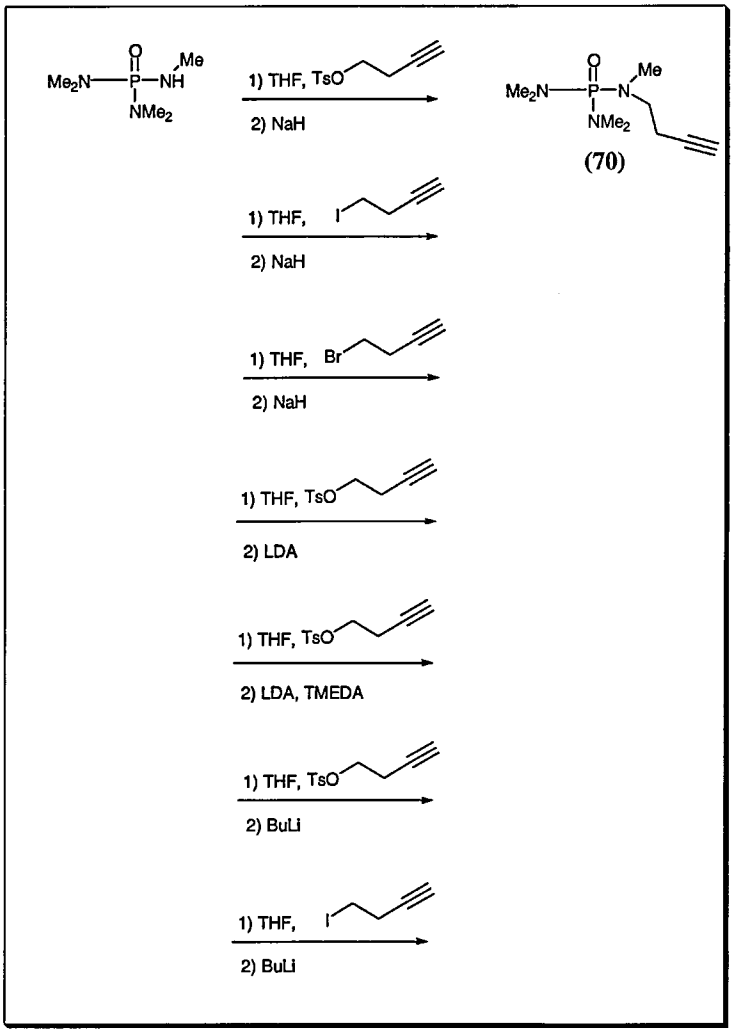

Scheme 60

In none of the above experiments was the desired phosphoramide derivative made, only PMPA being recovered. One possible explanation for the reactions not accomplishing the desired transformation is that the nitrogen anion is insufficiently nucleophilic to undergo substitution. To improve the strength of the anion different bases were used (BuLi, NaH, LDA and ^{t}BuOK) in the hope that by varying the metal cation the strength of the anion could be increased. In the event this was not observed. Another method of increasing the strength of the anion is by complexing the metal cation. Thus TMEDA was employed with the bases derived from lithium salt. Again, the reaction failed.

An alternative approach involved altering the leaving group on the butyne; in this case, the tosyl group was replaced by bromine or iodine. In no case was the synthesis successful.

For route (B) Scheme 59, a variation of the Mitsunobu reaction was carried out. This should have resulted in the coupling of the amide with the alcohol. However, the only butyne-substituted product obtained was (71).

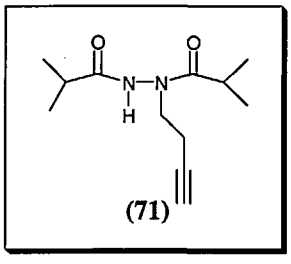

For route (C), the idea was to form the 4-aminobutyne from the parent alcohol then perform a substitution reaction with the phosphoramide acid chloride equivalent. 4-Aminobutyne was prepared according to Scheme 61.

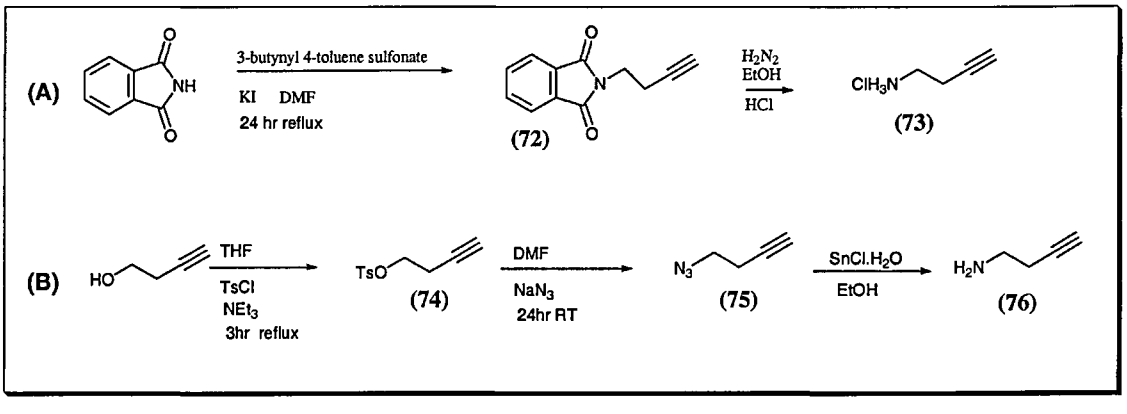

Scheme 61

In Scheme 61, pathway (A), the N-(3-butynyl)phthalimide (72) is made from a Mitsunobu reaction involving phthalimide, 3-butyn-1-ol and DIAD. Unfortunately, the

following step involving hydrazine and salt formation proved too difficult to purify, so the longer approach (Scheme 61, pathway B) was undertaken.

Pathway B involves the conversion of an alcohol to the corresponding tosylate (**74**); this is then converted to an azide (**75**), which is subsequently reduced to the amine (**76**). Formation of the amine was achieved but on a small scale. Attempted coupling of the amine to an acid chloride failed but this may be due to the scale, and so may work on a larger scale. This line of research was stopped due to a lack of time, but it can be seen that the basis for further research has been set in place with (**76**) having been synthesised. This leaves only the coupling of the amine to the relevant acid chloride to prepare the desired butynyl derivative. When this is prepared the butynyl derivative should be exposed to the same oxidation conditions as those previously used for HMPA. When this is achieved analysis of the reaction products will determine if a C-centred radical is formed as an intermediate (The formation or absence of the relevant cyclised products indicating formation of a C-centred radical).

3.5.2 Investigating the deuterium isotope effect on DMPU

This study demonstrates that oxidation of DMPU *via* model studies occurs on the ring. Previous studies of amide solvents show how oxidation results in the formation of a C-centred radical. DMPU has a similar functional group to amides, hence if DMPU forms a C-centred radical during oxidation it is to be expected that H-atom abstraction will occur. Such H-atom abstraction must occur at the ring methylene, given the observed product analysis. This being the case, an investigation into the deuterium isotope effect will add weight as to whether or not H-atom abstraction occurs. DMPU is a symmetric molecule, hence there are two sites in the ring with equal opportunity

for attack. To allow accurate determination of the deuterium isotope effect both need to be fully deuterated. The following Scheme shows several possible route of synthesis for **(77)**.

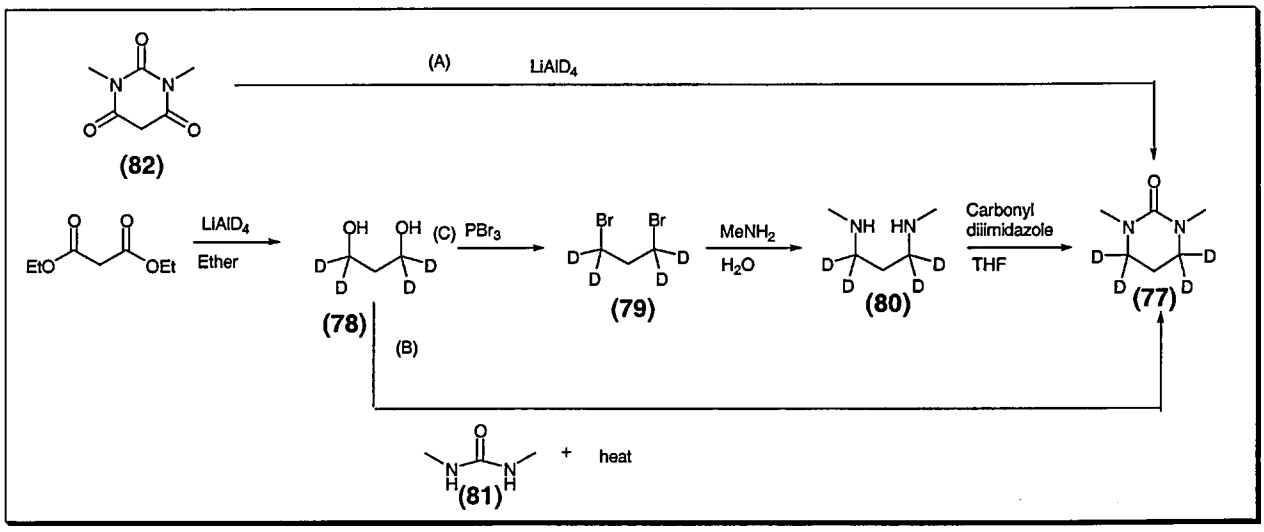

Scheme 62

The above synthese were attempted using $LiAlH_4$ to determine their feasibility prior to carrying out the experiment with expensive $LiAlD_4$. In pathway (A) Scheme 62 reduction of dimethylbarbituric acid was attempted. This did not give the required product; in retrospect this reaction is unlikely to work due to the acidic protons lying between the two carbonyl groups. These will be removed easier than reduction of the carbonyl groups, so negating the desired carbonyl reduction. At this stage, a retrosynthetic analysis was undertaken. According to this, the desired deuterium insertion is carried out by reduction of diethyl malonate. This reaction was carried out using $LiALH_4$ and afforded **(78)** in a 52 per cent yield. Using this latter material, it is possible to follow two routes. The most obvious is pathway (C) Scheme 62, bromination of the diol **(78)** to **(79)**, followed by conversion to the diamine **(80)** and finally coupling with carbonydiimidazole to form the desired product. Bromination of the diol was successful but the following conversion to the amine gave a large mixture

of products. Because of this, pathway (B) Scheme 62 was attempted. This allows direct coupling of the diol **(78)** to dimethylurea **(81)** affording the desired product. This was attempted and afforded the desired product in 42 per cent yield. The final deuterated product was not synthesised due to a lack of time but the methodology has been set in place for future work in this area. This is an adaptable methodology since the diethyl malonate may be replaced with 3-hydroxypropanoic acid ethyl ester, this allows reduction with $LiAlD_4$ to the alcohol at only one site. Final coupling of this will give DMPU but with only one ring site deuterated.

Future work will undoubtedly focus on microsomal oxidation of DMPU. To study the deuterium isotope effect with microsomal oxidation consideration must be given to how microsomes attack specific sites on a molecule. Previous work with amides has shown on that although ring oxidation is preferred in model studies, when microsomal oxidation is carried out significant amounts of N-methyl oxidation also occurs. To allow determination of the deuterium isotope effect on N-methyl oxidation a method was developed where deuterium was incorporated on to the N-methyl groups (Scheme 63)

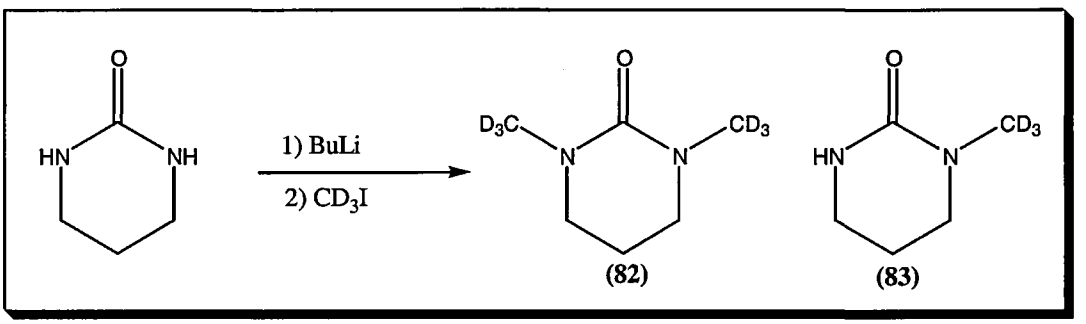

(82) (83)

Scheme 63

The above synthesis was carried out but only **(83)** was obtained. Further reaction of this compound would afford **(82)**. This methodology can also be adapted to making

DMPU with deuterium incorporated at one methyl site and hydrogen at the other. This could be accomplished by replacing tetrahydropyrimidinone with 1-methyltetrahydropyrimidin-2-one.

Analytical techniques and synthetic protocols should make the final stages of this project easily obtainable for future workers in this area. This would be a profitable line of research with results hopefully giving insight into why DMPU is non-toxic. Using this knowledge should allow the development of new, safer solvents.

4.0 Experimental

4.1 HPLC

Separation of amides was achieved using a 5μm C18 25cm Waters Symmetry column with an eluent system of 50% acetonitrile, 50% H_2O (flow rate 1ml/min, loop: 20μl). Identification was achieved by comparison of retention times and diode array UV-VIS spectra with those of synthetic standards.

Separation of phosphoramides was achieved using a 5μm 25cm PLRP column with an eluent system: time t=0 to 5 min, 5% acetonitrile, 95% H_2O; time t=5.1 to t=25.0 min, 10% acetonitrile, 90% H_2O; time t=25.1 to t=35 min, 100% acetonitrile (flow rate 1ml/min, loop: 20μl). Identification was achieved by comparison of retention times with those of synthetic standards.

4.2 Gas Chromatography

Separation of phosphoramides was achieved using a Perkin Elmer chromatograph with direct on-column injection (column: BP5 20m x 0.5mm 0.22μm i.d.; gradient: isothermal at 70 °C for 1 minute, thermal gradient from 70 °C to 300 °C with a ramp rate of 10 °C/min, isothermal at 300 °C for 10 min; detector: FID at 250 °C; injection temperature 210 °C).

4.3 Spectroscopy

NMR spectra were recorded using JOEL Lamda 300 spectrometer operating at 300 MHz for ^1H chemical shifts, δ, are reported in p.p.m. from tetramethylsilane and

coupling constants are reported in Hz. IR spectra were recorded using a Nicolet 205 FTIR spectrometer.

4.4 Solvents and Reagents

All chemicals were obtained from commercial sources.

Solvents were dried by CaH and distilled onto molecular sieves.

4.5 Synthesis

For all compounds purity was determined by ^{1}H NMR where only the peaks relevent to the compound were observed indicating >96% purity.

N-Methylbenzamide[86] (50)

To a solution of methylamine (0.33 mol, 10.25 g,) and NaOH (0.2 M, 400 cm^3), benzoyl chloride was added drop-wise with stirring. After stirring for 10 min the N-methylbenzamide product was extracted with DCM and recrystalised from EtOH/H_2O to give long white crystals.

m.p. 81°C lit m.p. 82°C

Yield 86%

$\delta_H(CDCl_3)$: 3.01 (3H, d, *J*=5.1, N-**Me**), 6.24 (1H, s, N-**H**), 7.39-7.52 (3H, m, **Ph**CO) 7.75 (2H, d, *J*=5.0, **Ph**CO)

$\delta_C(CDCl_3)$: 26.85 (N**Me**), 126.82 128.56 (*ortho/meta*-**Ph**), 131.35 (*para*-**Ph**), 143.5 (*ipso*-**Ph**), 170.00 (N**C**O)

m/z: 135 ($PhCON^+CH_2$), 105 ($PhCO^+$), 77 (Ph^+)

N-Formyl-N-methylbenzamide[86] (51)

Dimethylbenzamide (500 mg, 0.0336 mol) and TPPFeCl (23.7 mg, 33.6 μmol) were dissolved in dry DCM (25 cm^3). *tert*-Butylhydroperoxide (20.74 mg, 1.65 mmol) was added. The mixture was heated to 30 °C with agitation. At 2, 4, 6 and 8 h intervals further portions of *tert*-butylhydroperoxide (1.65 mmol) were added. The mixture was left overnight, treated with activated charcoal, filtered and purified using silica gel column chromatography (hexane/ethyl acetate 5:2) to yield a viscous oil.

Yield 7.3%

$\delta_H(CDCl_3)$: 3.21 (3H, s, N-**Me**), 7.38 (5H, m, **Ph**CO) 8.92 (1H, s, **H**CO)

$\delta_C(CDCl_3)$:27.48 (N-**Me**), 128.80 128.9 (*ortho/meta*-**Ph**), 132.16 (*para*-**Ph**), 133.40 (*ipso* -**Ph**), 164.36 (N**C**OH), 172.34 (**C**CON)

ν_{max}/cm^{-1} 1692 (C=O)

.4.5.1 HMPA derivatives

N-Chloromethylpentamethylphosphoramide (55)

Under nitrogen, pentamethylphosphoramide (0.02 mol, 3.3 g) was dissolved in chlorotrimethylsilane (TMSCl) (50 cm^3). Paraformaldehyde (2 g) was then added and the solution heated under reflux for 2 h. The solution was filtered and TMSCl removed under reduced pressure to yield N-chloromethyl-N-pentamethylphosphoramide quantitatively in 100% conversion to yield a clear viscous oil.

Yield 100%

$\delta_H(CDCl_3)$: 2.72 (12H, d, J=10.1, N-**Me**$_2$), 2.84 (3H, d, J=13.9, N-**Me**), 5.31(2H, d,

20.3, N**CH$_2$**Cl)

N-Alkylphosphoramides[108]

The appropriate amine (0.179 mol) was dissolved in dry ether (40 cm^3) at -10°C. To this was added dropwise an ethereal solution of tetramethylphosphorodiamidic chloride (0.059 mol, 4.94 g). The solution was warmed to room temperature and stirred for 2-3 h. The resulting hydrochloride salt was filtered off, the ether solution washed with water, then dried ($MgSO_4$), and the ether removed under reduced pressure. The crude mixture was separated by column chromatography (chloroform/EtOH 7:1 v/v).

Pentamethylphosphoramide[108]**(42)**

Yield (5.8g, 68.0%) as a clear liquid

$\delta_H(CDCl_3)$: 2.08 (1H,s, N-**H**), 2.47 (3H, dd, *J*=11.5, 15.8, N-**Me**), 2.56 (12H, d, *J*=9.52, N-**Me$_2$**)

$\delta_C(CDCl_3)$:27.12 (N-**Me**), 36.77 (N-**Me$_2$**)

ν_{max}/cm^{-1} 3251w (H-N), 2948 (C-H), 1218s (P=O), 776s (P-N)

N-Formylpentamethylphosphoramide[101] **(45)**

To an ice-cold solution of HMPA (1.8 g, 0.01 mol) in H_2O (20 cm^3) a solution of $KMnO_4$ (3.2 g, 0.2 mol) in H_2O (100 cm^3) was quickly added. The mixture was allowed to stir for 5 min then the ice bath was removed and the solution left to stir at

room temperature for 45 min. A cold solution of Na_2SO_3 (5 g, 0.04 mol) in H_2O (50 cm^3) was added, followed by 2M H_2SO_4 (dropwise) till the solution turned clear (approx. 30 cm^3). The solution was extracted with chloroform (3 x 50 cm^3), the organic extract washed with brine (1 x 20 cm^3), dried ($MgSO_4$) and evaporated under reduced pressure to yield the product as a clear liquid.

Yield 66%

$\delta_H(CDCl_3)$: 2.64 (12H, d, *J*=10.1, N-**Me**$_2$), 2.65 (3H, d, *J*=8.6, N-**Me**), 8.65 (1H, s, **NH**CO)

$\delta_C(CDCl_3)$: 27.50 (N-**Me**), 36.54 (N-**Me**$_2$), 165.34 (**C**O)

ν_{max}/cm^{-1} 2816w (C-H), 1685s (HNC=O), 1284s (P=O), 755m (P-N)

Bis(dimethylamino)-N-(*tert*-butylhydroperoxymethyl)-N-methylphosphoramide (54)

PMPA (0.5 g, 0.003 mol) was added to a 37% formaldehyde solution (0.73 g, 0.009 mol). This solution was allowed to stir at room temperature for 24 h. The solvent was removed under reduced pressure, then *tert*-butylhydroperoxide (3 cm^3) was added, followed by two drops of TFA. The solution was allowed to stir for a further 3 h, after which the solvent was removed under reduced pressure to yield to product as a clear liquid.

Yield 95%

$\delta_H(CDCl_3)$: 1.21 (12H, s, O-O-C(**CH**$_3$)$_3$), 2.64 (8H, d, *J*=9.51, P(N**Me**$_2$)$_2$, 2.74 (3H, d, *J*=8.25, PN**Me**CH$_2$OOtBu) 4.79 (2H, d, 4.77, *J*=11.73, NC**H**$_2$OOtBu

$\delta_C(CDCl_3)$: 26.38 (C(**C**H$_3$)), 34.35 (N**C**H$_3$), 36.81 (N(**C**H$_3$)$_2$, 80.50 (**C**(CH$_3$)), 92.15 (N**C**H$_2$OOC)

ν_{max}/cm^{-1} 2800 (C-O), 1365s ($C(CH_3)_3$), 1250s (P=O), 750m (P-N),

Accurate Mass ES+, [M+H]: obtained 268.1793, expected 268.1790

3-Butynyl 4-toluenesulfonate[109] (74)

Under a nitrogen atmosphere, 3-butyn-1-ol (0.1 mol, 7.01 g) and triethylamine (0.11 mol, 11.1 g) were dissolved in dry THF (100 cm^3). To this, a solution of THF containing 4-toluenesulfonyl chloride (0.1 mol, 19.1 g) was added dropwise and the reaction mixture was heated at reflux for 2 h. After cooling a white precipitate was filtered and the solvent removed under reduced pressure, to give a dark oil. The oil was resuspended in ether (50 cm^3), washed with 1M hydrochloric acid (2 x 20 cm^3), saturated sodium hydrogen carbonate (2 x 20 cm^3) and washed again with water (2 x 20 cm^3). The organic layer was dried ($MgSO_4$) and the solvent removed under reduced pressure. The resultant oil was purified by column chromatography on silica (10:1 hexane/EtOAc) to give the desired product as a clear pale yellow liquid.

Yield 74%.

$\delta_H(CDCl_3)$:1.95 (1H, t, *J*=2.6, **CH**), 2.43 (3H, s, **Me**), 2.58 (2H, dt, *J*=2.6 7.7, CH_2CCH), 4.06 (2H, t, *J*=7.8, CH_2O), 7.28 (2H, d, *J*=8.4, *meta*-**Ph**), 7.78 (2H, d, *J*=8.3, *ortho*-**Ph**)

$\delta_C(CDCl_3)$: 19.43 (CH_2CCH), 21.64 (**Me**), 67.39 (OCH_2), 70.74 (CH_2CCH), 78.34 (CH_2CCH), 127.96 129.88 *ortho/meta* **Ph**), 132.81 144.99 (*ipso*-**Ph**)

N-(3-Butynyl)phthalimide[110,111] (72)

3-Butynyl 4-toluenesulfonate (0.067 mol, 14.2 g), potassium iodide (3.6 mmol, 0.6 g) and potassium phthalimide (0.074 mol, 13.65 g) were dissolved in dry

dimethylformamide (200 cm^3) and refluxed for 24 h under a nitrogen atmosphere. After cooling, the solution was poured onto crushed ice (200 g). Extraction with diethyl ether (4 x 200 cm^3) was followed by washing with sodium hydroxide (200 cm^3), water (2 x 100 cm^3), and 0.5M hydrochloric acid (200 cm^3). The organic layer was dried ($MgSO_4$) and the solvent removed under reduced pressure to leave the product which was recrystallised from diethyl ether/hexane as a white solid.

m.p. 134-135 °C lit m.p. 133-134 °C

Yield 86%

$\delta_H(CDCl_3)$: 1.95 (1H, t, *J*=2.55, CH_2CCH), 2.6 (2H, dt, *J*=2.58, 6.96, NCH_2CH_2), 3.85 (2H, t, *J*=6.96, NCH_2), 7.75 (4H, m, **Aryl**)

$\delta_C(CDCl_3)$: 18.32 (CH_2CCH), 36.49 (NCH_2), 70.22 (CCH), 80.01 (CH_2CCH) 123.36 (Aryl CH), 132.23 (Aryl CHCCO), 134.02 (Aryl CH), 172.20 (NCO)

ν_{max}/cm^{-1} 3200s (-C≡C-H) 2140w (C≡C), 1650 (C=O)

4-Aminobutyne hydrochloride[112] **(73)**

NaN_3 (5.62 g, 117.2 mmol) was added to a solution of 3-butynyl 4-toluenesulfonate (5.25 g, 23.44 mmol) in dry dimethylformamide (30 cm^3), and the resulting suspension was stirred for 24 h. The mixture was partitioned between water (100 cm^3) and diethyl ether (100 cm^3), the aqueous phase was extracted with diethyl ether (50 cm^3) and the combined organic phase thoroughly washed with water (5 x 25 cm^3), dried with $MgSO_4$, and concentrated to remove most of the ether. The resulting clear liquid containing 3-butynyl azide was used without further purification. This solution was dissolved in methanol (75 cm^3), $SnCl_2.2H_2O$ (10.58g, 46.88 mmol) was added, the solution was stirred at room temperature for 24 hr, after which time the solvent was

evaporated under reduced pressure, and the residue dissolved in 10% aqueous NaOH. This solution was extracted with dichloromethane (5 x 40 cm^3). The combined organic phase was dried (Na_2SO_4), then a saturated solution of HCl in diethyl ether (20 cm^3) was added, and the resulting precipitate collected by filtration affording the required hydrochloride. The filtrates were concentrated to dryness to afford additional hydrochloride as yellow prisms.

Yield 21%

$\delta_H(D_2O)$: 2.42 (1H, t, *J*=1.5, **CH**), 2.54 (2H, dt, *J*=1.5, 4.2, **CH_2**CH), 3.10 (2H, t, *J*=5.1, N**CH_2**)

$\delta_C(D_2O)$:17.66 (**CH_2**CCH), 39.00 (N**H_3CH_2**), 73.38 (**CH**), 80.24 (**CH_2C**CH)

ν_{max}/cm^{-1} 3200s (-C≡C-H) 2140w (C≡C), 2700 (-NH_2^+)

4.5.2 DMPU Derivatives

1-Methyltetrahydropyrimidin-2-one[113,114] (61)

Under nitrogen, N-methyl-1,3-propanediamine (0.02 mol, 1.48 g) was dissolved in THF (10 cm^3) and carbonyldiimidazole (0.02 mol, 3.24 g) dissolved in THF (30 cm^3) was added dropwise with stirring. The solution was allowed to stir at room temperature for 48 h, then acidified using 2M HCl. Both THF and water were removed under reduced pressure and the crude mixture washed through silica plug with MeOH to afford 1-methyltetrahydropyrimidin-2-one.

m.p. 91-92 °C lit m.p. 90-92 °C

Yield 46%

δ_H ($CDCl_3$): 1.88(4H, quintet, *J*=5.7 $CH_2\mathbf{CH_2}CH_2$), 2.86 (3H, s, N-**Me**), 3.18 (2H, dt, *J*=2.6, 5.7, HN$\mathbf{CH_2}CH_2$), 3.24 (2H, t, *J*=5.9, $\mathbf{CH_2}CH_2$NMe), 4.92 (1H, s, N-**H**)

δ_C($CDCl_3$): 21.53 ($CH_2\mathbf{CH_2}CH_2$), 35.31 (N-**Me**), 40.02 (MeN-$\mathbf{CH_2}$), 47.45 (HN-$\mathbf{CH_2}$), 118.69 (**C**O)

ν_{max}/cm^{-1} 3387b (N-H), 1650 (NCON)

1,3 Dimethyl-5,6-dihydropyrimidine-2,4-dione[115] (59)

1,3-Dimethylurea (0.1 mol, 8.81 g), acrylic acid (0.05 mol, 3.6 g) and hydroquinone (0.0004 mol, 0.05 g) were added together under N_2 then heated at reflux for 2 h. After cooling the reaction was quenched in H_2O (20 cm^3) and extracted with chloroform (5x20 cm^3). The combined extracts were washed with K_2CO_3 (0.5M, 20 cm^3), dried ($MgSO_4$) and the solvent removed under reduced pressure to afford a crude mixture that was purified by column chromatography (hexane/EtOAc 1:1) to give 1,3-dimethyl-5,6-dihydropyrimidine-2,4-dione as white prisms.

m.p. 47-49 °C lit m.p. 48-49 °C

Yield 54.8%

δ_H($CDCl_3$): 2.71 (2H, t, *J*=6.9, CO$\mathbf{CH_2}$), 3.03 (3H, s, CON**Me**), 3.15 (3H, s, CONMeCO), 3.34 (2H, t, *J*=6.9, NMe$\mathbf{CH_2}$)

δ_C($CDCl_3$): 27.81 (OCN**Me**CO), 31.67 (O$\mathbf{CCH_2}$), 36.11 (OCN**Me**$\mathbf{CH_2}$), 43.15 (MeN$\mathbf{CH_2}$), 153.23 (CH_2 NCO), 169.63 (N**C**ON)

ν_{max}/cm^{-1} 1714s (NCOC), 1661s (NCON)

1-Methyl-5,6-dihydropyrimidine-2,4-dione[115] (64)

N-Methylurea (0.1 mol, 7.4 g), acrylic acid (0.05 mol, 3.6 g) and hydroquinone (0.0004 mol, 0.05 g) were added together under N_2 then heated at reflux for 2 h. After cooling the reaction mixture was quenched in H_2O (20 cm^3) and extracted with chloroform (5 x 20 cm^3). The combined chloroform extracts were washed with K_2CO_3 (0.5 M, 20 cm^3), dried ($MgSO_4$) and the solvent removed under reduced pressure to afford a crude mixture that was purified by column chromatography (hexane/EtOAc 1:2, EtOAc) to yield white prisms.

m.p. 129-130 °C lit m.p. 129-130 °C

Yield 21%

$\delta_H(CDCl_3)$: 2.65 (2H, t, *J*=6.8, $COCH_2$), 2.98 (3H, s, N-**Me**), 3.4 (2H, t, *J*=6.9, $HNCH_2$), 8.64 (1H,s, N-**H**)

$\delta_C(CDCl_3)$: 30.86 ($OCCH_2$), 34.81 (N-**Me**), 43.99 (NCH_2), 153.29 ($NCOCH_2$), 170.16 (NCONCO)

ν_{max}/cm^{-1} 3220 (N-H), 1712 (NCON), 1700 (NCOC)

3-Methyl-5,6-dihydropyrimidine-2,4-dione[116 117] (63)

Succinimide (10 g) was shaken with aqueous methylamine (25 cm^3; 33%). On standing, the solution deposited a crystalline solid, which was collected and recrystallised from ethanol to give N-methylsuccinamide as prisms. N-Methylsuccinamide (1.0 g) was then stirred at 60-70°C for 2 h with lead tetra-acetate

(3.5 g) in dimethylformamide (10 cm^3), and the mixture evaporated under reduced pressure. Extraction of the residue with hot ether, and crystallisation of the extracted material from ethanol gave the title compound (0.51 g).

m.p. 171-173 °C lit m.p. 170-172 °C

Yield: 50%

$\delta_H(CDCl_3)$: 2.73 (2H, t, *J*=6.78, OC-C**H**$_2$), 3.17 (3H, s, N-**Me**), 3.41 (2H, dt, *J*=2.76, 6.78, NH-C**H**$_2$), 5.96 (1H, bs, N-**H**)

$\delta_C(CDCl_3)$:27.03 (OC**C**H$_2$), 31.45 (N-**Me**), 35.32 (N**C**H$_2$), 157.0 (N**C**OCH$_2$), 169.79 (N**C**ONCO)

ν_{max}/cm^{-1} 3210 (N-H), 1750 (NCON), 1700 (NCOC)

Synthesis of N-Formylamides[118]

Dimethylformamide (0.006 mol, 0.44 g) was treated dropwise, under cooling and stirring, with phosphoryl chloride (0.008 mol, 1.23 g). The mixture was stirred at room temperature for 15 min, then cooled using an ice bath before the appropriate amide (0.003 mol) in acetonitrile (10 cm^3) was added dropwise. The reaction mixture was then allowed to warm to room temperature, then heated to reflux for 15 min. The reaction mixture was cooled, and quenched with ice, then extracted with chloroform. The organic layer was washed to neutrality with sodium hydrogen carbonate solution, dried ($MgSO_4$) and concentrated under reduced pressure. The crude mixture was purified by column chromatography (DCM containing 1.5%MeOH)

1,3-Diformyltetrahydropyrimidin-2-one (65)

m.p. 108-109 °C

Yield 2.3%

$\delta_H(CDCl_3)$: 2.01 (2H, quintet, *J*=6.1), 3.68 (4H, t, *J*=6.1), 9.43 (2H, s)

$\delta_C(CDCl_3)$: 19.92 ($CH_2\mathbf{C}H_2CH_2$), 39.31 ($\mathbf{N}CH_2$), 153.18 (**N**CON), 161.90 (**N**COH)

ν_{max}/cm^{-1} 1662 (C=O)

1-Formyltetrahydro-pyrimidin-2-one (60)

m.p. 90-95 °C

Yield 0.4%

$\delta_H(CDCl_3)$: 1.96 (2H, quintet, *J*=5.9, $CH_2\mathbf{C}H_2CH_2$), 3.34 (2H, dt, *J*=2.6, 6.0, $NH\mathbf{C}H_2$), 3.67 (2H, t, *J*=6.1, $CON\mathbf{C}H_2$), 6.35 (1H, s, N**H**), 9.35 (1H, s, CO**H**)

$\delta_C(CDCl_3)$: 20.79 ($CH_2\mathbf{C}H_2CH_2$), 38.97 ($HN\mathbf{C}H_2$), 39.77 ($CON\mathbf{C}H_2$), 153.95 (**N**CON), 162.43 (**N**COH)

ν_{max}/cm^{-1} 3240 (NH), 1690 (CO)

4-Hydroxy-1,3-dimethyltetrahydropyrimidin-2-one[119] **(58)**

To a stirred solution of 1,3-dimethyldihydropyrimidine-2,4-dione (1.6 g, 11.3 mmol) in toluene (20 cm^3) was added DIBAL 1M (12 cm^3, 12 mmol) dropwise. The reaction mixture was stirred for 6 h (endpoint determined by HPLC). Methanol was added to quench the reaction then the mixture was filtered, the toluene removed under reduced pressure and the resultant crude product analysed by HPLC mass spectrometry

m/z: 167 (M-Na), 145 (M^+), 127 (M^+-OH_2)

$\delta_H(CDCl_3)$: 1.87 (2H, m, $CH_2\mathbf{C}H_2$CHOH), 2.85 (3H, s, N-**Me**), 2.90 (3H, s, H_2OCN**Me**), 3.14 (1H, m, NMeC**H**H), 3.54 (1H, dt, *J*=4.2, 12.1, NMeC**H**H), C**H**OH, 4.81 (1H, t, *J*=3.0, OC**H**N)

1,3-Dibromopropane [120] (79)

Phosphorus tribromide (5.13 g, 0.019 mol) and 1,3-propanediol (1.12 g, 0.014 mol) were mixed at 0 °C and permitted to react slowly as the temperature rose. The mixture was stirred at 125 °C for 3 h, then allowed to cool; 10 cm^3 of water were added and a small amount of orange precipitate was removed by filtration. The filtrate was extracted 4 times with 20 cm^3 of DCM and the combined organic fractions were dried over $MgSO_4$; 1,3-dibromopropane was isolated as a clear liquid without further purification.

Yield 82%

$\delta_H(CDCl_3)$: 2.40 (2H, quintet, *J*=4.9,$CH_2\mathbf{CH_2}CH_2$), 3.57 (4H, t, *J*=4.8, $\mathbf{CH_2}CH_2\mathbf{CH_2}$)

1,3-Propanediol[121] (78)

Diethylmalonate (3.5 g, 0.016 mol) in diethyl ether (10cm^3) was added dropwise to lithium aluminium hydride (2 g, 0.53 mol) in ether (50 cm^3) and the reaction mixture refluxed for 2 h after addition was complete. Water (5 cm^3) was added cautiously, followed by 10_N-H_2SO_4 (40 cm^3). The aqueous solution was saturated with sodium chloride and extracted with diethyl ether. The organic fractions were combined, dried with $MgSO_4$ and the solvent removed to afford the desired product as a clear liquid.

Yield 43%

$\delta_H(CDCl_3)$: 1.79 (2H, quintet, *J*=5.5, $CH_2\mathbf{CH_2}CH_2$), 3.64 (2H, s, **OH**), 3.81 (4H, t, *J*=5.3, $\mathbf{CH_2}CH_2\mathbf{CH_2}$)

1,3-Dimethyl-3,4,5,6,-tetrahydro-2(1H)-pyrimidinone (57)

1,3-Propanediol (10 g, 0.13 mol) and 1,3-dimethylurea (11.56 g, 0.13mol) were added together, the reaction mixture was then heated for 24 h at 160 °C. The reaction mixture was distilled under reduced pressure to afford the desired product as a clear liquid

Yield 64%

$\delta_H(CDCl_3)$: 1.76 (2H, quintet, *J*=5.7, $CH_2CH_2CH_2$), 2.73 (6H, s, N**Me**), 3.76 (4H, t, *J*=5.5, NCH_2)

1-(Trideuteromethyl)tetrahydropyrimidin-2-one (83)

Under nitrogen, tetrahydropyrimidinone (1 g, 0.01mol) was added to dry toluene (50 cm^3). Whilst stirring BuLi (0.011mol) was added and the mixture stirred for 30 minutes. Iodomethane-d_3 (2.9 g, 0.02 mol) was then added dropwise. The solution was stirred for a further 24 h, after which water (2 cm^3) was added. The resultant solution was filtered, solvent removed under reduced pressure and purified by column chromatography (10% MeOH in EtOAc).

m.p. 90-91 °C

Yield 39%

$\delta_H(CDCl_3)$: 1.93 (2H, quintet, *J*=6.0, $CH_2CH_2CH_2$), 3.21 (2H, t, *J*=6.0, CH_2CH_2NMe), 3.27 (2H, dt, *J*=2.6, 5.5, $HNCH_2CH_2$)

$\delta_C(CDCl_3)$: 21.19 ($CH_2CH_2CH_2$), 30.92 (N-**Me**), 40.51 (MeN-CH_2), 47.34 (HN-CH_2), 118.72 (**CO**)

m/z: $M^+ = 118$

4.5.3 Model Study reactions[86]

For N,N-dimethylbenzamide

5,10,15,20-Tetraphenyl-21H,23H-porphine iron(III) chloride (0.001 M) and substrate (0.2M) were allowed to stir in DCM (10 cm^3) at 30°C for 10 min; *tert*-butylhydroperoxide (170 µl, 0.2M in DCM) was then added. At regular intervals a 100 µl aliquot was quenched in methanol (200 µl). This was subsequently treated with 1M methanolic KOH (200 µl), after a further 30 min, the solution then neutralised with 1M methanolic HCl (200 µl). The treated aliquot was evaporated under nitrogen, resuspended in acetonitrile and analysed by either HPLC or GC

For all other substrates

The above methodology was followed, but the 100 µl aliquot was made up to 1 cm^3 using MeOH and did not undergo the base/acid treatment.

Accuracy

For all model study experiments each sample was tested twice. This gave an error of ± 5%.

4.5.4 Molecular orbital calculations

Structural determination and heats of formation (ΔH_f) for the cyclic ureas and their postulated intermediate radicals, were calculated using the semi-empirical AM1 self-consistent-field molecular-orbital program within the MOPAC package.[122] Radical structures were determined using unrestricted Hartree-Fock calculations. All the structures were geometrically optimised using the Broyden-Fletcher-Goldfarb-Shanno

procedure. Computations were performed using a Silicon Graphic Indy workstation computer.

Differences in the heats of formation between the parent urea and the radical intermediate ($\Delta\Delta H_f$) were used as an estimate for the energy of activation E_a, from which relative rate constants could be calculated as seen on p 52-53.

5.0 References

(1) Klingenberg, M. *Arch. Biochem. Biophys.* **1958**, *75*, 376-380.
(2) Garfinkel, D. *Arch. Biochem. Biophys* **1958**, *77*, 493-509.
(3) Poulos, T. L.; Finzel, B. C.; Howard, A. J. *J. Mol. Biol.* **1987**, *195*, 687-700.
(4) Dawson, J. H.; Eble, K. S. *Adv. Inorg. Bioinorg. Mech.* **1986**, 41-64.
(5) McMurry, T. J.; Groves, J. T. *Cytochrome P-450: Structure, Mechanism and Biochemistry*; Plenum Press: New York, 1986.
(6) Suslick, K. *New J. Chem.* **1992**, *16*, 633-642.
(7) Hanson, L. K.; Sligar, S. G. *Croat. Chem. Acta* **1977**, *49*, 237-250.
(8) Muramaki, K.; Mason, H. S. *J. Biol. Chem.* **1967**, *242*, 1102-1110.
(9) Bangcharoenpaurpang, O.; Champion, P. M. *Biochemistry* **1986**, *25*, 2374-2378.
(10) Groves, J. T.; Watanabe, Y. *J. Am. Chem. Soc.* **1988**, *110*, 8433-8452.
(11) Poulos, T. L.; Fizel, B. C.; Howard, A. J. *Biochemistry* **1986**, *25*, 5314-5322.
(12) Schenkman, J. B.; Sligar, S. G.; Cinti, D. L. *Pharmacol.and Therapeut.* **1981**, *12*, 43-71.
(13) Poulos, T. L.; Howard, A. J. *Biochemistry* **1987**, *26*, 8165-8174.
(14) Raag, R.; Poulos, T. L. *Biochemistry* **1993**, *32*, 4571-4578.
(15) Porter, T. D.; Coon, M. J. *J. Biol. Chem.* **1991**, *266*, 13469-13472.
(16) Dawson, J. H.; Sona, M. *Chem. Rev.* **1987**, *87*, 1255-1276.
(17) Ishimura, Y.; Ulkrich, I. C.; Peterson, J. A. *Biochem. Biophys. Res. Commun* **1971**, *42*, 140-146.
(18) Sligar, S. G. *Biochemistry* **1976**, *15*, 5399-5406.
(19) White, R. F.; Loon, M. J. *Ann. Rev. Biochem.* **1980**, *49*, 315-356.
(20) Horecker, B. L. *J. Biol. Chem.* **1952**, *237*, 587-595.
(21) Lyanagi, T.; Mason, H. S. *Biochemistry* **1973**, *12*, 2297-2308.
(22) Vermilion, J. L.; Coon, M. J. *J. Biol. Chem.* **1978**, *253*, 8812-8819.
(23) Lyanagi, T.; Makino, N.; Mason, H. S. *Biochemistry* **1974**, 1701-1710.
(24) Karlin, K. D. *Science* **1993**, *26*, 701-708.
(25) Groves, J. T.; Nemo, T. E. *J. Am. Chem. Soc.* **1979**, *101*, 1032-1033.
(26) Valentine, J. S. *Bioinorganic Chemistry*; University Science Books: Mill Valley, California, U.S.A.,, 1994.
(27) Collman, J. P.; Hampton, P. D.; Brauman, J. I. *J. Am. Chem. Soc.* **1990**, *112*, 2977-2986.
(28) Traylor, T. G.; Hill, K. W.; Fann, W.-P.; Tsuchiya, S.; Dunlap, B. E. *J. Am. Chem. Soc.* **1992**, *114*, 1308-1312.
(29) Tullman, R. N. *Drug Metab. Dispos.* **1984**, *15*, 1163-1182.
(30) Bartoli, J. F.; Bat-tioni, P.; De Foor, W. R.; Mansuy, D. *J. Chem. Soc., Chem. Commun.* **1994**, 23-24.
(31) Goh, Y. M.; Nam, W. *Inorg. Chem.* **1999**, *38*, 914-920.
(32) Lim, H. M.; Jin, S. W.; Lee, Y. J. *Bull. Korean Chem. Soc.* **2001**, *22*, 93-96.
(33) Musher, J. I. *Angew. Chem., Int. Ed. Engl.* **1969**, *8*, 54-68.
(34) Collman, J. P.; Zhang, X.; Lee, V. J.; Uffelman, E. S.; Rauman, J. I. *Science* **1993**, *261*, 1404-1411.
(35) Ostovic, D.; Bruice, T. C. *Acc. Chem. Res.* **1992**, *25*, 314-320.

(36) Zhang, W.; Loebach, J. L.; Wilson, S. R.; Jacobsen, E. N. *J. Am. Chem. Soc.* **1990**, *112*, 2801-2803.
(37) Holm, R. H. *Chem. Rev.* **1987**, *87*, 1401-1449.
(38) Holm, R. H.; Donahue, J. P. *Polyhedron* **1993**, *12*, 571-589.
(39) Traylor, P. S.; Dolphin, D.; Traylor, T. G. *J. Chem.Soc., Chem. Commun.* **1984**, 279-280.
(40) Arasasingham, R. D.; Cornman, C. R.; Balch, A. L. *J. Am. Chem. Soc* **1989**, *111*, 7800-7805.
(41) Lindsay-Smith, J. R.; Lower, R. J. *J. Chem. Soc., Perkin Trans. 2* **1991**, 31-42.
(42) Traylor, T. G.; Ciccone, J. P. *J. Am. Chem. Soc.* **1989**, *111*, 8413-8420.
(43) Traylor, T. G.; Tsuchita, S.; Byun, Y. S.; Fann, W. P. *J. Am. Chem. Soc* **1993**, *115*, 2775-2781.
(44) Traylor, T. G.; Kim, C.; Fann, W. P.; Perrin, C. L. *Tetrahedron* **1998**, *54*, 7977-7986.
(45) Traylor, T. G.; Kim, C.; Richards, J. L. *J. Am.Chem. Soc.* **1995**, *117*, 3468-3474.
(46) Traylor, T. G.; Xu, F. J. *J. Am. Chem. Soc.* **1990**, *112*, 178-186.
(47) He, G. X.; Bruice, T. C. *J. Am. Chem. Soc.* **1991**, *113*, 2747-2753.
(48) Bruice, T. C. *Acc. Chem. Res* **1991**, *24*, 243-249.
(49) Almarsson, O.; Bruice, T. C. *J. Am. Chem. Soc.* **1995**, *117*, 4533-4544.
(50) Nam, W.; Choi, H. J.; So, H.; Lee, J. H.; Han, S. Y. *Chem. Commun.* **1999**, 387-388.
(51) Nam, W.; Han, H. J.; Oh, S. Y.; Lee, Y. J. *J. Am. Chem. Soc.* **2000**, *122*, 8677-8684.
(52) Yang, S. J.; Nam, W. *Inorg. Chem.* **1998**, *37*, 606-607.
(53) Shapiro, S.; Piper, J. H.; Caspi, E. J. *J. Am. Chem. Soc.* **1982**, *104*, 2301-2305.
(54) Hjemeland, R. *Biochem. Biophys. Res. Commun.* **1977**, *76*, 541-548.
(55) Groves, J. T.; McClusky, G. A.; White, R. E. *Biochem. Biophys. Res. Commun* **1978**, *81*, 154-156.
(56) Groves, J. T. *J. Am. Chem. Soc.* **1976**, *98*, 859-861.
(57) Atkinson, J. K.; Ingold, K. U.; Hollenberg, P. F.; Johnson, C. C.; Tadic, M.; Newcomb, M.; Putt, D. A. *Biochemistry* **1994**, *33*, 10630-10637.
(58) Groves, J. T.; Watanabe, Y. *J. Am. Chem. Soc.* **1986**, *108*, 507-508.
(59) Ostovic, D.; Bruice, T. C. *J. Am. Chem. Soc.* **1989**, *111*, 6511-6517.
(60) Komives, E. A.; Ortiz de Montellano, P. R. *J. Biol. Chem.* **1987**, *262*, 9793-9802.
(61) Kunze, K. L.; Mangold, B. L. K. *J. Biol. Chem.* **1983**, *258*, 4202-4207.
(62) Boyd, D. R.; Daly, J. W.; Withep, P. *J. Am. Chem. Soc.* **1968**, *90*, 6525-6531.
(63) Kasperek, G. J.; Bruice, T. C. *J. Chem. Soc., Chem. Commun.* **1972**, 784-784.
(64) Burka, L. T.; Plucinski, T. M.; McDonald, T. L. *Proc. Natl. Acad. Sci. USA.* **1983**, *80*, 6680-6684.
(65) Riley, P.; Hanzlik, R. P. *Xenobiotica* **1994**, *24*, 1-16.
(66) Guengerich, F. P. *Pharmacol. Ther. A.* **1979**, *6*, 99-103.
(67) Lu, A. Y. H.; West, S. B. *Pharmacol. Rev.* **1980**, *31*, 277-295.
(68) Wiley, R. A.; Sterson, L. A. *Biochem. Pharmacol.* **1972**, *21*, 3235-3241.
(69) Seto, Y.; Guengerich, F. P. *J. Biol. Chem.* **1993**, *268*, 9986-9997.
(70) Guengerich, F. P. *J. Med. Chem.* **1984**, *27*, 1101-1103.
(71) Guengerich, F. P.; Macdonald, T. L. *Acc. Chem. Res.* **1984**, *17*, 9-16.
(72) Miwa, G. T.; Walsh, J. S.; Lu, A. Y. H. *J. Biol. Chem.* **1984**, *259*, 3000-3004.
(73) Guengerich, F. P. *J. Biol. Chem.* **1987**, *262*, 8459-8462.

(74) Miwa, G. T.; Lu, A. Y. H. *Cytochrome P450: Structure, Mechanism and Biochemistry*; Plenum Press: New York, 1986.
(75) Foster, A. B. *Chem.- Biol. Inter.* **1974**, *9*, 327-331.
(76) Macdonald, T. L.; Zirvi, K.; Burka, L. T.; Peyman, P.; Guengerich, F. P. *J. Am. Chem. Soc.* **1982**, *104*, 2050-2052.
(77) Hanzlik, R. P.; Tullman, R. H. *J. Am. Chem. Soc.* **1982**, *104*, 2048-2050.
(78) Hall, L. R.; Hanzlik, R. P. *J. Biol. Chem.* **1990**, *265*, 12349-12355.
(79) Hall, L. R.; Hanzlik, R. P. *Xenobiotica* **1991**, *21*, 1127-1138.
(80) Iley, J.; Rosa, E. *Biochem. Pharmacol.* **1992**, *44*, 651-658.
(81) Constantino, L. PhD Thesis, University of Lisbon, 1994.
(82) Twiner, M. J.; Hirst, M.; Valenciano, A.; Zacharewski, T. R.; Dixon, S. J. *Toxicol. appl. Pharmacol.* **1998**, *153*, 143-151.
(83) LeTallec, N.; Lacroix, P.; deCertaines, J. D.; Chagneau, F.; Levasseur, R.; LeRumeur, E. *J. Pharmacol. Toxicol. Methods* **1996**, *35*, 139-143.
(84) Klug, S.; Merker, H. J.; Jackh, R. *Toxicol. Vitro* **1998**, *12*, 123-132.
(85) Angerer, J.; Goen, T.; Kramer, A.; Kafferlein, H. U. *Arch. Toxicol.* **1998**, *72*, 309-313.
(86) Tolando, R. PhD Thesis, Open University, 1997.
(87) Halliwell, B. *Free radicals in biology and medicine*; Oxford University Press: New York, 1985.
(88) Lloyd, J. W. *J. Am. Ind. Hyg. Ass.* **1975**, *36*, 917-919.
(89) Keller, D. A.; Marshall, C. E.; Lee, K. P. *Fundam. Appl. Toxicol.* **1997**, *40*, 15-29.
(90) Thornton Manning, J. R.; Nikula, K. J.; Hotchkiss, J. A.; Avila, K. J.; Rohrbacher, K. D.; Ding, X. X.; Dahl, A. R. *Toxicol. Appl. Pharmacol.* **1997**, *142*, 22-30.
(91) Holden, I.; Segal, Y.; Kimmel, E. C.; Casida, J. E. *Tetrahedron Lett.* **1982**, *23*, 5107-5110.
(92) Jones, A. R. *Experimentia* **1968**, *24*, 326-327.
(93) Jones, A. R.; Jackson, H. *Biochem.Pharmacol.* **1968**, *17*, 2247-2252.
(94) Jones, A. R. *Biochem. Pharmacol.* **1970**, *19*, 603-604.
(95) Bull, D. L.; Borkovec, A. B. *Arch. Environ. contam. Toxicol.* **1973**, *1*, 148-158.
(96) Akov, S.; Oliver, J. E.; Borkovec, A. B. *Life Sci.* **1968**, *7*, 1207-1213.
(97) Longo, V.; Citti, L.; Gervasi, P. G. *Toxicol. Lett.* **1988**, *44*, 289-297.
(98) Koulkes-Pujo, A. M.; Gilles, L.; Lesigne, B.; Sutton, J. *J. Chem. Soc., Chem. Commun.* **1974**, 71-72.
(99) Cook, H. *J. Am. Chem. Soc.* **1958**, *80*, 49-51.
(100) Collin, G. *Can. J. Chem.* **1959**, *37*, 1093-1950.
(101) Zijlstra, J. A.; Brussee, J.; Vandergen, A.; Vogel, E. W. *Mutat. Res.* **1989**, *212*, 193-211.
(102) Dahl, A. R.; Hadley, W. M. *Toxicol. appl. Pharmacol.* **1983**, *67*, 200-205.
(103) Anon *Chimia* **1985**, *39*, 147-148.
(104) Akesson, B.; Jonsson, A. G. *Drug Metabolism and Disposition* **1997**, *25*, 267-269.
(105) Iley, J.; Constantino, L.; Norberto, F.; Rosa, E. *Tetrahedron Lett.* **1990**, *31*, 4921-4922.
(106) Constantino, L.; Iley, J. *Biochem. Pharmacol.* **1994**, *47*, 275-280.
(107) Constantino, L.; Rosa, E.; Iley, J. *Biochem. Pharmacol.* **1992**, *44*, 651-658.
(108) Arceneaux, R. L. *J. Am. Chem. Soc.* **1959**, *24*, 1419-1421.
(109) Eglinton, G.; Whiting, M. C. *J. Chem. Soc.* **1950**, 3650-3653.

(110) Li, Y.; Marks, J. *J. Am. Chem. Soc.* **1996**, *118*, 9295-9306.
(111) L'abbe, G.; Leurs, S.; Sannen, I.; Dehaen, W. *Tetrahedron* **1993**, *49*, 4439-4446.
(112) Perez, D.; Bures, G.; Guitian, E.; Castedo, L. *J. Org. Chem.* **1996**, *61*, 1650-1654.
(113) Fox, J.; Praag, V. *J. Am. Chem. Soc.* **1960**, *82*, 486-489.
(114) Butler, A. R.; Hussain, I. *J. Chem. Soc., Perkin Trans. 2* **1981**, 317-319.
(115) Scannell, M. P.; Prakash, G.; Falvey, D. E. *J. Phys. Chem. A* **1997**, *101*, 4332-4337.
(116) Spring, F. S.; Woods, J. C. *J. Chem. Soc* **1945**, 625-628.
(117) Beckwith, A. L. J.; Hickman, R. J. *J. Chem. Soc* **1968**, 2757-2759.
(118) Flitsch, W.; Schindler, S. R. *Synthesis* **1975**, 685-700.
(119) Nagao, Y.; Kawabata, K.; Seno, K.; Fujita, E. *J. Chem. Soc., Perkin Trans. 1* **1980**, 2470-2474.
(120) Menard, D.; St-Jacques, M. *Can. J. Chem.* **1981**, *59*, 1160-1168.
(121) Alder, W.; Sessions, R. *J. Chem. Soc. Perkin Trans. II* 1984, 411-415.
(122) MOPAC 4.0 ed.; Indiana University: Indiana, 1989.